ANNUAL REPORT

Nuclear Physics Laboratory

University of Washington

April, 1995

Supported in part by the United States Department of Energy under Grant DE-FG06-90ER40537

INTRODUCTION

This has been a year of change at the Nuclear Physics Laboratory. We are pleased to have added several new faculty members to our group. R.G. Hamish Robertson and John Wilkerson have joined the Department of Physics as Professors. Peter Doe and Steve Elliott have joined the Research faculty as Professor and Assistant Professor, respectively. The primary interest of these new faculty is solar neutrino physics. They are presently playing a major role in the design and construction of detectors for the Sudbury Solar Neutrino Observatory (SNO). John Lestone has also recently joined the Research faculty as Assistant Professor. His primary interest is in nuclear reactions, particularly fission.

The Nuclear Physics Laboratory of the University of Washington has for over 40 years supported a broad program of experimental physics research. The current program includes "in-house" research using the local tandem Van de Graaff and superconducting linac accelerators and non-accelerator research in double beta decay and gravitation as well as user-mode research at large accelerator and reactor facilities around the world. We are also now actively using or developing solar neutrino observatories in Canada and Russia.

In June 1994 we completed an upgrade of the tandem accelerator. We now have a pelletron charging system, new resistors, a terminal control computer system and spiral inclined field beam tubes in the tandem. The position, energy and pulse transit time stability of the beam accelerated by this completed system as well as the transmission of the accelerator for heavy ions is significantly improved.

Some highlights of our research activities during the past year are given below.

Motivated by nuclear structure and astrophysical considerations, we have continued our studies of the distribution of Gamow-Teller strength. We focused on the high-energy-release beta decays of 37Ca and 36Ca, and find in both cases considerably more integrated Gamow-Teller strength than predicted by the shell model with effective operators. The GT matrix elements for 37Ca decay can be compared to the isospin-mirror GT matrix elements inferred from 37Cl(p,n) studies; to the extent that isospin symmetry is valid this comparison tests the procedure for extracting GT matrix elements from hadronic charge-exchange reactions. We find that the charge-exchange values can vary by up to a factor of two compared to the beta-decay values. Both of the discrepancies mentioned here provide challenges to nuclear theory.

We have considered the gravitational lensing properties of a plausible model for naturally-occurring wormholes, and find that they should be detectable by MACHO searches currently in progress. We find that the expected dipole anisotropy in the distribution of gamma ray bursts is not large enough to determine if they are cosmic in origin.

The Russian-American Gallium experiment (SAGE) continues to give a flux well below the Standard Solar Model. A calibration with 51Cr is in progress.

The University of Washington group continues to have major involvement in several aspects of the SNO project. The research and development effort for the acrylic vessel which holds the 1000 tons of heavy water has been completed. We are involved in the development of the data acquisition system for the readout of the SNO detector. In collaboration with groups at LASL and LBL we will provide an independent detector array for recording the neutral current signal of the SNO detector.

In our studies of sub-barrier fusion reactions we have measured the distributions of barriers for a prolate and an oblate target nucleus bombarded with 40Ca. The barrier distributions demonstrate important contributions

from the hexadecapole as well as from the sign of the quadrupole moment.

A study of entrance channel effects on the energy spectra of light charged particles has revealed significant effects. The spectral shape for 12C + 144Sm is hotter than for 64Ni + 96Zr when the bombarding energies are chosen to match the excitation energy in the compound nucleus.

Recent results from the APEX collaboration on the positron spectra for uranium projectiles do not reveal peak structures and call into question previous GSI results.

The AMS group, with partial support from NSF, has continued its development and refinement of techniques for the isolation of essentially pure pollen fractions from lake sediment and peat samples for AMS radiocarbon (14C) dating. These techniques were successfully applied, for the first time, to a low-organic-carbon-content core taken from an Arctic lake. An apparent age-depth reversal in earlier "bulk carbon" results obtained by others for this core was rectified.

The ultra-relativistic heavy ion group participated in a very successful initial run of CERN experiment NA49, which used two large time-projection chambers to track charged reaction products from the new CERN 33 TeV lead beam on a fixed lead target. The University of Washington group played a major role in developing the tracking software used with the main time-projection chamber of the experiment. They also developed new general purpose slow control software used in the experiment.

We have devised an approximate procedure for analyzing Bose-Einstein correlation data without background generation which may be useful for single-event physics at CERN and RHIC. We have made progress in analyzing expected "wiggles" in multi-particle Bose-Einstein correlation data arising from non-Gaussian source shapes.

As always, we welcome applications from outsiders for the use of our facilities. As a convenient reference for potential users, the table on the following page lists the vital statistics of our accelerators.
For further information, please write or telephone:

Professor Derek W. Storm, Director
Nuclear Physics Laboratory
University of Washington
Box 354290
Seattle, WA 98195
(206) 543-4085
e-mail: storm@npl.washington.edu

We close this introduction with a reminder that the articles in this report describe work in progress and are not to be regarded as publications or to be quoted without permission of the authors. In each article, the names of the investigators have been listed alphabetically, with the primary author underlined, to whom inquiries should be addressed.

Robert Vandenbosch
Editor

Barbara Fulton
Assistant Editor

1. NUCLEAR PHYSICS

1.1 Beta-delayed alpha-particle emission of ^{16}N and the E1 S-factor of the $^{12}C(\alpha,\gamma)^{16}O$ reaction

E.G. Adelberger, P. Chan, L. De Braeckeleer, P.V. Magnus, D.M. Markoff, D.W. Storm, H.E. Swanson, K.B. Swartz, D. Wright and Z. Zhao

The $^{12}C(\alpha,\gamma)^{16}O$ cross section at astrophysical energies is an incoherent sum of the electric dipole (E1) and electric quadrupole (E2) components. The E1 component is dominated by a broad level at 9.6 MeV and a subthreshold level at 7.12 MeV (alpha particle threshold 7.16 MeV) and the interference between them. The E2 component is dominated by a subthreshold level at 6.92 MeV, and direct capture, and the interference between these two terms. The beta-delayed alpha spectrum of ^{16}N provides a unique way to determine the alpha-particle width of the 7.12 MeV level, which is crucial to our understanding of the E1 cross section at low energies.

We have measured the alpha-particle spectrum using the rotating arm apparatus built for the mass-8 beta-alpha correlation measurements. The deuteron beam (30 μA at 3.5 MeV) from the FN tandem was incident on a rotating target which consisted of Ti^{15}N on a Ni backing. When the beam was on, the recoiling ^{16}N nuclei were collected by a carbon catcher foil of 10 or 20 $\mu g/cm^2$. When the beam was off, the catcher was transferred to the counting area. There are two silicon surface barrier detectors in the counting area. The energies of the alpha-particles and the carbon nuclei were detected simultaneously. The slow timing between the two particles was recorded at the same time to determine the random coincidences between two counters. The lifetime of the decay, measured by clocking each event relative to the arm rotation, is found consistent with the known lifetime of the ^{16}N nuclei. In addition, the absolute efficiency to measure carbon ions and detector response to low energy carbon ions were also studied using the $^{12}C(p,p)^{12}C$ reaction. Our results are consistent with previous measurements of TRIUMF[1] and Yale.[2]

The data were analyzed in an R-matrix formalism using a 3-level approximation. In Fig. 1.1-1, we show an R-matrix fit to our data. Possible $l = 3$ contribution is included in the fit.

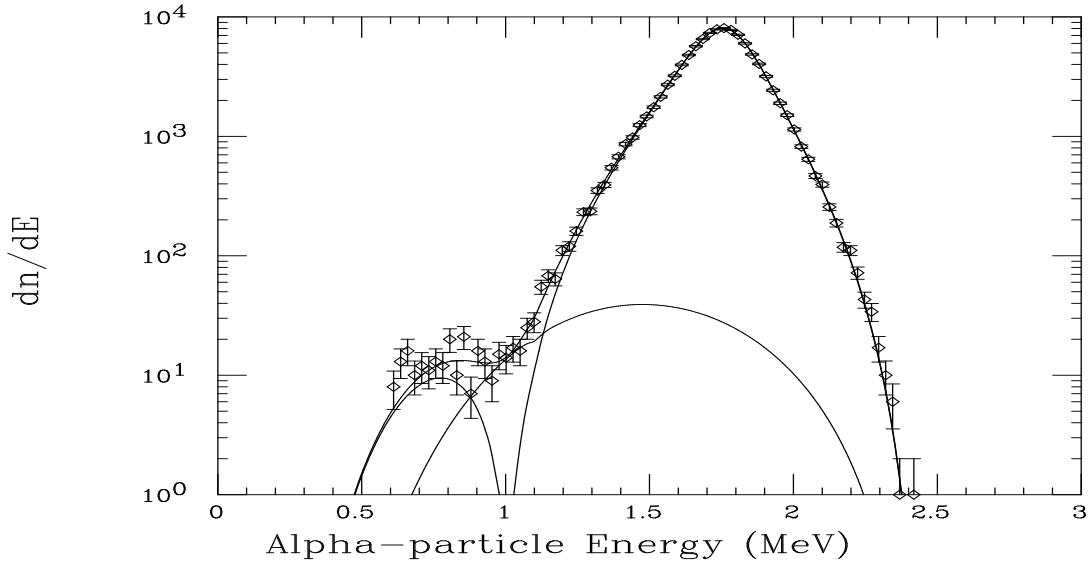

Fig. 1.1-1. Alpha energy spectrum.

[1]L. Buchmann *et al*., Phys. Rev. Lett. **70**, 726 (1993).
[2]Z. Zhao *et al*., Phys. Rev. Lett. **70**, 2066 (1993).

1.2 Detector tests for a measurement of the $^{12}C(\alpha,\gamma)^{16}O$ cross section at low energies

L. De Braeckeleer and Z. Zhao

The main uncertainties in the E1 component of the $^{12}C(\alpha,\gamma)^{16}O$ cross section were the uncertainty in the alpha-particle width of the subthreshold 7.12 MeV level and also the uncertainty in the sign of the interference between 7.12 MeV level and 9.6 MeV level. The beta-delayed alpha spectrum of ^{16}N provides a unique way to determine the alpha-particle width of the 7.12 MeV level, as discussed in the previous report,[1,2,3] but provides no new information on the sign of the interference in the $^{12}C(\alpha,\gamma)^{16}O$ reaction. The E2 component is obtained by measuring the angular distribution of the gamma rays, and the extrapolation to astrophysical energies is also largely uncertain.

Although the combined four sets of previous cross section measurements[4,5,6,7] favors constructive interference in the E1 $^{12}C(\alpha,\gamma)^{16}O$ reaction, examination of individual data sets reveals inconsistency among them especially regarding the sign of the interference in the E1 channel. Since the alpha-particle width of the subthreshold level is determined by the ^{16}N data, the constructive and destructive interference in the E1 channel of the $^{12}C(\alpha,\gamma)^{16}O$ reaction should differ by a factor of two at energy $E_{c.m.}$ = 1.2 MeV. A 10% measurement at this energy should allow us to distinguish between two interference schemes. We plan to do measurements in two steps; step one is a two-detector assembly at 90° to determine the E1 component (mainly the sign); step two is a measurement of the angular distribution of the gamma rays to determine the E2 component.

Recently, technological advancements have made available a high intensity pulsed ion beam and large volume germanium counters. We plan to surround the Ge counter with a NaI(Tl) annulus and plastic scintillator. The Ge counter will be running in escape mode (requiring coincidence with 511 keV gamma rays in the NaI(Tl) counter). Therefore the Ge counters provide good energy resolution, and escape gamma rays in the NaI(Tl) provide excellent timing relative to the pulsed beam. We expect a significant background reduction relative to previous measurements. Using two Ge counters (8 cm long and 8 cm in diameter), the total efficiency of this detector system is 1×10^{-3}. For a 120 $\mu g/cm^2$ target, the expected count rate is 4.5/day at $E_{c.m.}$ = 1.2 MeV. The E2 contamination in the 90° detector arrangement is less than 10% for the entire accessible energy range. We expect the beam independent background to be negligible.

We are currently testing such a concept using a smaller Ge and BGO counters. We also studied the beam independent background in such a system. We plan to study the beam related background in the near future.

---

[1] L. Buchmann *et al*., Phys. Rev. Lett **70**, 726 (1993).
[2] Z. Zhao *et al*., Phys. Rev. Lett. **70**, 2066 (1993).
[3] Z Zhao *et al*., to be published.
[4] P. Dyer and C.A. Barnes, Nucl. Phys. **A233**, 495 (1974).
[5] A. Redder *et al*., Nucl. Phys. **A462**, 385 (1987).
[6] R.M. Kremer *et al*., Phys. Rev. Lett. **60**, 1475 (1988).
[7] J.M.L. Ouellet *et al*., Phys. Rev. Lett. **69**, 1475 (1992).

1.3 On the dipole distribution of gamma ray bursts

J.G. Cramer and P.B. Cramer*

Gamma ray bursts (GRB) constitute an outstanding puzzle of contemporary astrophysics. In recent satellite experiments GRB have been observed to occur in a time scale of milliseconds to seconds at the rate of a few per day from directions uncorrelated with the galactic plane and to deliver the remarkably large integrated energy of about 6 MeV per cm^2 of detector area. No radio, optical, or X-ray counterparts of GRB have been observed, lending ambiguity to their origin and distance scale. The leading scenarios for GRB source locations are: (1) GRB are at galactic halo distances, perhaps produced by unusual neutron stars or quiet supernovas, or (2) GRB are at cosmological distances, perhaps produced by merging neutron stars. If GRB are galactic and are emitted in an angular cone with a half-angle θ (expressed as a fraction of π), the energy release of each GRB is $10^{51}\ \theta^2$ ergs (or, with θ =1, roughly the mass of Mars' largest moon Phobos converted entirely into gamma ray energy). On the other hand, if GRB are cosmological, each GRB has an energy release of $10^{51}\ \theta^2$ ergs (with θ =1, this is roughly a Jupiter-mass converted completely into gamma rays in a few seconds). In either case, both the generation and the transport of this quantity of energy constitute very formidable and unsolved theoretical problems.

We here consider the possibility of using the motion-induced dipole moment of the GRB distribution as an indication of the GRB source. COBE data shows that the Earth is moving through the microwave background radiation with a velocity of $\beta_{CB} = 1.23 \times 10^{-3}$ in the direction $\ell^{II} = 264.4^o \pm 0.3^o$ and $b^{II} = 48.4^o \pm 0.5^o$ in galactic coordinates. On the other hand, the Sun moves with respect to the galactic center with a velocity of $\beta_{gal} = 7.92 \times 10^{-4}$ in the direction $\ell^{II} = 91.1^o \pm 0.4^o$ and $b^{II} = 0^o$ in galactic coordinates. These vectors thus point in nearly opposite directions, making an angle of about 130º with each other.

The solid angle of a moving source is modified by its proper motion, an effect well known in nuclear and high energy physics. This solid angle modification will induce a dipole component in the GRB angular distribution of magnitude 2β with its peak pointing in the direction of β, i.e. the GRB events will be distributed on the sky with a probability given by $P(\theta,\phi) = 1 + 2\beta \cos\theta$. Consider an observed sample of *N* observations of GRB, with the *i*th event detected at a polar angle of θ_i with respect to the source velocity direction of interest and with an observational efficiency ε_i. The estimated boost is $\langle\beta_{obs}\rangle = \sum_{i=1}^{N} \omega_i \cos\theta_i / \sum_{i=1}^{N} \omega_i$, where $\omega_i = 1/\varepsilon_i$. Assuming ω_i=1 and treating the dipole component as small, the values of $(\omega_i \cos\theta_i)$ will fall on a uniform flat distribution of values between -1 and +1. The mean of such a distribution is zero and its standard deviation is $\sigma = 1/\sqrt{3}$. Therefore, for *N* observations, the observed standard deviation of $\langle\beta_{obs}\rangle$ will be $\sigma_{obs} = 1/\sqrt{3N}$.

We conclude that a determination of the dipole distribution at the 1σ level for the COBE velocity would require 220,000 GRB observations and for the galactic velocity vector would require 532,000 GRB observations. Unfortunately, the most recent catalog of GRB events contains only 1121 events. Thus, because the proper motion of the solar system is relatively small and the number of detected GRB is still quite small, it is not feasible to use the expected dipole distribution as an indication of GRB origin.

* Max-Planck-Institut für Physik, Föhringer Ring 6, D-80805 München, Germany.

1.4 Natural wormholes as gravitational lenses

J.G. Cramer, R.W. Forward,* M.S. Morris,† M. Visser,‡ G. Benford£ and G.A. Landis§

Visser has suggested a wormhole configuration, a flat-space wormhole that is framed by a variant of the cosmic string solutions of Einstein's equations with a negative string tension of -1/4G and therefore a negative mass density. The inflationary phase of the early universe might produce closed negative-mass string loops framing stable Visser wormholes or expand microscopic wormholes in the Planck-scale spacetime foam to macroscopic dimensions, thereby creating stable natural wormholes.

When a massive object passes through a wormhole, from back-reaction the entrance mouth should gain mass and the exit mouth lose mass. If the mass flow occurs in the early universe from a high to a low density region, the exit wormhole mouth could acquire a stellar-scale negative mass. We have christened such objects "gravitationally negative anomalous compact halo objects" (GNACHOs).

We have considered the gravitational lensing of such objects as a way of detecting them. We find that the lensing of a negative mass is not analogous to a diverging lens. In certain circumstances, it can produce more light enhancement than does the lensing of an equivalent positive mass.

The intensity modulation of a background star that occurs when the GNACHO lensing mass crosses near the source-detector line of sight shows light enhancement profiles that are characteristically bounded by two caustics, each of which provides a very sharp increase in light intensity. Between these caustics is an umbra region with no transmitted light at all. This light enhancement profile is qualitatively different from that of a positive lensing mass of the same magnitude and geometry. In particular, the negative mass light curves is much sharper, showing stronger but briefer light enhancements, and a precipitous drop to zero intensity in the central region.

Our calculations show that objects of negative gravitational mass, if they exist, can provide a very distinctive light enhancement profile. Since three groups are presently conducting searches for the gravitational lensing of more normal positive mass objects, we have suggested that these searches be broadened so that the signatures of the objects discussed above are not overlooked by over-specific data selection criteria and software cuts. While the analysis of this brief report is phrased in terms of wormholes, the observational test proposed is more generally a search for compact negative mass objects of any origin. The question of whether quantum field theory is consistent with negative mass in a spacetime that is asymptotically flat and semiclassical near infinity is as yet undecided. Observation of GNACHOs would give an experimental and definitive answer to this question. We recommend that MACHO search data be analyzed for evidence of GNACHOs.

This work has been accepted for publication in Physical Review D, and is available as electronic preprint astro-ph/9409051 on World Wide Web at http://babbage.sissa.it.

*Forward Unlimited, P.O. Box 2783, Malibu, CA 90265.
†Department of Physics and Astronomy, Butler University, Indianapolis, IN 46208.
‡Physics Department, Washington University, St.Louis, MO 63130-4899.
£Physics Department, University of California at Levine, CA 92717-4575
§NASA Lewis Research Center, Mail Code 302-1, Cleveland OH 44135-3191.

1.5 ^{36}Ca β – decay and the Isobaric Multiplet Mass Equation

E.G. Adelberger and A. Garcia*

This work was a byproduct of our study of ^{37}Ca decay at ISOLDE, which is presented elsewhere in this report. The ^{36}Ca activity was produced in a fluorinated Ti target, and data were taken with both A = 36 (for ^{36}Ca) and A = 55 (for ^{36}Ca ^{19}F) beams. The A = 36 beam was dominated by ^{36}K; the A = 55 beam was extremely pure but had such a low intensity (because the fluorine leak in the target had expired) that we detected only the intense proton group corresponding to the superallowed decay of ^{36}Ca.

The delayed proton energy scale was calibrated using well-known proton groups from ^{37}Ca and ^{36}K decays. We found that the superallowed ^{36}Ca group had a lab energy of $E_p - 2550.2 \pm 2.2$ keV, which corresponds to a mass excess of -13135.6 ± 2.4 keV for the lowest T = 2 level in ^{36}K. When combined with the well-known masses of the ^{36}S, ^{36}Cl, and ^{36}K members of the isospin quintet and the less well-known mass of ^{36}Ca, our result provides one of the most precise tools of the isobaric multiplet mass equation (IMME)

$$M(A_1 T_1 T_3) = a(A_1 T) + b(A_1 T) T_3 + c(A_1 T) T_3^2.$$

The results of fitting these data to the IMME (plus extensions containing T_3^3 and T_3^4 terms) are shown in Table 1.5-1.

Table 1.5-1. Coefficients of multiplet mass equation for the lowest quintet in A = 36.

a (keV)	b (keV)	c (keV)	d (keV)	e (keV)	χ^2 / ν	$P(\chi^2, \nu)$[a]
-19378.4±1.0	-6043.8±1.3	200.5±0.7			1.5	0.22
-19377.6±1.5	-6044.5±1.6	199.1±1.9	0.8±1.0		2.4	0.12
-19.3771±1.5	-6043.6±1.3	197.6±2.5		0.6±0.5	1.6	0.21
-19377.1±1.5	-6039.2±3.8	195.4±3.1	-4.2±3.4	2.7±1.8		

[a]Probability of getting a χ^2 as large as that in the previous column.

*Dept. of Physics, University of Notre Dame, South Bend, IN.

1.6 Gamow-Teller strength in ^{36}Ca β^+ decay

E.G. Adelberger, B.A. Brown,* Z. Janas,† H. Keller,† K. Krumbholz,‡ V. Kunze,‡ P. Magnus F. Meissner,‡ A. Piechaczek,† M. Pfützner,£ E. Roeckl,† K. Rykaczewski,£ W.-D. Schmidt-Ott,‡ W. Trinder† and M. Weber†

We have used the FRS projectile fragment separator at GSI to study the decay of ^{36}Ca. Beta delayed γ's and protons were observed using the same detector setup we used for the ^{37}Ca decay study discussed in the following report.. A secondary ^{36}Ca beam with an intensity of 0.25 atoms/s was produced by a primary beam of 300 MeV/u ^{40}Ca impinging on a 1g/cm^2 ^{9}Be target. A total of 2.8 x 10^4 ^{36}Ca atoms were implanted during the experiment. The ^{36}Ca lifetime, 102 ± 2 ms, was extracted from the time distribution of proton events with energies above 2.5 MeV, mainly originating from the superallowed transition. We observed strong transitions to γ emitting states in ^{36}K at 1112.8(4) and 1619.0(2) keV, and to proton decaying ^{36}K states at 3370(41), 4287(39), 4451(33), 4687(37), 5947(47) and 6798(71) keV.

Fig. 1.6-1 compares our measured B(GT) values to shell model predictions using the USD interaction. We find a situation strikingly similar to that observed in ^{37}Ca decay[1] where the theory with "quenched" GT operators gives a good account of the strengths to transition at low energy ($E_x \lesssim$ 3.5 MeV), but predicts much too little strength at higher energies. In fact the B(GT) integrated strength up to our experimental cutoff (see Fig. 1.6-1) agrees much better with that predicted by the unquenched theory. There are now three examples of high energy-release β decays (^{37}Ca, ^{36}Ca, and ^{33}Ar) where the shell model fails, in similar ways, to predict the distribution of GT strength. This systematic shortcoming poses an important problem for nuclear structure calculations.

This work has been published in Physics Letters B.

WWW: Select "Fig 1.6" from Table of Contents page

Fig. 1.6-1. The heavy lines show the $\pm 1\sigma$ error band of the summed *B(GT)* strength in ^{36}Ca decay as a function of final state E_x. Curves b) and c) are shell model calculations using free and renormalized *GT* operators, respectively.

* Michigan State University, East Lansing, MI.
†GSI, Darmstadt, Germany.
‡II. Phys. Inst., Univ. Göttingen, Germany.
£ Inst. of Exp. Physics, Univ. of Warsaw, Poland.

[1]E.G. Adelberger, *et al.*, Phys. Rev. Lett. **67,** 3658 (1992).

1.7 Study of ^{37}Ca β decay at GSI and the ^{37}Cl cross section for ^{8}B neutrinos

E. G. Adelberger, Z. Janas,* H. Keller,* K. Krumbholz,† V. Kunze,† P. Magnus, F. Meissner,† A. Piechaczek,* M. Pfützner,‡ E. Roeckl,* K. Rykaczewski,‡ W.-D. Schmidt-Ott,† W. Trinder,* and M. Weber*

The observation of significant discrepancies between mirror B(GT) values extracted from ^{37}Ca β decay and ^{37}Cl(p,n) studies (mentioned elsewhere in this report) motivated this measurement that provided absolute intensities of the previously observed[1] β-delayed proton groups and, for the first time, detected the beta-delayed gamma rays following ^{37}Ca decay. In addition we obtained a precise measurement of the ^{37}Ca halflife.

The FRS projectile fragment separator at GSI produced a secondary ^{37}Ca beam of about 30 atoms/s, from the bombardment of a $1\,g/cm^2$ Be target with a 300 MeV/u beam of ^{40}Ca. A total of 2.6 million ^{37}Ca ions were stopped in the central element of a 3 counter Si telescope that was surrounded by 2 large-volume Ge detectors. Beta delayed protons were detected in the central Si counter, and delayed gammas were detected by the Ge detectors in coincidence with a β pulse in the outer two Si counters.

The ^{37}Ca halflife was obtained from the time distribution of the intense proton group corresponding to the superallowed decay. Our value of 181(1) ms is two standard deviations larger than the previously accepted result. A high-quality spectrum of γ-rays following ^{37}Ca decay (see Fig. 1.7-1) showed peaks at 1370.9(2), 2750.4(2) and 3239.3(2) keV with branching ratios of 2.1(1)%, 2.8(1)%, and 4.8(2)% respectively. Combining these results with the delayed proton intensities from ref. 1 we find that the 3239 keV state of ^{37}K has $\Gamma_\gamma / \Gamma_p = 22(2)$. This is a surprisingly large value for a level that lies nearly 1.4 MeV above proton threshold, and explains most of the discrepancy noted earlier regarding the mirror B(GT)'s for this level.

We have used our results to recompute the cross section for ^{8}Be neutrinos on a ^{37}Cl detector. Our result $1.09(3)\times10^{-42}\,cm^2$ is consistent with Bahcall's standard value of $1.06(10)\times10^{-42}\,cm^2$.

WWW: Select "Fig 1.7" from Table of Contents page.

Fig. 1.7-1. γ-ray spectrum from the decay of ^{37}Ca. The dominant lines are labeled by the residual nucleus in which the transitions occur. Weaker lines are from weaker transitions in ^{36}Ar or are single or double escape peaks. This work has been published in Physics Letters B.

---

*GSI, Darmstadt, Germany.
†II. Phys. Inst., Univ. Göttingen, Germany.
‡ Inst. of Exp. Physics, Univ. of Warsaw, Poland.

[1] A. Garcia, *et al.*, Phys. Rev. Lett. **67,** 3654 (1991).

1.8 Study of ^{37}Ca decay at ISOLDE

E. G. Adelberger, A. Garcia,* P.V. Magnus, H.E. Swanson, D.P. Wells,† F.E. Wietfeldt,‡
O. Tengbald,£ and the ISOLDE Collaboration

Comparison of the isospin analog *B(GT)* values from our β-delayed proton work on ^{37}Ca [1] and a new, high-resolution study[2] of ^{37}Cl(p,n) showed some large discrepancies. The discrepancies at low E_x could arise if γ-decay competed successfully with proton decay for a few of the low-lying final states in ^{37}K.[3] We studied β-delayed γ emission in ^{37}Ca at ISOLDE and found unexpectedly significant γ-ray branches from 2 of the unbound daughter states in ^{37}K.

Our ^{37}Ca source was produced using a ^{37}CaF beam from the ISOLDE general-purpose on-line isotope separator at the CERN PS/booster. The fluorinated A = 56 beam had very little radioactive contamination. In particular, it had virtually no ^{37}K activity that in an A = 37 beam is so intense that it would have been impossible to do our experiment. The fluorination process was very efficient; the A = 56 beam had about 30 ^{37}CaF ions per second, 50% of the ^{37}Ca intensity observed in the A = 37 beam. The ^{37}CaF beam was focused onto a three-element particle telescope that was surrounded by an annular eight-segment NaI detector that covered $\Delta\Omega / 4\pi \approx 0.9$. We observed β-delayed γ branches of (1.5±0.4)%, (3.6±0.8)%, and (4.4 ±0.6)% to ^{37}K levels at 1.37, 2.75, and 3.24 MeV. These results are consistent with Ge detector data taken at GSI (see Section 1.7 of this report). Combining this β-delayed γ work with our earlier β-delayed proton results[1] we find the *B(GT)* values listed in Table 1.8-1. It is apparent that although the larger anomalies have essentially been eliminated, problems remain at the factor of 2 level.

This work was recently published in Physical Review C.[4]

Table 1.8-1. Analog B(GT) values obtained from ^{37}Ca β decay and ^{37}Cl(p,n).

E_x(^{37}K)	$B(GT;\ \beta^+)$[a]	E_x(^{37}Ar)	$B(GT;\ p,n)$[b]
0.00	$(4.8 \pm 0.1)\times10^{-2}$	0.00	$(4.8 \pm 0.1)\times10^{-2}$
1.37	$(9.2 \pm 2.5)\times10^{-3}$	1.41	$(1.4 \pm 0.1)\times10^{-2}$
2.75	$(1.2 \pm 0.1)\times10^{-1}$	2.80	$(7.0 \pm 0.2)\times10^{-2}$
3.24	$(8.2 \pm 1.6)\times10^{-2}$	3.17	$(1.28 \pm 0.04)\times10^{-1}$
3.62	$(7.5 \pm 0.4)\times10^{-2}$	3.60	$(5.8 \pm 0.3)\times10^{-2}$
3.84	$(9.4 \pm 0.5)\times10^{-2}$	3.94	$(1.9 \pm 0.1)\times10^{-2}$
4.19	$(2.0 \pm 0.7)\times10^{-3}$		
4.41	$(4.3 \pm 0.2)\times10^{-2}$		
4.50	$(6.0 \pm 0.3)\times10^{-2}$	4.57	$(8.5 \pm 0.2)\times10^{-2}$

[a]From this work.
[b]From the $E_p \approx 100$ MeV ^{37}Cl(p,n) data of Ref. 2. Data are normalized so that the ground-state transition has the correct value determined by the ^{37}Ar lifetime.

*Department of Physics, University of Notre Dame, South Bend, IN.
†Department of Health, Washington State, Olympia, WA.
‡Lawrence Berkeley Laboratory, Berkeley, CA.
£ CERN, Switzerland.

[1] A. Garcia, *et al*., Phys. Rev. Lett. **67,** 3654 (1991).
[2] D.P. Wells, private communication regarding experiment at Indiana University Cyclotron Facility.
[3] C.D. Goodman, *et al*., Phys. Rev. Lett. **69,** 2446 (1992).
[4] A. Garcia, *et al*., Phys. Rev. C **51,** R439 (1995).

2. NEUTRINO PHYSICS

2.1 Solar neutrino research

Q.R. Ahmad, J. Beck, P.J. Doe, S.R. Elliott, J.V. Germani, A.W.P. Poon, T.D. Steiger, R.G.H. Robertson and J.F. Wilkerson

Understanding the properties of neutrinos ranks as one of the major unresolved issues in nuclear and particle physics. In particular, we do not know if neutrinos have mass or not. Neutrinos with mass would provide conclusive evidence of new physics beyond the minimal Standard Model of elementary particles and fields while possibly also comprising a significant portion of the dark matter thought to abound in the universe. Increasingly, the "solar neutrino problem", in which all four of the existing experiments observe far fewer neutrinos from the Sun than predicted by solar model calculations, appears to point to neutrino oscillations. Neutrino oscillations convert one "flavor" of neutrino into another, and can only occur if neutrinos have mass. Our experimental program to resolve this question includes a collaboration with the Russian Academy of Sciences, Los Alamos National Laboratory, and the University of Pennsylvania on a ^{71}Ga radiochemical measurement (SAGE) of the pp neutrino flux and participation in the Sudbury Neutrino Observatory (SNO), a joint Canadian, US, UK effort to measure the spectral distribution and flavor composition of the flux of the higher-energy, ^{8}B neutrinos from the Sun.

2.2 The Sudbury Neutrino Observatory

Q.R. Ahmad, J. Beck, P.J. Doe, S.R. Elliott, J.V. Germani, A.W.P. Poon, T.D. Steiger, R.G.H. Robertson and J.F. Wilkerson

The Sudbury Neutrino Observatory will be the first solar neutrino detector capable of registering and distinguishing both the flux of electron neutrinos and the total flux of all left-handed neutrinos from the Sun. As such, it can make an unambiguous statement that neutrino oscillations are occurring, if the total flux is found to be larger than the ν_e flux. The conclusions will be essentially independent of solar models.

The sensitive medium of the SNO laboratory is 1000 tonnes of ultra-pure D_2O. The charged-current interaction of electron neutrinos on deuterium produces a fast electron that emits Čerenkov radiation in the water. An array of 9500 photomultipliers records the amount of light and, therefore, the energy of the electron. Our group is involved in developing the data acquisition system for the readout of the SNO detector, directing the research and development effort for the acrylic vessel that separates the heavy water from the light water shield, coordinating the SNO detector turn-on and commissioning efforts, and providing an independent detector array for recording the neutral-current signal of the SNO detector. Neutral-current interactions of all flavors of neutrino disintegrate the deuteron into a proton and a neutron, and the rate of these interactions can be determined by measuring the rate of neutron production.

2.3 Development of a compact 20 MeV gamma-ray source for energy calibration at the Sudbury Neutrino Observatory

M.C. Browne,[*] N.P. Kherani,[†] A.W.P. Poon, R.G.H. Robertson and C.E. Waltham[‡]

A compact 20 MeV gamma-ray source is being developed for energy calibration at the Sudbury Neutrino Observatory (SNO). The gamma-rays are produced through the radiative capture reaction $^3H(p,\gamma)^4He$.

There are several constraints in designing the source. It has to be compact and portable, as it will be lowered to the center of the SNO detector through the 57" diameter deck of the acrylic vessel. The neutron production rate has to be low to ensure SNO's neutral current sensitivity to supernova neutrinos during the scheduled high energy γ calibration. Even though the Q-value of $^3H(p,n)^3He$ is -0.763 MeV, which corresponds to a reaction threshold of 1.02 MeV, impurities in the beam and the target will give rise to undesired neutrons through the $^2H(t,n)^4He$, $^3H(d,n)^4He$, and $^3H(t,nn)^4He$ reactions. So the discharge hydrogen gas and the target tritium must be of very high purity. The solid tritium target must also have a high thermal stability to minimize tritium gas mixing into the discharge gas.

Fig. 2.3-1 shows the design of the source. It can be divided into two sections: a cold cathode Penning ion source and a target chamber. The anode E2 is biased at +2 kV, while the cathodes E1, and E3 are grounded. Pyrex®-stainless steel couplings (C) are used to isolate high voltages. Permanent magnet rings M provide a ~1 kG axial magnetic field causing the electrons to spiral around the field lines, generating more ions. A SAES® getter pump is attached to E1. The getter pump serves as the dispenser of hydrogen gas. Ions (H^+, H_2^+ and H_3^+) are accelerated through a -15 to -20 kV bias towards the target mounted at the end of the beam line. In this scheme, the construction of complicated accelerating and focusing electrodes is avoided, thus keeping the length of the source to a minimum. In fact, the length of the source is only 16".

The target selected for this source is a solid scandium tritide (Sc^3H_2), primarily because of its good thermal stability. It will be prepared at the Tritium Laboratory of Ontario Hydro Technologies in Toronto, Canada. It is clear from the drawing that the source is a sealed one, minimizing the hazard of tritium contamination.

The electro-optics of the ion source were first computer simulated and subsequently tested experimentally. The beam current has been measured using two independent methods: by measuring temperature change of a copper target and by integrating the beam profile measured using a Faraday cup. In the thermal measurement, the temperature of the copper target was monitored by a type T thermocouple. The beam power was later calibrated by an electric heater embedded in the target. We designed and constructed a special Faraday cup for measuring the beam profile. The cup was biased such that the secondary electron effects were minimized. Fig. 2.3-2 shows the results of the beam current measurements.

We also designed and constructed a mass spectrometer to measure the mass composition of the ion beam. Ions of different masses are separated by a magnetic field perpendicular to the ion beam propagation. Our experiment showed that protons compose (63±15)% of the beam, the rest being H_2^+ and H_3^+ molecular ions. We are now building a target evaporation chamber, similar to that used by Kherani *et al.*,[1] to test fully the target fabrication procedure of Sc^3H_2 before using the tritium facility at Ontario Hydro Technologies.

---

[*]Department of Physics, North Carolina State University, Raleigh, NC.
[†]Ontario Hydro Technologies, 800 Kipling Avenue, Toronto, Ontario, Canada M8Z 5S4.
[‡]Department of Physics, University of British Columbia, Vancouver, B.C., Canada V6T 1Z1.

[1]N.P. Kherani and W.T. Shmayda, Fusion Tech., **21**, 334 (1992); N.P. Kherani, Ph.D. thesis, University of Toronto, 1994 (submitted to University Microfilm Inc., Ann Arbor, Michigan).

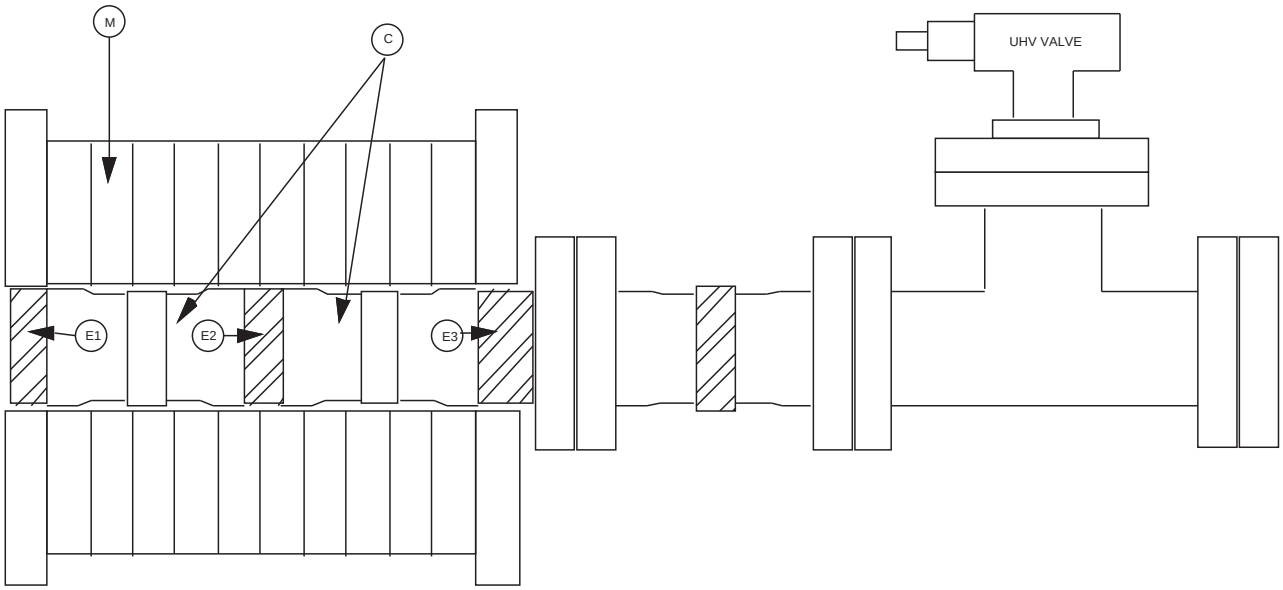

Fig. 2.3-1. Design of the SNO $^{3}H(p,\gamma)^{4}He$ 20 MeV gamma-ray source.

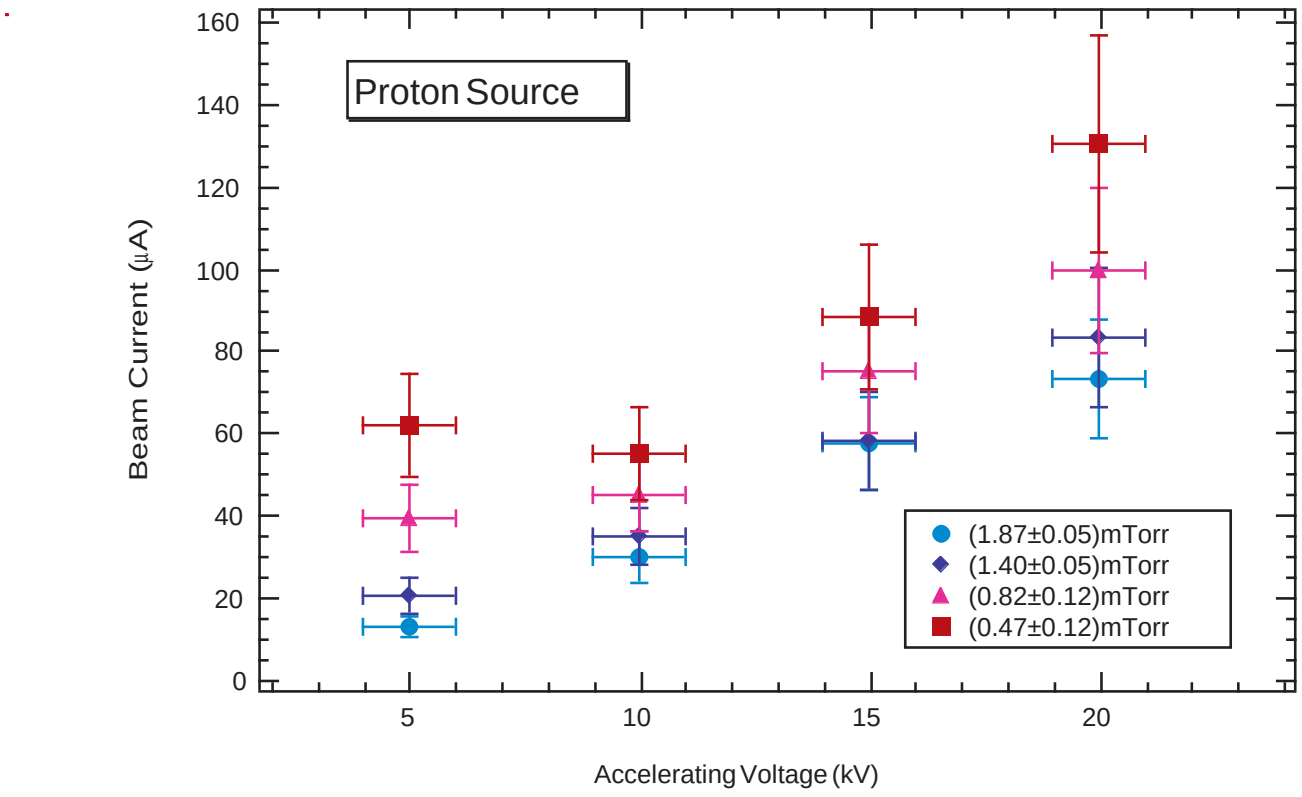

Fig. 2.3-2. Measured beam current of the ion source as a function of the beam accelerating voltage.

2.4 A neutral current detector array for Sudbury Neutrino Observatory

P.J. Doe, S.R. Elliott, J.V. Germani, A.W.P. Poon, T.D. Steiger, R.G.H. Robertson and J.F. Wilkerson

Neutrons can be detected with high efficiency in ^{3}He-filled proportional counters without interfering significantly with the Cerenkov light from charged-current processes. We plan to install in SNO an array of such counters, with a total length of 800 meters, and constructed of highly purified materials.

Our rationale follows: ^{3}He proportional counters offer fundamental advantages. Neutral-current and charged-current events are recorded separately and distinguished event by event. The effective CC rates are doubled and the NC rates quadrupled in comparison with the dissolved-salt method. For the basic dissolved-salt method, the rate of neutron capture is obtained by subtraction of data without salt, after correcting for capture in deuterium. Recently, however, it has been suggested that gamma and electron events can be distinguished to some degree on-line. The secular variation in the NC rate due to the Earth's orbital eccentricity would become observable at the 95% confidence level. Time variations in the neutrino flux could be followed simultaneously in the NC and CC channels on the time scale of milliseconds to years. All signals and backgrounds can be determined at the same time, and there is no need to compare and subtract data taken at different times and under different conditions. The method is fully compatible with the dissolved-salt approach, allowing, by two different techniques, a valuable systematic check of important physics results. The duty factor for full-efficiency NC detection rises from 50 to 100%, and the possibility of missing NC data from a supernova or other interesting event is correspondingly diminished. Even if salt is present in the water, the conversion of NC events to Čerenkov light makes inferences about which events are CC and which NC indirect. Event-by-event NC detection offers the prospect of determining a ν_μ or ν_τ mass (especially in the cosmologically interesting range of 20-100 eV) if a supernova should occur.

We are collaborating with scientists at Los Alamos National Laboratory and Lawrence Berkeley Laboratory to design, fabricate, and deploy this array of ^{3}He proportional counters. The key issue in building such an array is to select materials that will minimize the amount of radioactive U and Th chain elements. A special chemical vapor deposition (CVD) process to produce ultra-pure nickel has been found that meets these requirements. The research and design phase is nearly complete and preparations are underway for full scale construction of the array.

2.5 SNO neutral-current detector position readout

J.V. Germani, S. Konsek,* R.G.H. Robertson, A. Myers and T. Van Wechel

Development is underway to permit modest, ~1 meter resolution, position readout of the ^{3}He filled proportional counter detector strings that will be used as neutral-current detectors in the SNO experiment. Position readout along the length of the proportional counters is desirable for several reasons. The identification of backgrounds internal to the counters, as well as localized concentrations of Th or U in either the counters or the acrylic vessel, will be easier to identify with position information. Furthermore, the ability to construct spherical radial distributions of neutron events will improve our ability to identify, and correct for, backgrounds from Th and U uniformly distributed in the acrylic vessel.

Single-ended readout of the detectors is highly desirable in order to minimize the amount of material in the heavy water and to keep the mechanical design and string deployment as simple as possible. The method presently under development relies on leaving the remote end of the counter unterminated. The pulse that propagates toward the remote end is reflected back with the same sign and adds with the pulse that heads directly to the preamp. The maximum delay time between the leading edge of the direct and reflected pulses is approximately 100 ns for an 11 m string of counters. A delay line of approximately 25 ns will be used at the remote end to define the minimum time delay for pulses originating close to that end. Thus, the time delays will range from 50 to 150 ns. Since the widths of current pulses range from 20 ns to 4 ms, the position signal in the combined pulse shape will vary from a double-peaked shape to a kink in the leading edge.

We have set up a facility at NPL for studying position readout techniques and pulse propagation in the detector strings. A two-meter proportional counter is used to approximate one segment of a neutral-current string. This counter is coupled to six meters of transmission line, which simulates other counters in the string. The low-noise current preamplifier is a custom Robertson design that is built by the laboratory's electronics staff. Pulse shapes are digitized with a digital oscilloscope with sample rates as high as 1 GS/s, and are then analyzed off-line for pulse reflections. In addition, the affect of log amplification is being studied, as a means of begin able to cope with the large dynamic range required to digitize current pulses.

Initial results show that position resolution of 1 meter is possible. This is consistent with the requirements of the neutral-current array, since the neutrons liberated in neutral-current interactions travel one meter on average before being absorbed by a proportional counter. Further measurements are planned with the present apparatus. Several digital signal processing techniques are being studied for the extraction of position information, and improvements in preamplifiers and log amplifiers are ongoing.

*Department of Physics, University of Washington, Seattle, WA.

2.6 SNO DAQ: Development of a 100 channel noise test system

Q.R. Ahmad, J. Beck, S.R. Elliott and J.F. Wilkerson

The SNO data acquisition (DAQ) system will acquire data on an event-by-event basis from the 9500 PMTs that comprise the SNO detector. An integral part of this system is the Front End Card (FEC). It will provide dead timeless sub-nanosecond time and charge (Q&T) measurement for photomultiplier pulses in the range of 1 - 1000 photoelectrons. The FEC will handle 32 PMT signals per 9U x 280 or 340 mm card. The electronics is implemented using three full custom integrated circuits as well as commercial ADCs, memory and logic. The DAQ interface is VME compatible.

In close collaboration with the University of Pennsylvania SNO group we are finishing up tests of the prototype FECs (pFECs) which consist of 8 instead of the final 32 channels per board. Results from these tests are providing valuable information as we finalize the design of the Front End Cards. The mass production of custom chips and boards will start before the end of 1995.

We are developing a 100 channel PMT noise test data acquisition system using the pFEC boards and a single VME crate that will be used to perform noise test of the PMTs and cables as they are installed in the upper hemisphere of our underground detector in Sudbury.

We are developing the software to perform this task under the Object Oriented Progamming (OOP) environment of Macintosh's Think C compiler using a realtime data acquisition OOP code developed by McGirt and Wilkerson at Los Alamos. This task can serve as a quick and simple DAQ/Electronics diagnostic. The task will first initialize all channels and then calculate the noise rate as the voltage is ramped to the PMT's operating voltage. During the course of the test it will provide the user with a real-time histogram of noise rate per channel. Drastic deviation from the norm would be indicative of tube or cable problems. The noise data will also be written to disk so that one can later look at the time history of the noise for each individual PMT.

Furthermore, we are developing the necessary software to look at the Charge and Time (Q&T) information for each channel which we can compare to the acceptance testing Q&T database provided by Queen's University.

2.7 The SNO PMT test facility

Q.R. Ahmad, J. Beck, A. Goldberg, K.P. Issacson, J.Knox, A.W.P. Poon, W.G. Weitkamp and J.F. Wilkerson

The SNO Data Acquisition group has been developing a PMT test facility that will utilize 96-120 SNO PMTs (including reflectors) to perform the following series of tests (in order of priority):

Test and debug the SNO electronics and data acquisition (DAQ) systems with a reasonable number of PMTs.

Develop and test calibration sources.

Determine calibration constants, attenuation coefficients, and possibly even total efficiency of PMTs and reflectors.

The initial tests of the electronics and DAQ systems can be done in air, but a series of more sophisticated tests to check out calibration constants and more realistically simulate the SNO detector must be done in water. The second and third items also require that the PMTs be immersed in water.

The original plan for a PMT test facility was to share space in the neutral current detector test pool at Los Alamos. However, when the SNO data acquisition development effort moved to the University of Washington, it quickly became clear that the water shield room of the old 60-inch cyclotron could be made into a suitable test facility. The room is 14 feet wide by 20 feet long and can be filled to a depth of 14 feet. It was originally designed to shield the cyclotron scattering chamber from neutrons coming directly from the cyclotron. The room is accessible through a 20 in high x 28 in wide port located 56 in above the floor.

The room has several advantages as a test facility: it is not used now (the cyclotron has been turned off since 1986), it has held water in the past, it is easier to install detectors inside provided they fit through the port, and it can be overhauled to make a suitable test volume with relatively modest amount of work. The adjacent experimental cave also offers a reasonable laboratory space to set up the SNO electronics and data acquisition systems.

The first question was whether gamma ray background levels might not be too high for the tests in question. A 5" diameter x 4" NaI detector was set up to measure the radioactive background inside the water room. It was found that the backgrounds in the water room are similar to the ambient backgrounds in the adjacent laboratory and are dominated by low energy ^{40}K decays. At this point the dominant background to the test array is expected to be from cosmic rays.

The next problem to be addressed was conversion of the water room into a suitable SNO PMT test facility. An aluminum duct which traversed the room was removed. Access holes near the ceiling for cables running to the test detectors have been cut and plugs for all the ports in the walls have been fabricated. A contractor will complete resealing the room in the near future.

We have been working with collaborators at Lawrence Berkeley Laboratory to design the optimized PMT support structure that will fit within the room. The current design has a spherical geometry and can accommodate from 96-120 PMTs. Installation of the support structure should commence after initial wet tests of the water room are completed.

2.8 Acrylic vessel activities 1994-1995

P. Doe

The principal activity on the acrylic vessel over the past year has been the fabrication of the individual components from which the vessel is constructed.

The spherical shell of the acrylic vessel is constructed by bonding together 120 panels in the underground laboratory. These panels are first thermoformed from flat sheet into spherical shapes, machined to exact dimensions and then annealed to relieve machining stress. Careful monitoring is required throughout this fabrication process to ensure that the components are radioactively and mechanically acceptable.

80% of the panels required to form the sphere have been completed. To ensure that the machined panels were of the correct dimensions, the whole upper hemisphere of the vessel was dry assembled at the fabricator's facility in Colorado. This also allowed testing of the final assembly jigs, fixtures and survey technique and refining of assembly procedures. After dry assembly the individual panels are being cleaned, packed and shipped to the SNO site. The five cylindrical castings that comprise the vessel chimney have also been fabricated, machined and shipped to the SNO site.

A second "qualification wall", measuring 20' long by 15' high and consisting of 8 spherically formed panels has been successfully completed by the fabricator, thus completing the demonstration of the bonding techniques required in the vessel assembly and for the attachment anchor points for the neutral current detectors.

The acquisition of the 10 Kevlar@ suspension ropes has begun following successful completion of the selection, R&D and radioassay program established and overseen by LANL.

The coming year will be a challenging one. Installation of the vessel chimney begins in early June '95 followed by the upper hemisphere in August '95. The suspension ropes will be required in October '95. Once the upper hemisphere is suspended, the lower hemisphere along with the neutral current detector anchors will be installed. The vessel is expected to be complete in May 1996. Ways of improving the schedule are being investigated.

2.9 The Russian-American Gallium Experiment (SAGE)

S.R. Elliott and J.F. Wilkerson

The Russian-American Gallium Experiment (SAGE) is a radiochemical solar neutrino flux measurement based on the inverse beta decay reaction $^{71}Ga(\upsilon_e, e^-)^{71}Ge$. The threshold for this reaction is 233 keV which permits sensitivity to the p-p neutrinos which dominate the solar neutrino flux. The target for the reaction is in the form of 55 tonnes of liquid gallium metal stored deep underground at the Baksan Neutrino Observatory in the Caucasus Mountains in Russia. About once a month, the neutrino-produced Ge is extracted from the Ga. ^{71}Ge is unstable with respect to electron capture ($t^{1/2}$ = 11.43 days) and, therefore, the amount of extracted Ge can be determined from its activity as measured in small proportional counters. The experiment has measured the solar neutrino flux in 31 extractions between January 1990 and October 1993 with the result; 69±10 (statistical) +5/-7 (systematic) SNU. Additional extractions through the end of 1994 are awaiting analysis.

The collaboration is currently using a 500-kCi ^{51}Cr neutrino source to test the experimental operation. The energy of these neutrinos is similar to the solar ^{7}Be neutrinos and the source thus makes an ideal check on the experimental procedure. The extractions for the Cr experiment took place in January and February of 1995 and the counting of the samples will continue through the summer. The University of Washington plays a major role in the statistical analysis of the data and in the determination of systematic uncertainties. We are very active in the planning and analysis of the Cr experiment data.

3.0 NUCLEUS-NUCLEUS REACTIONS

3.1 Distributions of fusion barriers extracted from cross section measurements on the systems $^{40}Ca + ^{192}Os, ^{194}Pt$

J.D. Bierman, P. Chan, J.F. Liang, M.P. Kelly, A.A. Sonzogni and R. Vandenbosch

As described in last year's report,[1] the goal of this project is to experimentally determine the fusion cross sections of the two systems to high precision spanning the entire barrier region. These data may then be twice differentiated to yield the distribution of barriers. These distributions should differ as a result of the difference in permanent quadrupole deformations of the targets. This will be a valuable test of the sensitivity of the barrier distribution or "fingerprint" method of determining the relative importance of different coupling channels.

We have measured fission fragment angular distributions at energies both well above and within the barrier region. The differences in these distributions were very small. More importantly, the center of mass angle where the angular distribution intersects a properly normalized isotropic distribution is constant over the entire energy region. As a result, rather than measure the entire distribution at each energy, we simply measure the differential cross section at this angle for each energy and then convert this measurement to a total fusion cross section as if the distribution were isotropic. This allows us to acquire data of sufficiently high statistics spanning the entire barrier region in fairly small energy steps in a reasonable amount of beam time.

To this point, fusion cross sections have been measured for the $^{40}Ca + ^{192}Os$ system in roughly 1.25 MeV energy steps covering the entire barrier region. The measured cross sections range from 400 mb down to 0.1 mb. Measurements were also made at energies well above the barrier for this system. Analysis of these data is nearly complete. The product of energy and cross section has been differentiated to extract the distribution of barriers for the osmium system which is shown in Fig. 3.1-1. This "fingerprint" is similar to that expected for a spherical projectile and a target with a prolate quadrupole and small negative hexadecapole deformation. Data have also recently been taken for the $^{40}Ca + ^{194}Pt$ system in roughly 1.25 MeV energy steps spanning its barrier region. The analysis of these data is currently being performed.

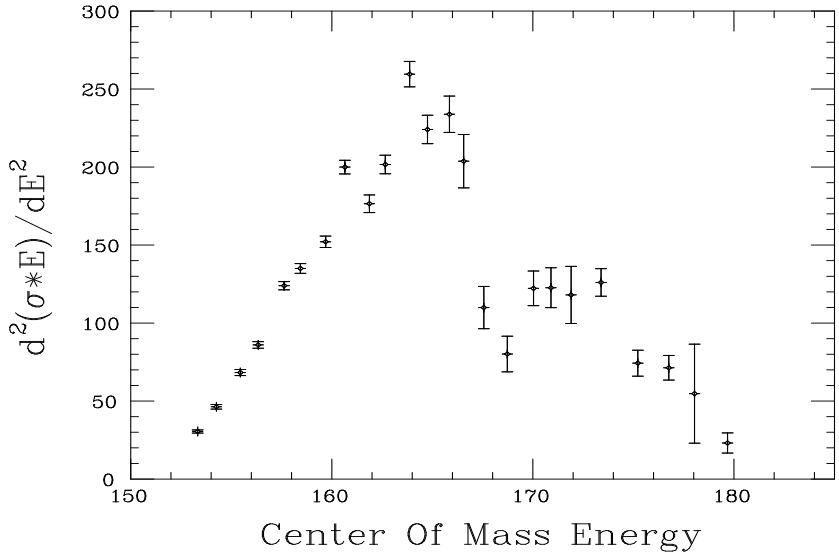

Fig. 3.1-1. Fusion barrier distribution extracted from experimentally measured cross sections for $^{40}Ca + ^{192}Os$.

[1]Nuclear Physics Laboratory Annual Report, University of Washington (1994) p. 10.

3.2 Sub-barrier fusion for $^{40}Ca + ^{46,48,50}Ti$

J.D. Bierman, P. Chan, J.F. Liang, A.A. Sonzogni and R. Vandenbosch

Several mechanisms have been used to explain the observed enhancement in the sub-barrier fusion cross section, among them nuclear deformation, coupling to inelastic channels and transfer reactions. The $^{46,48,50}Ti$ isotopes exhibit a decrease in β_2 with increasing mass number and simultaneously the neutron transfer Q-values become more positive, which implies that collective motion should counteract transfer reactions as responsible for the enhancement. A measurement of the enhancement for the three isotopes should indicate which process is stronger. The projectile was the doubly magic ^{40}Ca to minimize projectile structure effects.

Details of the experiment can be found in a previous report.[1] Briefly, evaporation residue angular distributions were taken at a selected set of energies and integrated over angles. From these complete angular distributions we calibrated the relation between the differential cross section at 5 degrees and the integrated one. For a far larger set of energies, the differential cross section at 5 degrees was measured and the integrated one was then obtained. Results for ^{46}Ti are presented in Fig. 3.2-1. The full line is from a coupled channel calculation, which includes inelastic and transfer couplings. For the inelastic part we considered the 2^+ and 3+ states for both projectile and target with strengths taken from the literature. The pickup of 1 and 2 neutrons was considered for the transfer part and their coupling strengths were adjusted to match the data. The dashed line is from an uncoupled calculation.

A preliminary analysis suggests that for these systems, neutron transfer reactions are playing the most important role in the sub-barrier enhancement of the fusion cross section. A future experiment is being planned, where we will extend and improve the data already taken.

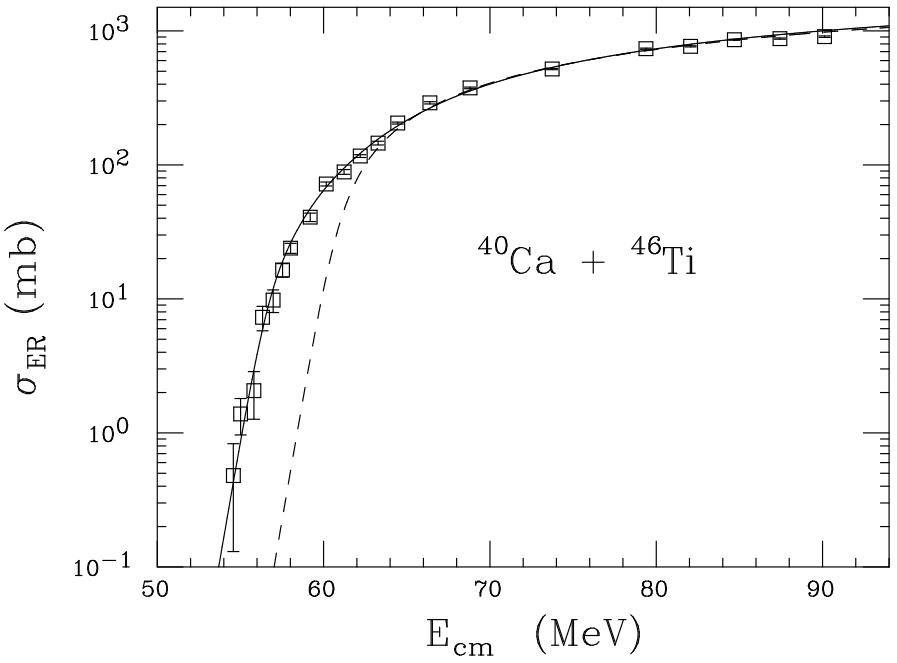

Fig. 3.2-1. Fusion excitation function for $^{40}Ca + ^{46}Ti$.

[1] Nuclear Physics Annual Report, University of Washington (1994) p. 11.

3.3 Properties of light charged particles produced by 25 A MeV ^{16}O on $^{159}_{65}$Tb, $^{181}_{73}$Ta, $^{197}_{79}$Au and 35 A MeV ^{14}N on $^{nat}_{62}$Sm, $^{181}_{72}$Ta

D. Bowman,* G. Cren,* R. DeSouza,† J. Dinius,* A. Elmaanni,‡ D. Fox,† C. K. Gelbke,* W. Hsi,* C. Hyde-Wright,§ W. Jiang, W. G. Lynch,* T. Moore,† G. Peaslee,* D. Prindle, C. Schwarz,* A. A. Sonzogni, M. B. Tsang,* R. Vandenbosch and C. Williams*

In last year's Annual Report we reported on our analysis[1] of an experiment performed at the National Superconducting Cyclotron Laboratory at Michigan State University using the miniball array.[2] In this experiment we measured light charged particles (LCPs) in coincidence with fission fragments (FF tag) or evaporation residues (ER tag). The ER tagged events were from more central collisions than the FF tagged events and by varying the target mass we change the average impact parameter over a large range while changing the total fusion cross section only slightly.[3] In last years report we stated that we observed a substantial variation in the LCP multiplicity depending on the tag. For every target the observed LCP multiplicity is higher for the ER tag than it is for the FF tag. We show the characteristics of these "extra" LCPs by plotting in Fig. 3.3-1 the number of observed protons as a function of energy for 10,000 ER and 10,000 FF tagged events from the 25 A-MeV ^{16}O on $^{181}_{73}$Ta. At high energies the spectra are essentially identical. For lower, evaporative energies, there is a clear excess of protons. This excess is clearly observed for protons and alphas from all targets and beam energies used in this experiment with the exception of the 35 A-MeV ^{14}N beam on the $^{nat}_{62}$Sm target which has a very low ER cross section. The excess is also observed but not as pronounced for deuterium and tritium emission.

It seems clear that the fission process must occur before the compound nucleus reaches the end of the particle emission de-excitation chain. We should be able to use the number of LCPs emitted after the time at which fission occurs to estimate how quickly fission must occur. We plan to pursue this through the use of statistical model calculations.

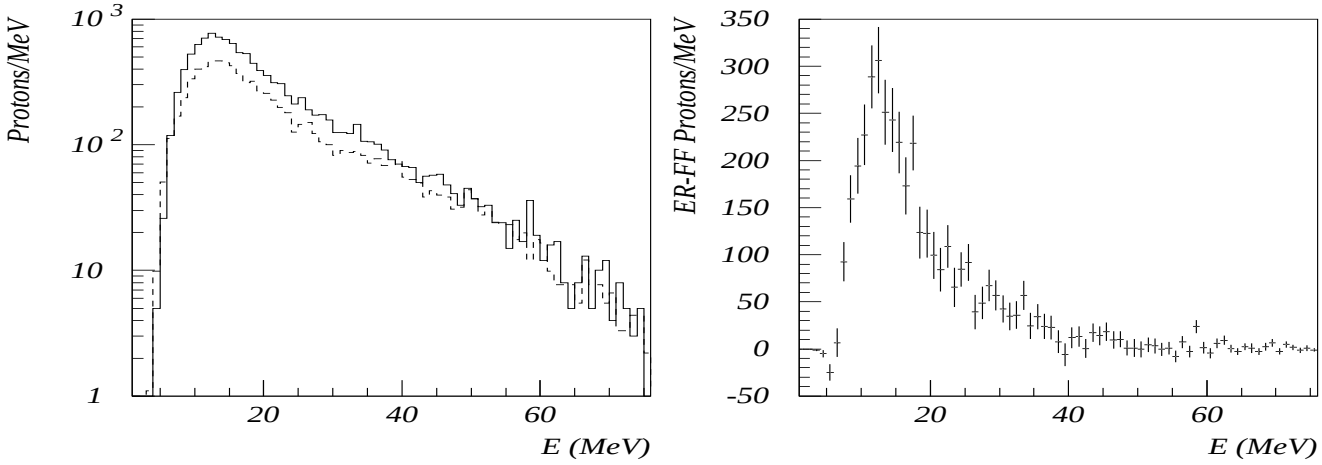

Fig. 3.3-1. Number of protons as a function of energy for 25 A-MeV ^{16}O on $^{181}_{73}$Ta data. The solid line is ER tagged data and the dashed line is FF tagged data. In the panel on the right we show the difference of the histograms.

*National Superconducting Cyclotron Laboratory, Michigan State University, East Lansing, MI.
†Indiana University Cyclotron Facility, Indiana University, Bloomington IN.
‡Present Address: Battelle Memorial Institute, Columbus, OH.
§Department of Physics, Old Dominion University, Norfolk VA.

[1]Nuclear Physics Laboratory Annual Report, University of Washington (1994) p. 14.
[2]R. DeSouza *et al.*, Nucl. Instrum. Methods A, **295**, 109 (1990).
[3]D. Prindle *et al.*, Phys. Rev. C **48**, 192 (1993).

3.4 Entrance channel dependence of light particle emissions in the ^{156}Er compound nucleus decay

J.D. Bierman, P. Chan, M.P. Kelly, J.F. Liang, A.A. Sonzogni and R. Vandenbosch

The decay of a compound nucleus can be described by a statistical theory where the decay processes are assumed to be independent of the formation channels.[1] Measurements on the decay of the ^{156}Er compound nucleus populated by ^{12}C + ^{144}Sm and ^{64}Ni + ^{92}Zr entrance channels gave mixed results as compared to the statistical model.[2] The ^{12}C + ^{144}Sm data were in good agreement with statistical model calculations. However, the statistical model overestimated the neutron multiplicity for the ^{64}Ni + ^{92}Zr reaction over a wide range of excitation energies.[3]

A program of studying the light-charged particles emitted from the ^{156}Er compound nucleus was initiated recently. The ^{156}Er compound nucleus was populated by ^{12}C + ^{144}Sm and ^{60}Ni + ^{96}Zr reactions at an excitation energy of 113 MeV where the fission barrier falls below the neutron binding energy and the maximum angular momentum, in the spin distribution, leading to evaporation residues is reached. The experiment was carried out in the Nuclear Physics Lab of the University of Washington. The angular distributions of light-charged particles were measured in coincidence with the evaporation residues by CsI scintillators coupled to PIN diodes. The evaporation residues were separated from the incident beam by a pair of electrostatic deflector plates and identified by energy vs. time-of-flight using the linac rf signal as stop.

The evaporated proton and α particle energy spectra are shown in Fig. 3.4-1 for the two reactions studied. The spectral shape of the C+Sm system is harder than that of the Ni+Zr system. It suggests that the protons and α particles were emitted from a hotter source for the mass asymmetric system. The result of statistical model calculations using the code PACE[4] are shown by solid curves. The level density parameter used in the calculations was A/10 for both systems. Good agreement between the data and the calculations can be seen for the ^{12}C induced reaction. For the Ni+Zr reaction, the calculation predicts a less steep slope than the measurement. More analyses comparing the entrance channel dependence of the ^{156}Er compound nucleus decay is underway.

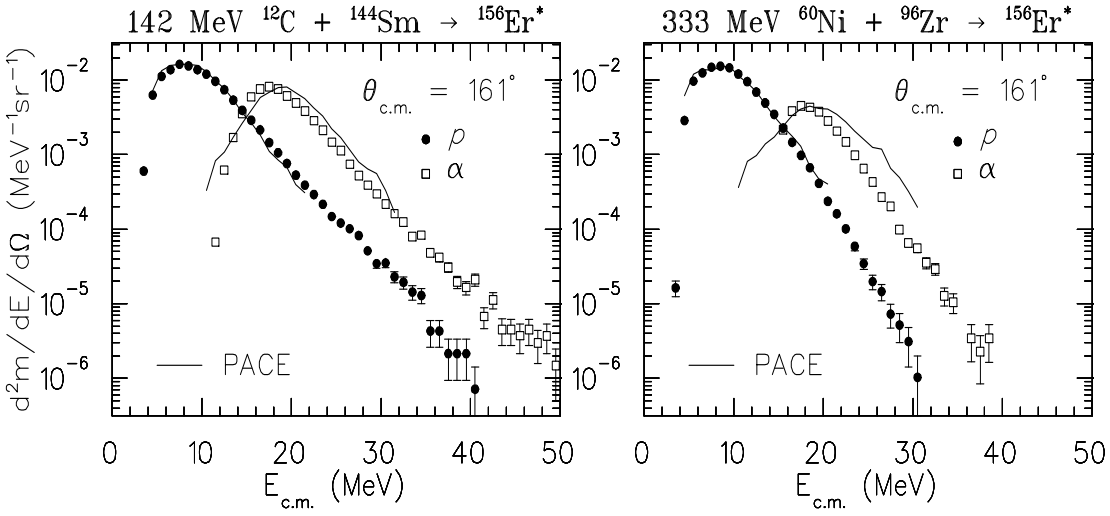

Fig. 3.4-1. Energy spectra of protons and α particles emitted from the decay of the ^{156}Er compound nucleus.

[1] N. Bohr, Nature (London) **137**, 344 (1936).
[2] B. Fornal *et al.*, Phys. Rev. C **42**, 1472 (1990).
[3] R.V.F. Janssens *et al.*, Phys. Lett. B **181**, 16 (1986).
[4] A. Gavron, Phys. Rev. C **20**, 230 (1980).

3.5 Bremsstrahlung and the GDR in $^{16,18}O + ^{92,100}Mo$ reactions

J.D. Bierman, M.P. Kelly, J.F. Liang and K.A. Snover

Recent measurements on C+Mo[1] and C+Sn[2] systems in the region 5-11 MeV/u bombarding energy have suggested a large target isotope effect on the production of high energy $\gamma-$rays ($E_\gamma \geq 30$ MeV). These $\gamma-$rays were presumed to be bremsstrahlung primarily from first chance neutron-proton collisions. Another measurement,[3] on the C+Sn system at 10 MeV/u bombarding energy finds, in conflict with the earlier measurements, no evidence for an enhanced bremsstrahlung yield when using the heavier target isotope. More recently, the Stony Brook group has presented results backing up earlier findings on the same system together with an explanation of the isotopic effect.[4] In this report, we present progress in the search for a similar effect in O+Mo systems. An important part of our procedure is the use of angular distributions to better define the relative contributions of bremsstrahlung and statistical decay.

We have measured the $\gamma-$rays produced in the four possible reactions of $^{16,18}O + ^{92,100}Mo$ using the Seattle 10" x 15" NaI spectrometer. The incident energy for both $^{16,18}O$ projectiles is 9.4 MeV/u. Gamma ray yields were measured at five angles between 40° and 140° in the lab frame relative to the beam axis. These $\gamma-$rays cross sections were transformed to the compound nucleus center-of-mass and fit to a linear combination of the first three Legendre polynomials. The coefficient of the first polynomial, $A_0(E_\gamma)$, is a measure of the $\gamma-$ray cross section, $\sigma(E_\gamma)$. The second coefficient, $a_1(E_\gamma)$, is a measure of the forward-backward anisotropy relative to the compound nucleus center-of-mass.

Fig. 3.5-1. shows the extracted $A_0(E_\gamma)$ and $a_1(E_\gamma)$ for the inclusive $^{18}O + ^{92}Mo$ data. In the left panel, a bremsstrahlung component (solid line) has been determined by manual iteration of the strength and slope parameters. The dashed line in the right panel shows the a_1 that results from this bremsstrahlung component alone. The bremsstrahlung component will always have a positive a_1 (for $A_{tgt} > A_{proj}$) since the nucleon-nucleon center-of-mass moves at half the beam velocity while the compound nucleus center-of-mass moves more slowly. In the region where GDR emission competes significantly with bremsstrahlung ($E_\gamma \leq 30$ MeV) the A_0 bremsstrahlung component of course falls below the data points. Since GDR emission has no forward-backward anisotropy in the compound nucleus center-of-mass, its effect is to dilute the a_1. Hence the data points in the right panel fall below the dashed curve. The bremsstrahlung a_1 diluted by the contribution of statistical $\gamma-$rays (solid line, right panel) follows the data reasonably well. Observed nonzero values of a_1 below approximately 16 MeV are due to some other reaction mechanism. The use of a multiplicity gate on the gamma spectrum has been shown to greatly reduce the nonzero a_1 at low E_γ, but has little effect on the region $E_\gamma \geq 20$ MeV other than to worsen the statistical errors.[5]

Efforts are underway using the CASCADE statistical model code to do a simultaneous fit of statistical and bremsstrahlung components to both the $A_0(E_\gamma)$ and the $a_1(E_\gamma)$ spectra.

---

[1]C.A. Gossett *et al*., Phys. Rev. C **42**, R1800 (1990).
[2]Vojtech *et al*., Phys. Rev. C **40**, R2441 (1989).
[3]R. Pfaff *et al*., Z. Phys. A **347**, 67-70 (1993).
[4]N. Gan *et al*., Phys. Rev. C **49**, 298-303 (1994).
[5]Nuclear Physics Laboratory Annual Report, University of Washington (1994) p. 8.

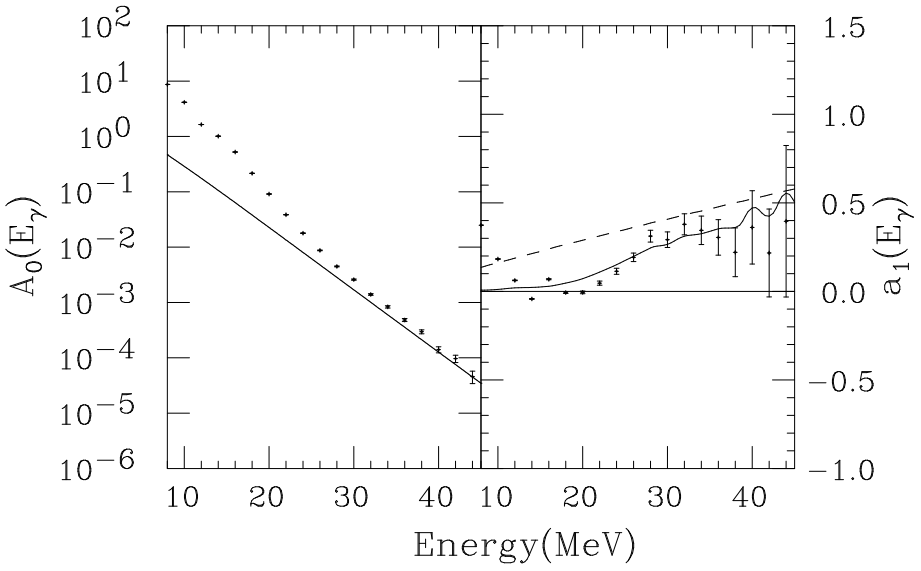

Fig. 3.5-1. The points are the inclusive data for $^{18}O + ^{92}Mo$ at 9.4 MeV/u bombarding energy and the curves are the calculated bremsstrahlung component. The dashed line in the right panel is the a_1 that results from the bremsstrahlung component alone, as shown by the solid line in the left panel. The solid line in the right panel is the bremsstrahlung a_1 diluted by the statistical $\gamma-$rays contribution.

3.6 APEX update

T.A. Trainor and the APEX collaboration

During the past year the full APEX detector system has accumulated several million positrons resulting from several-pnA beams of ≈6 MeV/u uranium projectiles incident on several targets. Under no conditions have narrow peaks in positron-electron coincidence or positron singles energy spectra been observed (except for the ^{206}Pb results described below). This overall result now constitutes a major disagreement with the results of several collaborations at the GSI in Darmstadt, Germany.

APEX was designed to investigate in a kinematically complete way the production mechanism for reported anomalous electron pairs in several very-heavy-ion collision systems. The initial null results from APEX reported last year prompted an extensive study by Monte Carlo techniques of the detailed acceptance of APEX, especially as compared to the GSI experiments. This study has revealed no fundamental reason for a failure to observe anomalous pairs from an acceptance standpoint.

More recently two collision systems have been used both to calibrate the APEX ability to detect such pairs and to examine the 'best case' GSI result. For the former the collision system ^{206}Pb- ^{206}Pb was used to produce pairs from internal conversion of a $3^- \rightarrow 2^+$ transition. These pairs have been seen as a narrow peak in the coincidence spectrum. The detailed peak shape is now being compared with Monte Carlo studies to further elucidate the APEX acceptance.

In an attempt to examine the best-case GSI result (narrow peaks in positron singles spectra where the question of acceptance is much simpler) data were acquired for the uranium-thorium system. A total of 37,000 positrons was detected, 200 times that for the original GSI (EPOS) result and 20 times that for a more recent EPOS result. After a preliminary analysis no peak structures have been observed outside statistical fluctuations.

In light of these results the reality of the electron-pair phenomenon as reported by GSI is called into question. Further analysis of the APEX data and data acquisition are planned for the coming year.

4.0 FUNDAMENTAL SYMMETRIES AND WEAK INTERACTIONS

4.1 CVC and SCC in the mass-8 isotriplet

L. De Braeckeleer, E.G. Adelberger, K.A. Snover, D.W. Storm and D. Wright

The conserved vector current (CVC) hypothesis predicts the existence of a small weak magnetism correction to the β-decays of ^{8}Li and ^{8}B related to the isovector M1 and E2 decay strengths of the isospin analogue state in ^{8}Be. By measuring the difference in $\alpha-\beta$ angular correlations in the decays of these two nuclei,[1] we may extract the quantity $b/AC + d_{II}/Ac$, where b is determined by the M1 decay amplitude, c the GT decay amplitude, the first term is the CVC-predicted weak magnetism correction, and the second term represents second class current (SCC) contributions.

In previous experiments in this laboratory,[2] we have measured the GT strength of ^{8}Li and ^{8}B decay, as well as the isovector M1 strength of the decay of the isospin analogue doublet in ^{8}Be, to excited ^{8}Be. We have combined these measurements to produce a CVC prediction for the weak magnetism term, and compared this prediction to the $\alpha-\beta$ correlation data of both Tribble and Garvey[3] and McKeown, Garvey, and Gagliardi.[4] The CVC prediction and the two data sets are shown in Fig. 4.1-1. If we assume CVC to be correct, we may allow for the possibility of an SCC contribution by fitting the difference between our prediction and the data. We obtain d_{II}/Ac=0.0$\pm$0.3$\pm$0.3 from Tribble and Garvey's data, and d_{II}/Ac=-0.5$\pm$0.2$\pm$0.3 from the data of McKeown, Garvey, and Gagliardi. The first error bar quoted represents the uncertainty in the $\alpha-\beta$ correlation data, the second the uncertainty of our CVC prediction. If, on the other hand, we assume the absence of SCC, we may test the validity of CVC by comparing our prediction directly to the data. If we call the multiplicative difference between our prediction and the data κ, we obtain κ=1.00$\pm$0.04$\pm$0.05 for Tribble and Garvey's data, and κ = 0.93 $\pm$0.03$\pm$0.05 for the data for McKeown, Garvey, and Gagliardi. We thus conclude that present experimental data are consistent with both CVC and the absence of SCC.[5]

Uncertainties in the measured isovector gamma decay strength give a significant contribution to the uncertainty in the CVC prediction of the weak magnetism term. We are therefore planning improved measurements of both the total strength and its distribution to various excitation energies of ^{8}Be. To this end, we have carried out a careful investigation of the sources of background in the ^{4}He(α,γ) experiment used to measure the gamma decay strength.

Although difficulties in obtaining a correct normalization make it unattractive for a measurement of the total strength, the use of a long (~40cm) gas cell target which allows the center of the cell to be viewed by a detector while its Kapton windows are shielded by lead, eliminates an important source of γ-ray background and is therefore preferable for a measurement of the decay strength distribution. The remaining background may be attributed to γ-rays and neutrons produced when beam particles scattered by the windows or the target gas interact with the walls of the cell. By subtracting the γ-ray spectrum observed with the cell empty from the spectrum observed with a He-filled cell, we can compensate for the background produced by beam scattered from the cell windows, but not for background produced by beam scattered from the target gas. Crude estimates of the magnitudes of each of these backgrounds are consistent with experimentally observed spectra before and after subtraction.

---

[1] Nuclear Physics Laboratory Annual Report, University of Washington (1994) p. 19.
[2] Nuclear Physics Laboratory Annual Report, University of Washington (1994) pp. 20-21.
[3] R.E. Tribble and G.T. Garvey, Phys. Rev. C **12**, 967 (1975).
[4] R.D. McKeown, G.T. Garvey and C.A. Gagliardi, Phys. Rev. C **22**, 738 (1980).
[5] L. De Braeckeleer *et al*., Phys Rev C, in press.

The remaining background after subtraction is unfortunately still comparable to the signal for γ -ray energies below ~8 MeV. To reduce this background, we have designed a new gas cell with a geometry chosen so that no α particle singly scattered by the target gas hits the cell wall in a region visible to our detector with an energy of more than ~20 MeV. We plan to line these portions of the gas cell wall with Tantalum metal, whose Coulomb barrier will greatly inhibit background-producing interactions.

The new cell will be used in a precision measurement of the gamma decay strength distribution.

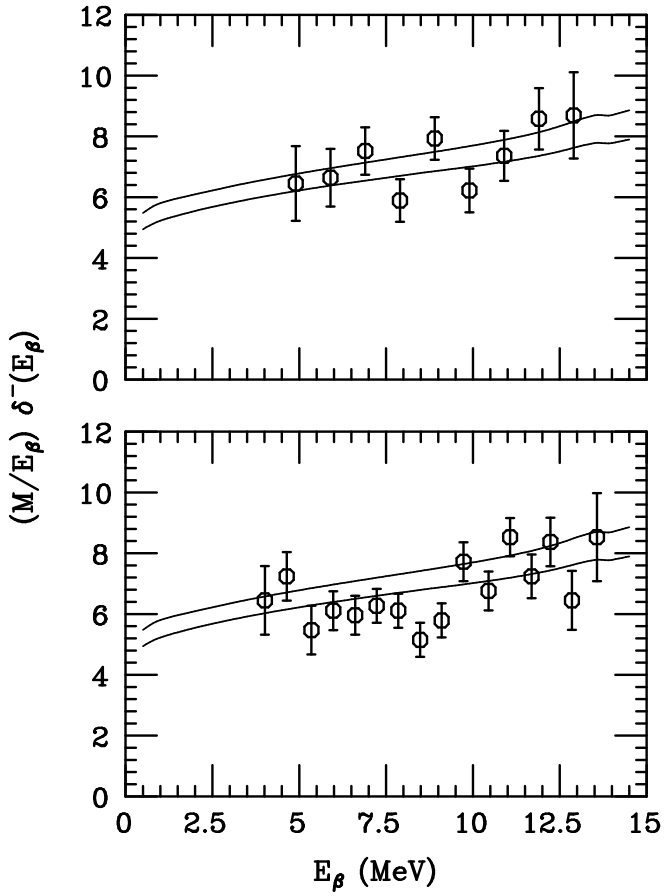

Fig. 4.1-1. The panels compare the $\pm 1\sigma$ CVC prediction (assuming no SCC), shown as a solid curve, to the data points of Tribble and Garvey (upper panel) and McKeown, Garvey, and Gagliardi (lower panel).

4.2 Measurement of the $\beta-\alpha$ angular correlation in mass-8

E.G. Adelberger, J.F. Amsbaugh, P. Chan, L. De Braeckeleer, P.V. Magnus, D.M. Markoff, D.W. Storm, H.E. Swanson, K.B. Swartz, D. Wright and Z. Zhao

Among the measurements needed to test CVC and/or search for second class current in the Mass-8 isotriplet, the measurements of the $\beta-\alpha$ angular correlations in ^{8}Li and ^{8}B are the most difficult to achieve with high accuracy. Both the weak magnetism and the weak electricity induced currents are proportional to the momentum transferred in the decay and therefore contribute to the observables at the percent level. The accuracy of these measurements determines the ultimate sensitivity of the symmetry tests. In particular, the β energy dependence of the a_2 term in the $\beta-\alpha$ angular correlation is presently quite uncertain. The two previous experiments[1,2] support a large quadratic term, a fact not compatible with CVC and our recent measurement of the E2/M1 ratio, (see Section 4.1). Our apparatus has been designed with particular attention to the response function of the beta counters (delta E, active veto and stabilization). The data accumulated in August (1 week) and November 93 (3 weeks) have been analyzed. The $\beta-\alpha$ angular correlation measured in ^{8}Li is fitted by $1 + a_1 \cos(\theta) + a_2 \cos^2(\theta)$; the a_1 and a_2 coefficients are shown in Figs. 4.2-1 and 4.2-2. The kinematical term a_1 shows a little deviation from the expected value at high energy. We are currently investigating the origin of this systematic effect. The a_2 coefficient does not have a significant quadratic energy dependence. Two additional β counters have been built and set up at 0 and 180 degrees. This has required a modification of both the alpha counters and the hardware/software of the acquisition and stabilization system. We are now in the process of testing this new apparatus. We will also spend a couple of weeks adding to the existing statistics of the ^{8}Li experiment. Finally, the ^{8}B run is awaiting the completion of the high intensity ^{3}He terminal ion source.

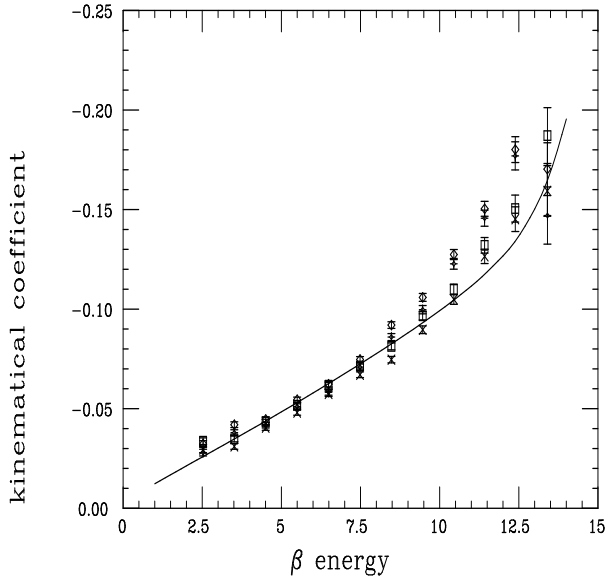

Fig. 4.2-1. The kinematical coefficient a_1 measured in the ^{8}Li decay.

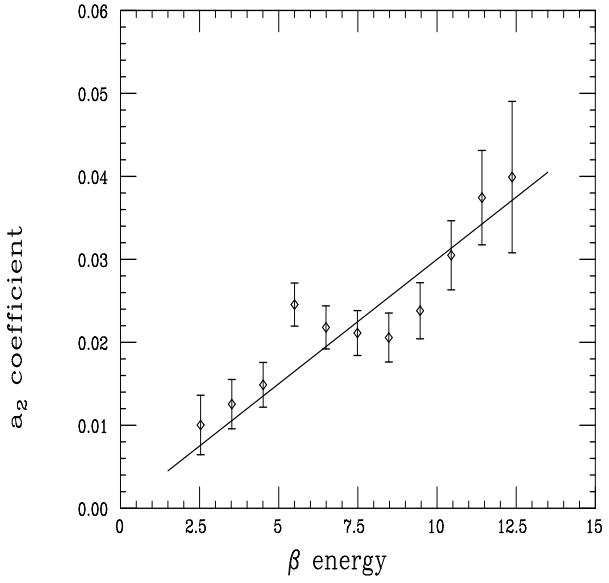

Fig. 4.2-2. The a_2 coefficient measured in the ^{8}Li decay.

[1]Tribble *et al.*, Phys. Rev. C **12**, 967 (1975).
[2]McKeown *et al.*, Phys. Rev. C **22**, 738 (1980).

4.3 Completion of an apparatus to measure the PNC spin rotation of cold neutrons in a liquid helium target

E.G. Adelberger, B.R. Heckel, D.M. Markoff, S.D. Penn and H.E. Swanson

The apparatus to measure the parity non-conserving (PNC) spin-rotation of transversely polarized neutrons through a liquid helium target is nearly complete. This apparatus is designed to measure a neutron spin-rotation predicted to lie between 0 and 5×10^{-7} radians[1,2] in 46 cm of helium with an error of 5×10^{-8} radians. This observable, in conjunction with $A_L(\vec{p} + \alpha)$,[3] will determine the PNC isovector pion-exchange amplitude of the NN interaction, F_π. This amplitude is sensitive to the neutral weak current contribution. Current experimental results provide upper limits for F_π that are smaller, by a factor of three, than the early theoretical calculations.[4] Recent QCD sum-rule calculations[5,6] predict a smaller value for F_π that is consistent with existing data, and an expected rotation of 2×10^{-7} radians in our targets. Our experiment is motivated by the need for a more precise measurement of F_π.

The two coaxial μ-metal shields have been constructed and tested. With the cryostat in place, we measured axial magnetic fields of 15-20 μG in the center region, rising to approximately 40 μG on the ends. This is comfortably below the maximum tolerable field of 100 μG, set by the requirement that spin-rotations arising from diamagnetic effects of helium will be within our desired errors.

The cryostat insert housing the liquid helium targets, the π-coil, and the pump and valve system that fill and empty the target chambers has been built. The feedthrough system which will drive the pump and valve will be completed shortly.

The neutron detector, a segmented ^{3}He ionization chamber, is currently under construction. It is designed so that neutrons of different velocity ranges can be detected separately. The PNC effect is velocity independent, while spin-rotations from magnetic fields are velocity dependent. Velocity separated detection will allow us to monitor the integrated magnetic fields along the neutron path. In addition, the detector signal plates are divided into four quadrants that will allow us to monitor false signals from geometric asymmetries.

The central π-coil has been constructed, wound, and assembled. Preliminary tests show the leakage fields to be on the order of 10^{-4}G near the coil, falling off to 10^{-5}G 5 cm away. The qualitative field shape was consistent with the sum of the coil symmetry (comparing favorably with computer predictions) and the winding asymmetry.

The input and output coil forms have been constructed and are currently being wound with 1 mm wire. With μ-metal pieces connecting the main coil with the return coils, we expect field homogeneities of a part in 10^4. The computer program to control the experiment and the data acquisition is currently being written and tested.

Our scheduled beam time at the NIST (National Institute of Standards and Technology) reactor facility in Maryland will begin approximately two months after reactor start-up following the scheduled down-time for facility improvements. We expect to take data in the fall of 1995.

---

[1]Y. Avishai, Phys. Lett. **112B**, 311 (1982).
[2]V.F. Dmitriev *et al*., Phys. Lett. **125**, 1 (1983).
[3]J. Lang *et al*., Phys. Rev. C **34**, 1545 (1986).
[4]E.G. Adelberger and W.C. Haxton, Ann. Rev. Nucl. Part. Sci. **35**, 501 (1985).
[5]E.M. Henley, private communications.
[6]G. Feldman *et al*., Phys. Rev. C **43**, 863 (1991).

4.4 Measurement of Newton's constant G

E.G. Adelberger, J.H. Gundlach, B.R. Heckel and H.E. Swanson

Newton's constant G is one of the most fundamental yet least precisely known constants of nature ($G = (6.6726 \pm 0.0008) \times 10^{-11} m^3 kg^{-1} s^{-2}$)[1] and recently even this value has also been brought into question. The PTB (the German Bureau of Standards) obtained a value 0.6% (~40 standard deviations!) higher[2] than the accepted value, a group from New Zealand reported a value which is 0.1% lower (~7 standard deviations)[3] while another German group[4] measured a value that is in accordance with the CODATA value. In addition a Russian group claims to observe a temporal variation of G at the 0.7% level.[5]

We are pursuing a novel and elegant technique that we believe may ultimately make a determination of G at the 10^{-5}-level possible.

We plan to use the new rotating torsion balance (described in Section 4.5) currently being developed for testing the universality of free fall. We will use the $l,m = 2,2$ gravitational coupling from two masses (30-70kg) on opposite sides of the pendulum to induce a torque on the torsion pendulum. The turntable rotation rate will be servoed so that the pendulum does not move with respect to the turntable i.e. so that the torsion fiber never twists. This essentially transfers the angular acceleration of the pendulum to the turntable. The angular acceleration will be measured using a high-quality shaft encoder attached to the turntable. We plan to use a flat vertical pendulum; the expression for the q_{22}-moment of a two-dimensional pendulum contains the same integral over the mass distribution as does the moment of inertia. This largely avoids the important experimental problem of knowing the dimensions and density uniformities of the small pendulum. To eliminate spurious torques caused by masses in the laboratory we will rotate the attractor masses on a second turntable at a different and possibly opposite rotation rate.

We made computer simulations to study this feedback scheme. From these we expect that a 10^{-5} acceleration measurement would ultimately be possible. We already implemented the rotation feedback in our existing rotating balance and were able to verify the computer simulations. The dominant noise source we encountered was due to gravitational effects from pedestrian and vehicular traffic in the vicinity of the apparatus. The site of the new rotating balance is in a relatively isolated spot on the campus and should reduce this problem. Furthermore the rotation rate of the attractor masses can be chosen to give a fairly high signal frequency which will reduce gravitational 1/*f*-noise.

---

[1]CODATA (Committee on Data for Science and Technology) 1986, based on "1986 Adjustments of the Fundamental Physical Constants" By E.R. Cohen and B.N. Taylor, Rev. Mod. Phys. **50**, 1121 (1987).

[2]W. Michaelis *et al*., presented at the Conference on Precision Electromagnetic Measurement, Boulder, CO, 27 June - 1 July, 1994.

[3]M. Fitzgerald and T. Armstrong, presented at the Conference on Precision Electromagnetic Measurement, Boulder, CO, 27 June - 1 July, 1994.

[4]H. Meyer, presented at the Seventh Marcel Grossmann Meeting on General Relativity, Stanford, July, 1994.

[5]V.P. Izmailov *et al*., Measurement Techniques **36**, no. 10 (1993).

4.5 Construction of a new rotating torsion balance instrument

E.G. Adelberger, J.H. Gundlach, B.R. Heckel, S. Penn, Y. Su and H.E. Swanson

We are preparing a new, more sensitive rotating torsion balance apparatus to search for violations of the Equivalence Principle over length scales ranging from 1 m to infinity.

The dominant limitations of our previous results arose from:

- Brownian motion of the torsion pendulum due to gas damping in the residual vacuum of ≈0.1 Torr.
- coherent imperfections in the turntable such as fluctuations in the rotation rate or vertical "rumble".
- residual gravity-gradient couplings.
- daily variations in the tilt of the laboratory floor that required corrections to the data.
- vertical seismic motion was suspected (but never proved) to contribute to our fluctuating errors.

Our new instrument is designed to minimize the first four of these problems.

- an ion-pump will be used to evacuate the chamber to $< 10^{-7}$ torr.
- the torsion balance will be rotated on a high-quality air-bearing turntable on which a state-of-the-art angle encoder and an eddy current motor are mounted directly. The turntable system is being manufactured by a commercial firm, and is scheduled for delivery in late spring.
- the tilt-sensitive parts of the apparatus will hang from a 2-axis gimbal constructed using flexures to avoid sticking and hysterisis.
- the pendulum will be more symmetric; it will have 8 testbodies that mate reproduceably in conical seats.
- the gravity gradient compensation will be improved by placing the compensators farther from the balance.

We will develop the apparatus in two phases. First we will upgrade our existing Eöt-Wash balance for high vacuum operation, and hang it from a gimbal mechanism attached to the new turntable. This will allow us to thoroughly test the turntable and identify the necessary improvements for the second phase. We have built a massive concrete platform 5 m above the floor of the old cyclotron cave on which the turntable will be mounted and below which the apparatus will hang. The pendulum will be 2.5m above the floor to reduce the ambient Q_{21} gravitational gradient. This initial setup should yield a factor of 5 more precise test of the Equivalence Principle.

The second phase will have a gimbaled structure inside the vacuum vessel to support the tilt-sensitive components and a much longer torsion fiber. We will explore using a liquid-nitrogen cooled jacket to reduce thermal noise and fiber relaxation noise. With this second phase we hope to probe the Equivalence Principle with a substantially improved sensitivity.

4.6 Progress with the rotating-source torsion balance experiment

E.G. Adelberger, J.H. Gundlach, M.G. Harris, B.R. Heckel, G.L. Smith and H.E. Swanson

In last year's Annual Report,[1] we reported preliminary results that were apparently limited by systematic errors from gravity gradients arising from imperfections in the 3 ton Uranium source. The largest systematic error arose from the l, m=3,1 coupling.

- the stray Q_{31} gradient of the source (due to machining imperfections) could not be measured precisely (and therefore minimized) because the Q_{51} gradient of the earlier source did not vanish by design.
- the coupling to the stray q_{31} moment of the pendulum (due to small test body misplacements) led to variations larger than the statistical error.

We therefore modified our 3 ton Uranium source mass to have vanishing $Q_{31}$and Q_{51} moments. This was accomplished by introducing two horizontal gaps above and below the midplane of the Uranium brick stacks. We used flat aluminum bearing plates as spacers; these allow us to rotate the central stack by 180° into a configuration which maximizes the Q_{31} moment. Using this source configuration to measure the stray q_{31} moment of the pendulum and special q_{31} test bodies to measure the stray Q_{31} gradient of the source in its normal configuration, we were able to demonstrate that most of the offset (torques that are independent of the test body configuration on the pendulum tray) is due to the $Q_{31}q_{31}$-coupling. We have tuned the source and the pendulum so that $Q_{21}q_{21}$ offset torques are small, and we verified that the corrections due to $Q_{41}q_{41}$ coupling are negligible.

In addition we have built a set of new Pb and Cu precision test bodies that seat more reproduceably in the pendulum tray.

We now operate our instrument at high vacuum and take data with the source mass rotating faster ($\approx 1\text{rev}/20\,\text{min}$) than before and we achieve a statistical error of $5\text{nrad}\sqrt{\text{day}}$.

We have made several tests for non-gravitational systematic sources of error, and established that magnetism, thermal variations, and apparatus tilt now lead to insignificant uncertainties. To reduce our thermal sensitivity we installed a glass tube which surrounds the fiber. The Ag coated tube increases the pendulum time response to temperature changes to approx. 10h.

[1]Nuclear Physics Laboratory Annual Report, University of Washington (1994) p. 28.

4.7 New tests of the universality of free fall

E.G. Adelberger, M. G. Harris, B. R. Heckel, G. Smith and Y. Su

Our tests of the Universality of Free Fall (UFF) have reached the practical limits of the current version of the Eöt-Wash torsion balance. We studied differential accelerations of Be-Cu and Be-Al test-body parts in the fields of Earth, the Sun, or Galaxy, and in the direction of the cosmic microwave dipole. We also compared the acceleration towards the Sun and our galactic center of Cu and single-crystal Si in an Al shell (this pair of bodies approximates the elemental compositions of Earth's core and the Moon or Earth's crust, respectively). In terms of the classic UFF parameter η, our Earth-source results are $\eta(\mathrm{Be,Cu}) = (-1.9 \pm 2.5)\times 10^{-12}$ and $\eta(\mathrm{Be,Al}) = (-0.2 \pm 2.8)\times 10^{-12}$ where all errors are 1σ. Thus our limit on UFF violation for Be and a composite Al/Cu body is $\eta = (-1.1 \pm 1.9)\times 10^{-12}$. Our solar-source results are $\Delta a(\mathrm{Be,Cu}) = (-3.0 \pm 3.6)\times 10^{-12}$ cm / s^2, $\Delta a(\mathrm{Be,Al}) = (+2.4 \pm 5.8)\times 10^{-12}$ cm / s^2, and $\Delta a(\mathrm{Si/Al,Cu}) = (+3.0 \pm 4.0)\times 10^{-12}$ cm / s^2. This latter result, when added to the lunar laser-ranging results that senses both composition-dependent forces and gravitational binding-energy anomalies, yields a nearly model-independent test of the UFF for gravitational binding energy at the 1% level. A fivefold tighter limit follows if composition-dependent interactions are restricted to vector forces. Our galactic-source results test the UFF for ordinary matter attracted toward dark matter, yielding $\eta^{\mathrm{DM}}(\mathrm{Be,Cu}) = (-1.3 \pm 0.9)\times 10^{-3}$, $\eta^{\mathrm{DM}}(\mathrm{Be,Al}) = (+1.8 \pm 1.4)\times 10^{-3}$, and $\eta^{\mathrm{DM}}(\mathrm{Si/Al,Cu}) = (+0.7 \pm 1.0)\times 10^{-3}$. This provides laboratory confirmation of the usual assumption that gravity is the dominant long-range interaction between dark and luminous matter. We also tested Weber's claim that solar neutrinos scatter coherently from single crystals with cross sections $\sim 10^{23}$ times larger than the generally accepted value and rule out the existence of such cross sections.

These results have recently appeared in print.[1] We are now designing a new instrument with improved sensitivity (discussed elsewhere in this report).

[1] Y. Su *et al.*, Phys. Rev. D **50**, 3614 (1994).

4.8 Search for γ rays following the $\beta\beta$ decay of ^{100}Mo to the first excited 0^+ state of ^{100}Ru

L. De Braeckeleer, M. Felton* and A. Poon

A natural attempt to reduce the background of a very low counting rate measurement is to set up a coincidence experiment. It has been known for a long time that the ultimate sensitivity of a $0^+ \rightarrow 2^+$ $\beta\beta$ $0-\nu$ decay search could exceed the one of $0^+ \rightarrow 0^+$ because the photon deexcitation provides an additional signature that can be used to reject the background. Moreover, the physics of a $0^+ \rightarrow 2^+$ 0ν $\beta\beta$ decay has its own particular features. The neutrinoless $0^+ \rightarrow 2^+$ transition is extremely interesting for particle physics since its observation would imply both a finite value of the neutrino mass and the existence of a right handed current. It is also interesting for nuclear physics because it involves the $\Delta \leftrightarrow$ nucleon transition, a process strictly forbidden for the $0^+ \rightarrow 0^+$ case. However, the pessimistic estimates of the rates for $0^+ \rightarrow 2^+$ transitions due to both phase space suppression and small nuclear matrix elements have limited the enthusiasm of experimentalists for the search of this process. Is it possible to use the experimental advantage of the extra signature of the $\gamma-$rays of the nuclear deexcitation and to avoid the theoretical disadvantage of the small matrix elements governing the rate of $0^+ \rightarrow 2^+$ transitions? In the long wavelength approximation, the double beta decay operators can connect an initial 0^+ state with 0^+, 1^+, 2^+states in the daughter nucleus. As a general rule, a decay to the 1^+ is kinematically forbidden due to its higher excitation energies. In some cases, the decay to the first excited 0^+ state is allowed. A favorable case is ^{100}Mo, with a Q value of 2 MeV to the first excited 0^+ state in ^{100}Ru. Recently, two groups have attempted the observation of the $\beta\beta$ decay of ^{100}Mo to the first excited 0^+ state of ^{100}Ru. Assuming similar matrix elements as the ones governing the transition to the ground state, one expects a partial half-life of 10^{21} years. Presently the two groups report conflicting results: $(8.1^{+2.4}_{-1.5}) \times 10^{20}$ years[1] and a null result at the level of 2×10^{21} years.[2] Previous experiments have focused on a very low background, special materials and underground laboratory. We are investigating a different approach: the detection in coincidence, of the 2 γ rays following the $\beta\beta$ decay of ^{100}Mo to the first excited 0^+ state of ^{100}Ru. As a preliminary test, we are using 2 medium size (55%) BGO suppressed Germanium detectors (side mounted). We are measuring the coincidence background between these 2 counters. The BGO's are used to veto the cosmic ray background as well as the natural radioactivity. The apparatus is covered by a 4" thick layer of OFHC copper and a 4" thick layer of lead.

The background level at the energies of 540 and 590 keV is (0.02 ± 0.01) count per $(1 \text{ keV})^2$ per year. We are now measuring the coincidence background with a small sample of molybdenum (35 g.) to find out how the apparatus responds to the radioactivity inserted in the sample itself. A Monte Carlo calculation of the efficiency of an apparatus equipped with 2 large detectors (170%) is under development.

*Department of Physics, University of Washington, Seattle, WA 98195.

[1]A.S. Barabash *et al*., Nucl. Phys. B, **S28A**, 236 (1992).

[2]D. Blum *et al*., Phys. Lett. B **274**, 506 (1992).

4.9 Test of time reversal symmetry: The emiT experiment

S.R. Elliott, R.G.H. Robertson, T.D. Steiger, D.I. Will and J.F. Wilkerson

The fact that CP (combined charge conjugation and parity symmetry) conservation is violated in kaon decays was discovered over three decades ago.[1] Despite the considerable efforts of numerous researchers, however, this phenomenon remains to be adequately explained. The observation of CP symmetry violation combined with the CPT theorem implies that T (time reversal) symmetry must also be violated. Thus, tests of T symmetry provide a probe of the thirty-year-old CP puzzle which complements direct CP symmetry tests. Scientists at the Nuclear Physics Laboratory along with colleagues from Los Alamos National Laboratory, the National Institute of Standards and Technology (NIST), Notre Dame University, the University of California at Berkeley/Lawrence Berkeley National Laboratory, and the University of Michigan, have formed the emiT Collaboration to carry out the most precise test of T symmetry ever performed using neutron decay.

The complete neutron beta-decay distribution may be written:

$$\frac{dP(\mathbf{p}_e,\mathbf{p}_\nu)}{d\Omega_e d\Omega_\nu dE_e} = G(E_e)\left(1 + a\frac{\mathbf{p}_e\cdot\mathbf{p}_\nu}{E_e E_\nu} + A\sigma_n\cdot\frac{\mathbf{p}_e}{E_e} + B\sigma_n\cdot\frac{\mathbf{p}_\nu}{E_\nu} + D\sigma_n\cdot\frac{\mathbf{p}_e\times\mathbf{p}_\nu}{E_e E_\nu}\right)$$

where $\mathbf{p}_e$ and E_e are the momentum and energy of the electron, $\mathbf{p}_\nu$ and E_ν represent the emitted neutrino, σ_n is the spin direction of the neutron, and $G(E_e)$ includes phase-space factors and the Fermi function. In this equation, the term proportional to the triple correlation $\sigma_n\cdot(\mathbf{p}_e\times\mathbf{p}_\nu)$ is the only term which is odd under time reversal. Thus, the goal of the emiT experiment is to measure or place limits on the coefficient, *D*, which describes the strength of time reversal violation.

The experiment will be performed by observing in-flight decay of low-energy (<10 meV) neutrons from the Cold Neutron Research Facility at NIST in Gaithersburg, MD. Using energy and momentum conservation, the unobservable variables describing the neutrino may be replaced by measurable variables describing the proton. Thus, *D* may be written in terms of $\sigma_n\cdot(\mathbf{p}_e\times\mathbf{p}_p)$, and this quantity may be measured by detecting both the electron and the proton, and monitoring the angular correlation between their momenta as the neutron polarization is flipped.

The emiT detector consists of four plastic scintillator paddles for electron detection and four arrays of large-area PIN diodes to detect the protons. These eight detector segments are arranged in an alternating octagonal array about the neutron beam so that each segment of one type lies at an angle of 135º relative to *two* segments of the other type. This geometry takes advantage of the fact that the electron-proton angular distribution is strongly peaked due to the disparate masses of the decay products.

The emiT experiment is currently concluding the design phase and entering the construction phase. Assembly on the floor of the NIST reactor will begin before the end of 1995. The primary responsibility of the UW team is the production of the proton detector segments including read-out electronics, detector support frame, and associated vacuum systems. The feasibility of the proposed proton detection scheme was decisively proven during a test run at the NIST reactor in 1992.[2] The proton detector segments and the front-end electronics are currently under construction at the Nuclear Physics Laboratory.

---

[1] J.H. Christenson *et al*., Phys. Rev. Lett. **13**, 138 (1964).

[2] E.G. Wasserman, Ph.D. thesis, *Time Reversal Invariance in Polarized Neutron Decay*, Harvard University, 1994.

5. ACCELERATOR MASS SPECTROMETRY (AMS)

5.1 Paleoclimate studies using AMS radiocarbon (^{14}C) dating of pollen from lake sediments and peat deposits

T.A. Brown,* G.W. Farwell and P.M. Grootes†

We have continued our development and refinement of techniques for the isolation and AMS ^{14}C dating of essentially pure pollen fractions from lake sediment and peat samples under partial funding through an NSF grant under the Paleoclimate from Arctic Lakes and Estuaries (PALE) Initiative of the ARCSS Program (Grant No. ATM91-23963). We have applied these techniques to a number of cores taken from lakes and bogs in Washington, British Columbia, and Alaska.

Some of our results were summarized in last year's Annual Report.[1] A comprehensive description of the work and a discussion of the results are given in the Ph.D. dissertation of Thomas A. Brown.[2] A paper describing the principal features of our ^{14}C AMS system and its performance (absolute accuracy, ± 0.5% or ± 40 years) has now been published.[3]

Radiocarbon dating of organic material from lake sediments and peat deposits has been used for decades in paleoclimate studies. During the past several years, AMS measurements have increasingly supplanted the traditional β-counting method of ^{14}C dating since they offer greatly increased sensitivity (sub-milligram samples can be dated) and, in many instances, greater accuracy; they are also very much faster. However, the typical "bulk carbon" sample preparation techniques used for both AMS and β-counting leave unanswered the question of just what is being dated, a grave disadvantage in palynological and other paleoclimate studies. In contrast, the extraction procedures[2] that have been developed here typically produce purified pollen samples which can be clearly identified under the microscope; thus, an unambiguous proxy climate indicator --pollen-- is dated, and nothing else. Additionally, our results to date[2,4] show that the extraction and dating of pollen fractions eliminates "hard water effects" as sources of dating errors (sometimes thousands of years) and demonstrate that significant age differences can exist between pollen and macrofossils at the same level in a sediment core.

Recent results from the application of our pollen extraction/AMS dating procedures to a low-organic-content Arctic lake sediment core[2] were useful in rectifying an apparent age-depth reversal in the results obtained from "bulk carbon" samples from the core. They also demonstrated a clear need for careful screening of prepared samples, through microscopic examination, for suitability in obtaining valid and consistent radiocarbon dates for palynological and other paleoclimate studies.

With the recent departures of Thomas A. Brown and Pieter M. Grootes it has become unfeasible to continue the program of radiocarbon AMS measurements here in the Nuclear Physics Laboratory. The NSF-PALE paleoclimate work will continue, however, as a collaborative effort, with the AMS measurements to be carried out at the Lawrence Livermore National Laboratory, Livermore, California.

---

*Now at Center for Accelerator Mass Spectrometry, L-397, Lawrence Livermore National Laboratory, Livermore, CA, USA 94551.

†Now at C-14 Leibnitz Labor, Leibnitzstrasse 19, Christian Albrechts Universität, 24118 Kiel, Germany.

[1]Nuclear Physics Laboratory Annual Report, University of Washington (1994) pp. 30-31.

[2]Thomas A. Brown, Ph.D. Dissertation (Geophysics), University of Washington (1994).

[3]T.A. Brown, G.W. Farwell, and P.M. Grootes, Proceedings of the 6th International Conference on Accelerator Mass Spectrometry (1993), Nucl. Instrum. Methods B **92**, 16 (1994).

[4]T.A. Brown, G.W. Farwell, and P.M. Grootes, presented at the 15th International Radiocarbon Conference, August 15-19, 1994, University of Glasgow, Scotland.

6. ATOMIC AND MOLECULAR CLUSTERS

6.1 Stopping powers of atoms and atomic clusters

J.F. Liang, R. Vandenbosch and W.G. Weitkamp

We have continued our effort to determine vicinage effects in the stopping power of small carbon clusters. We are particularly interested in the energy region where with decreasing energy electronic stopping gives way to nuclear stopping. In this energy region the differences in stopping are small as the nuclear and electronic vicinage effects tend to cancel each other. Last year we reported our results for the stopping of single carbon atom anions.[1] We have extended these measurements to C_2^- and to a lesser extent C_3^- anions. The measurements consist of comparing the energy loss of C^- with C_2^- at the same bombarding energy per carbon. This means the degraded carbon ions exiting from the stopping foil have close to the same energy, with any difference reflecting vicinage effects. Our first series of measurements were made with a surface barrier detector with a thin Au window.

We first determined that the vicinage effects were independent of the stopping foil thickness in the range explored, 5-25 $\mu g / cm^2$. This is to be expected as the clusters will break up and the atoms separate soon after they enter the stopping foil. In view of the independence of the vicinage effect on foil thickness it is more appropriate to express the effect as the difference in stopping power for clusters as compared to single atoms, rather than the ratio of the stopping powers. We have found that C_2^- clusters lose energy faster than C^- ions at the highest energy studied, 165 keV per carbon. As the energy decreases the difference disappears.

Since the vicinage effects are very small we have decided to explore an alternate detection technique based on energy analysis of the degraded ions in an electrostatic deflector. We have reoriented a 90 degree bend deflector originally built to deflect the polarized ion source beam into the injection line of the tandem accelerator. This deflector transmits more than 70% of undegraded beam to a Faraday cup. Our measurements to date with this deflector have concentrated on measurements with low energy beams and a 5 $\mu g / cm^2$ stopping foil, and have confirmed that vicinage effects are small in the 30-50 keV per carbon energy range.

---

[1] Nuclear Physics Laboratory Annual Report, University of Washington (1994) p. 59.

6.2 Size distributions for RbC_n clusters

R. Vandenbosch and D.I. Will

It has been known for some time that low-mass carbon clusters exhibit an odd-even intensity pattern largely independent of the method of production of the clusters. The yield of negative ions, C_n^-, is larger by typically a factor of 2 to 3 for even mass clusters through n about 8 or 10. This favoring of even-n clusters is attributed to the larger electron affinities of carbon chains with an even number of carbons, as can be understood from the occupancy of delocalized pi electron orbitals.[2]

Middleton[3] first reported a much stronger odd-even dependence in the yield of CsC_n^- clusters, for which the enhancement of even clusters is typically two orders of magnitude. No explanation of this striking effect has been offered. We decided to see if it occurs for mixed clusters with other alkali metals. We have measured the intensity of RbC_n^- clusters from the sputtering of graphite with Rb+ ions. The results are given in Fig. 6.2-1. As was observed for CsC_n clusters, the enhancement of even-n clusters is more than two orders of magnitude.

In an attempt to understand this enormous enhancement, we have initiated ab initio quantum chemical calculations of the electron affinities of C_n and RbC_n clusters. We are using the Gaussian 92 program[4] with the LANL2DZ basis functions. These basis functions are capable of reproducing the odd-even alternation in electron affinities of linear C_n chains. Our preliminary results for RbC_n indicate an odd-even variation of similar magnitude to that for C_n. The absolute values of the electron affinities however are much less, with the odd-n RbC_n clusters (with the exception of RbC) not having stable anions (not having positive electron affinities). Although the calculations may not be accurate enough to conclusively determine whether the odd-n clusters have negative affinities, the results of the calculations strongly suggest that the origin of the large enhancement is the much smaller absolute values of the electron affinities of RbC_n as compared to C_n.

In the course of these calculations we have also explored the relative energies of different geometrical configurations for the RbC_n clusters. We find that linear clusters with the Rb on one end are appreciably more stable than linear clusters with the Rb in the middle, or than for small bent clusters.

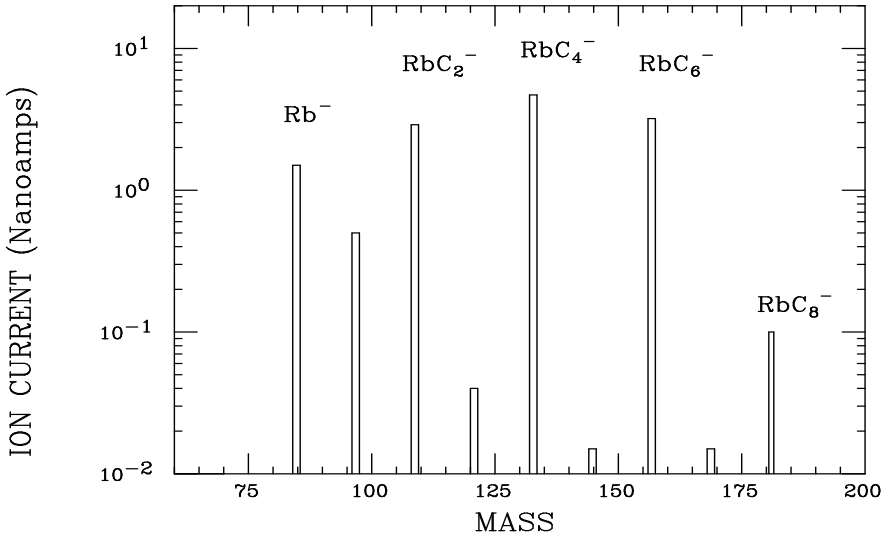

Fig. 6.2-1. Intensity distributions for RbC_n clusters produced by Rb sputtering of graphite. The small yields for n=3,5 and 7 are upper limits.

---

[2]R. Middleton, Nucl. Instrum. Methods B **58**, 161 (1977).

[3]R. Vandenbosch *et al.*, Nucl Instrum Methods B 88, 116 (1994).

[4]Gaussian 92, Revision G.1, M.J. Frisch *et al.*, Gaussian, Inc., Pittsburgh, PA, 1992.

6.3 High energy fragmentation of C_{60}

R. Vandenbosch

The unusual stability and high symmetry of C_{60} results in a great deal of interest in the mechanisms by which this molecule dissociates when sufficiently excited. Two rather different mechanisms have been put forward to account for the approximately exponential fall off in yield as the heavy fragment mass decreases from the mass of the parent molecule. One is the successive removal of a number of C_2 molecules. The other is a decreasing probability for emitting fragments of increasing mass in a binary process. We report here a semi-quantitative examination of the latter mechanism. It was motivated by a recent report of the C_n^+ yield distribution, where both the light (n < 20) and heavy (n > 40) fragments were reported.[5] A remarkable feature of the data, shown in Fig. 6.3-1, is the near-symmetry of the size distribution. This is exhibited by reflecting the yield of light fragments with $n \geq 19$ and plotting them as the closed symbols at 60-n. This symmetry is very suggestive of a binary fragmentation mechanism, $C_{60} \rightarrow C_n + C_{60-n}$.

We have developed a binary fragmentation model based upon the assumption of unimolecular dissociation from a statistically equilibrated system. One ingredient in such a model is the activation energy for a particular fragmentation channel leading to a C_{60-n} and a C_n primary product pair. DeMuro, Jelski, and George[6] have considered the general problem of removing carbon chains under a constraint to leave the resultant heavy fragment as close as possible to the original buckyball. They find that loss of 4, 6, 8 . . . atoms can occur via an "unzipping" process, yielding low-energy structures down to 44 atoms. The activation energy for a particular fragmentation channel should be approximately proportional to the number of bonds broken in this unzipping process. We have used the tabulated results of deMuro *et al.* for the number of bonds broken when chains of different length are extracted from C_{60} to estimate the relative yields of different fragmentation channels. A fit to the data yields the full curve shown in Fig. 6.3-1. This mechanism also leads to a natural explanation of the dominance of even-n for the heavy fragments. Odd-n primary heavy fragments cannot be produced by this unzipping process. The observed yields of odd-n fragments for the lighter fragments may be the consequence of C_1 and C_3 evaporation from excited chains. The chains produced by unzipping C_{60} will have considerable strain energy in addition to their share of the residual excitation energy.

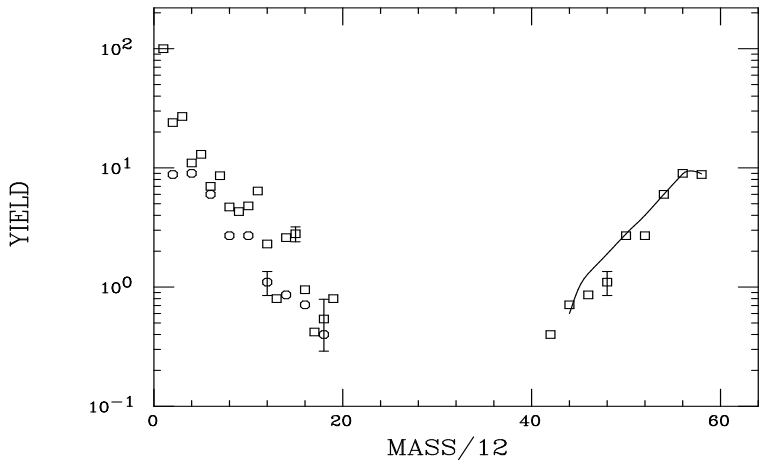

Fig. 6.3-1. The open squares represent the singly positive charged yields of LeBrun *et al.* for 625 MeV bombardment of C_{60} vapor. The open circles are the reflection of the heavy yields assuming binary fragmentation. The full curve is a binary fragmentation fit to the heavy fragment yields.

---

[5]T. LeBrun *et al.*, Phys. Rev. Lett. **72**, 3965 (1994).
[6]R.L. deMuro *et al.*, J. Phys. Chem. **96**, 10603 (1992).

7.0 ULTRA-RELATIVISTIC HEAVY ION COLLISIONS

7.1 URHI Group Overview

S.J. Bailey, H. Bichsel, P. Chan, J.G. Cramer, P.B. Cramer,* G.C. Harper, M.A. Howe, G. Odyniec,†
D.J. Prindle, J.G. Reid, R.J. Seymour, T.A. Trainor, P. Venable and J. Zhu

The major achievement for our group in the past year has been the highly successful first NA49 160 GeV/u lead beam run at CERN this past November and December. In preparation for this run the UW group has accepted a leading role in the production of Main TPC tracking software (Sections 7.5 and 7.6) and slow-controls system coordination software (Sections 7.4 and 9.4). The CERN and heavy ion communities have recognized that NA49 has carried out a major achievement by bringing into operation a highly complex experimental system with almost perfect functioning during its first running period. This experiment is considered to be the flagship experiment for the CERN heavy ion program through the year 2000.

The full NA49 system will consist of two 1.5T vertex magnets, with one vertex TPC installed in each magnet gap, and two large main TPCs on either side of the beam and 10 m downstream from the main target. Of these the second vertex TPC and the right Main TPC have been installed for this first lead beam run. The full TPC complement will be installed in time for the 1995 run next fall.

The Main TPCs are each 3.5 m square by 1.2 m high in active volume. Each TPC has about 64,000 electronics channels with 512 ADC samples per channel per event. This produces a data rate for one main TPC of about 3-4 Mb/s. The total data volume after five days of NA49 operation was about 1.5 Tbyte.

Successful Main TPC tracking was accomplished minutes after the first data were recorded. Track and charge distributions were displayed with a UW-produced display package (Section 7.7) and were used to check out and optimize the functioning of the TPC on line and to analyze the performance of the tracking software offline.

The UW group also played a lead role in preliminary analysis of Main TPC data (Section 7.3) in preparation for the Quark Matter 95 meeting at Monterey, CA in January. Charged-particle momentum spectra, collision system temperature distributions and net-charge momentum distributions were extracted during the week following the end of the run. These UW efforts, in combination with other VTPC and MTPC analysis efforts by NA49 collaborating institutions such as MPI-Munich, Lawrence Berkeley Laboratory, and IKF-Frankfurt provided a good preliminary description of this new lead-lead collision system only weeks after the first availability of beam.

In addition to our NA49 activities we have continued an active role in the STAR collaboration, which will mount a solenoidal detector at the RHIC accelerator in time for turn on in 1999. Some of these activities included development of STAR trigger algorithms based on correlation measures (Sections 7.11, 7.12 and 7.13), development of a servo-controlled TPC high voltage control system, and simulations in support of the STAR silicon vertex tracker (Section 7.8).

In addition to collaboration-specific activities we continue to pursue a strong interest in development of HBT or Bose-Einstein correlation determinations of collision system space-time geometry (Sections 7.9 and 7.10).

*Max-Planck Institut für Physik, Föhringer Ring 6, D-80805 München, Germany.
† Lawrence Berkeley Laboratory, Berkeley, CA.

7.2 NA49 Pb run first results

S.J. Bailey, H. Bichsel, P. Chan, J.G. Cramer, P.B. Cramer,* G.C. Harper, M.A. Howe, G. Odyniec,†
D.J. Prindle, J.G. Reid, R.J. Seymour, T.A. Trainor, P. Venable and J. Zhu

This past November and December NA49 carried out at CERN the first data acquisition with 33 TeV lead projectiles incident on a lead target. Operational detector elements included an in-magnetic-field vertex TPC, an out-of-field main TPC, a ring calorimeter covering the pseudorapidity region $2.1 < \eta < 3.4$, and a veto calorimeter covering the very forward pseudorapidity region which accepts spectator projectile particles, i.e., those which have not participated in the collision.

A minimum-bias correlation plot between E_{veto} and E_T for the veto and ring (transverse energy) calorimeters respectively shows an expected anticorrelation of these observables extending from E_{veto} = 33 TeV at E_T = 0 (no collision) to E_{veto} = 6 TeV at E_T = 0.5 TeV (central collision). Position of an event along this correlation is determined mainly by the particular collision geometry (impact parameter) for the event. The observed minimum E_{veto} energy is equivalent to about 38 noninteracting projectile particles (spectators) incident on this calorimeter, whereas simple model calculations predict about 13 spectator particles or 2 TeV. Therefore, about 4 TeV equivalent energy in *produced* particles must fall within the veto calorimeter acceptance.

Using these calorimeter data the degree of stopping of projectile particles while passing through the target can be compared for these new Pb-Pb results with that for S-Au obtained by NA35. The degree of stopping is found to be similar, for a corresponding mean number of interactions of projectile particles, indicating that collective effects in the stopping process do not seem to dominate.

More detailed analysis of calorimeter data indicate an energy density in the collision system of about 3 GeV/fm^3 in a volume (from HBT measurements) roughly 3.5 times larger than that for 200 GeV/c sulfur-sulfur.

Preliminary analysis of vertex and main TPC data indicate that the negative charged particle (mainly pion) distribution in pion rapidity has a peak value at midrapidity of about 230 per rapidity unit. This distribution is significantly broader than would be expected for particle emission isotropic in the CM. A preliminary study of Bose-Einstein correlations of negative particles indicate that the source size is about 7.4 fm, as compared to a source size of about 4.7 fm for sulfur beam.

These preliminary results indicate the achievement of energy densities and produced particle multiplicities consistent with predicted conditions for color deconfinement. The similarity of the degree of stopping for sulfur and lead on heavy targets indicates the absence of rescattering or other collective effect.

*Max-Planck Institut für Physik, Föhringer Ring 6, D-80805 München, Germany.
†Lawrence Berkeley Laboratory, Berkeley, CA.

7.3 NA49 Pb run preliminary spectrum analysis

P.Chan and T.A. Trainor

When the 160 GeV/u lead beam became available at the CERN SPS last fall, we carried out a preliminary spectrum analysis for experiment NA49's main TPC in order to provide an initial look at the data. This analysis also served as a check on the status of the hardware and analysis software.

The NA49 right main TPC is located 11 m downstream from the target and double magnet system with a lateral displacement of 2 m to the right of the beam. Straight tracks are deduced from correlation of ionization deposited by charged particles traversing the TPC active volume. For each reconstructed track, the corresponding particle's physical parameters, such as transverse momentum (p_t), rapidity assuming pion and proton mass (Y_π, Y_{proton}), and transverse mass ($m_t = \sqrt{p_t^2 + m_\pi^2}$) are determined. Due to the condition of the software environment in these early stages, only 100 events of negative particles (h_-) and 70 events of positive particles (h_+) were used for this analysis. On average, there are 320 reconstructed tracks per event for h_- and 390 for h_+.

The only correction applied to the raw spectrum was the TPC geometrical acceptance. Two acceptance correction factors were determined, one for p_t and one for m_t spectra. The p_t acceptance correction was determined by comparing the simulated output of GEANT with flat phase space input. On the other hand, a VENUS-generated phase space distribution was used to determined the acceptance correction factor for the m_t distribution. Due to the lack of statistical power over certain regions, the acceptance correction was most reliable for $4 \leq Y_\pi \leq 5$.

For a pion mass hypothesis, p_t acceptance corrected data are then used to produce event averaged p_t $< dN/dp_t >$ and rapidity $<dN/dY_\pi>$ distributions for h_- and h_+. The preliminary result shows a mean p_t of 370 and 440 MeV/c for h_- and h_+ respectively. The m_t acceptance correction factor is used to obtain the m_t distribution $1/m_t$ $<dN/dm_t>$ which is fitted with an exponential dependence on m_t. The fitted inverse slope parameter (or temperature) is 190 and 250 MeV for h_- and h_+ spectra respectively.

A "net baryon" distribution can be deduced from the charge excess between the h_+ and h_- spectra. The preliminary analysis shows a mean p_t of 580 MeV/c for this distribution. The rapidity distribution peaks near mid rapidity.

This set of results from the preliminary data analysis provides us with a first substantive glance at the data obtained from a new generation of ultrarelativistic heavy ion experiments. It also makes clear the challenge to our software analysis system in analyzing the bulk of data to be generated by NA49 in coming years.

7.4 Experience using SControl in CERN experiment NA49

J.G. Cramer, P.B. Cramer* and M.A. Howe

SControl was designed (see Section 9.4) for CERN Experiment NA49 and was used extensively in the initial Autumn 1994 run of NA49. The program operated on a dedicated HP-712 workstation in the NA49 counting room. In this application its function as a "control" system for actively changing experimental parameters was minimal. The principal tasks of SControl were: (a) to collect experiment-status information from 6 satellite processors, (b) to maintain an archive of this information by updating an archive file, (c) to maintain a data structure (BOS bank) that was read at irregular intervals by the data acquisition system, (d) to provide user-controlled displays of experiment parameters of interest, and (e) to generate and manage alarms.

The experiment was represented by pages organized in a hierarchical structure, with a "home" page at the top level showing an orthographic representation of the whole experiment. On this diagram the major subsystems were outlined in white, and each of these outlined regions provided a hyper-link to the top-level page of the subsystem. The subsystem top-level pages typically showed a block diagram of the subsystem, with blocks outlined in red providing hyper-links to the appropriate sub-sub-systems. This pattern of diagrams with hyper-links was repeated at one or more levels until a page was reached that was designed to monitor several related functions of a particular subsystem. For example, a page displayed as a strip chart the measured drift velocity of gas used in a TPC, the pressure and temperature at which the measurement was made, a "normalized" drift velocity that had been corrected for variations in temperature, pressure, and electric field, and a scatter plot correlation of measured drift velocity with measured pressure.

An alarm system was created which generated appropriate levels of alarms when (a) certain temperatures went out of range and (b) when one of the "heartbeat" signals provided by the satellite processors failed to recur at the expected interval.

Archives were updated every 10 minutes and organized into daily files, each initialized at midnight. About 200 Mb of archived parameter files were accumulated during the NA49 run. Measured gas temperatures, pressures, and other data from these files have already proved very valuable in providing comprehensive time-dependent estimates of the drift velocities in the NA49 TPCs.

Experience during the 1994 run of NA49 provided a number of lessons that bear on the application of SControl to future experiments and NA49 runs: (1) It is important to establish and enforce a naming convention for the slow control parameters archived. Names supplied by satellites were used to identify parameters in the archives. Parameters with time-dependent names proved troublesome. (2) Whenever an alarm link is created, a message describing the action to be taken when the alarm occurs should also be provided. No alarm is "obvious". (3) In the 1994 NA49 run, all slow control information was written each day to a master archive file. Because of the large volume of array information (up to 12 Mb/day) stored in the archive file by the two time-of-flight systems, this arrangement proved unwieldy. In future runs, when there will be more detectors on line, we will maintain separate archive file structures for several subsystems. (4) A better way of reviewing archived information is needed. We are considering a facility for converting slow control archives to a PAW ntuple for analysis. (5) One of the great advantages of SControl is the ease with which the user interface can be modified and expanded while running. However, this can lead to confusion and duplication unless the application developer exercises restraint.

*Max-Planck Institut für Physik, Föhringer Ring 6, D-80805 München, Germany.

7.5 NA49 main TPC tracking software

S.J. Bailey, P. Chan, D.J. Prindle, S. Schönfelder,* T.A. Trainor, P. Venable and X. Zhu

The original NA49 tracking software was an extension of NA35's TRAC program, modified to match the geometry and tracking needs of NA49. All steps of the analysis from reading the raw data through the momentum calculation were incorporated into a single large stand-alone program (TNT).

To allow a more modular design and interactive access to the data, the NA49 Server Environment (NASE) was created at IKF, Frankfurt, for use by all NA49 analysis programs. This server provided a central memory manager that separate client programs could access, thus sharing data. After a client had finished, its output data was stored in the central server where users could access the data to immediately view the results from a PAW-like environment.

The stand-alone tracking software was modified and split up into several separate clients for NASE. This collection of clients, STIRN, became the basis for NA49 MTPC tracking. STIRN includes modules for reading in init files with setup parameters, raw-data reading and space-point finding, tracking, dE/dx calculation, and momentum determination. It also comes with a collection of utility clients for matching simulated tracks to reconstructed tracks, calculating two-track resolution, and other programs for debugging and testing the primary clients.

Although improvements continue to be made to STIRN, the clients were ready and tested on simulated data before the first data acquisition run took place at CERN this last Fall. Thus, we were able to view reconstructed tracks literally within minutes of the initial raw data acquisition. The modular nature of STIRN allowed numerous improvements and suggestions to be rapidly implemented during the run.

Although useful, NASE suffers from being slow, using memory inefficiently, and instability. Because of these problems STIRN was recently converted to run under DSPACK, an alternate server system. Because DSPACK uses shared memory instead of copying data through Unix sockets, the performance of STIRN under DSPACK is significantly enhanced. DSPACK is also a more stable system than NASE and initial results have been promising.

Until both systems have been fully tested, STIRN is being simultaneously developed for both servers with the choice of which server to use being made at compile time. This allows both systems to be tested and compared while maintaining the same source code for the core of the analysis to ensure accountability between tests of the different systems.

*Max-Planck Institute für Physik (MPI), Föhringer Ring 6, D-80805 München, Germany.

7.6 NA49 InitEdit database editor

S. Bailey, P. Chan, J.G. Cramer, D.J. Prindle and T.A. Trainor

The NA49 main TPC tracking code (see previous section of this Annual Report) has had all parameters relating to track finding excised from the code and placed in initialization files. This makes it easy to check the effect of each parameter on track finding. The drawback is that we need an accountable way to check and modify what is in the initialization file. To do this we have written a program specifically to edit these files.

InitEdit can be thought of as a user interface to the tracking code parameter files. InitEdit uses Motif widgets as its interface elements. The tracking parameters are typically read from a file and after editing can be written back to a file or sent directly to the NASE server. This ability to send the parameters directly to NASE makes it very easy to test a variety of parameter values before committing them to a file.

The initialization data are divided into sections, with a given program module typically using only one section of the initialization data. InitEdit edits each section independently, making it easier for the user to worry only about the relevant parameters. InitEdit can check that the parameters are within an acceptable range. Typically it checks that the user has entered a valid number and makes no restriction on the range.

[due to imaging conflicts, this figure is viewed by selecting "Fig 7.6" on the Table of Contents.]

Fig. 7.6-1. Example of an InitEdit screen. This screen allows one to modify the track-finding parameters.

7.7 Na49 display

S. Bailey, P. Chan, J.G. Cramer, D.J. Prindle and T.A. Trainor

To help check our track finding and fitting algorithms we have developed an event display program. This program uses the Motif widget set for its user interface elements and draws to the screen using X primitives. This allows it to be used from any X terminal. Currently the program knows how to draw Monte-Carlo and reconstructed space points in all NA49 TPCs as well as Monte-Carlo and reconstructed tracks in the Main TPCs.

Navigation through the data can be done by holding one of the mouse buttons down while moving the mouse. Holding the left mouse button down while moving the mouse simply moves the display objects. Holding the middle mouse button down causes a zoom toward or away from the point under the cursor. Holding the right mouse button down while moving the mouse causes the objects in the display to rotate about the origin. One of the main features of the program is that it draws quite quickly, allowing one to view the wire frame TPC outlines and all tracks during a rotation. This makes it very easy to orient the display to look along a precise direction.

There are numerous other features, including the ability to select points or tracks, attach scales to points and hide categories of objects in addition to an extensive help selection.

[due to imaging conflicts, this figure is viewed by selecting "Fig 7.7" on the Table of Contents.]

Fig. 7.7-1. An example of the display screen.

7.8 Energy deposition and particle identification in a TPC

H. Bichsel

Because the individual detector cells in a TPC encompass a limited volume (of the order of 5x10x40 mm), the ionization J observed (which corresponds to the energy deposited in that volume) differs from the energy Δ lost by a charged particle traversing it. It is quite easy to calculate the energy lost.[1] It will include large energy losses which produce secondary electrons, "δ rays". If the path of a δ ray carries it outside of the measurement volume, the energy deposited will be reduced. It is also possible that δ rays from neighboring volumes will enter the volume under consideration ("crossers"), and the energy deposited will be increased.

Since J is related to particle speed, it is possible to determine from it the particle mass if the momentum of the particle is determined in another measurement. The process of mass determination is called "particle identification" (PID). The ionization is a stochastic quantity, thus a large number of values of J (of order 100) are measured in successive layers of a detector. Then, a suitable average value J_a must be selected from all the values of J to get the speed. Monte Carlo calculations simulating the process have been made, and the range of particle momenta for which PID is possible has been determined.

The energy loss spectrum for particles with charge $z = 1$ and $\beta\gamma = 5.2$ is shown by the solid line in the Fig. 7.8-1. The use of 60% of all Δ to obtain Δ_a excludes values above about $\Delta_c = 7$ keV. Thus the difference between Δ and J needs to be known only for $\Delta < 7$ keV. Monte Carlo calculations for the effect have been made. The result is shown by the dashed line: the difference between Δ and J is large[2] only for large Δ. The largest contribution to the difference is the presence of crossers: their energy deposition is at least 10 keV, thus any $\boldsymbol{J}$ which includes a crosser will be well above J_c and will not be relevant to PID. The total number of crossers is of order of 2%, depending on the geometry, and the net effect is simply that the energy deposition spectrum is reduced by 2% compared to the energy deposition spectrum. Electrons escaping from the counting volume occur for only 0.6% of all events.

The conclusion is that the difference between energy loss and energy deposition is negligibly small for purposes of PID.

$f(\Delta)$

$\Delta(\mathrm{keV})$

Fig. 7.8-1. Energy loss spectra for z=1 and $\beta\gamma = 5.2$.

---

[1]Nuclear Physics Laboratory Annual Report, University of Washington (1993) pp. 56-57.
[2]H. Bichsel, Radiat. Protection Dosimetry **13**, 91 (1985).

7.9 STAR SVT efficiency for D meson detection

S. Bailey, P. Chan, J.G. Cramer, D.J. Prindle and T.A. Trainor

One very interesting observable in ultra relativistic heavy ion collisions is D meson production. Previous attempts[1] to demonstrate that STAR is capable of observing D meson production have used the flight path of the D as a signature. The D^+ and D^- mesons have $c\tau = 320\mu m$ (in the rest frame) while the D^0 and $\overline{D}^0$ have $c\tau = 125.9\mu m$. An energetic D meson may travel a few millimeters before decaying, and a suitable vertex detector should be able to distinguish its decay point from the primary vertex.

However, STAR's acceptance is centered at mid-rapidity and the D mesons produced there are expected to be thermal and hence low velocity. This implies a very short flight path for the D mesons. Multiple scattering of the rather low energy decay products in the beam pipe and vertex detector material significantly modifies the track directions. This has led to the conclusion that the current STAR vertex detector design is not suitable for detecting D mesons produced in central Au-Au collisions via the detection of a secondary vertex.

We have therefore examined the possibility of using the special kinematics of the $D^{*+} \rightarrow \pi^+ D^0$ decay mode to detect D^0 mesons.[2] Briefly, the branching ratio of D^{*+} into $\pi^+ D^0$ is 55%. Since the mass difference is so small ($M_{D^{*+}} - M_{D^0} - m_{\pi^+} = 5.87$ MeV) the π^+ is essentially emitted with the D^{*+} meson velocity. Typically one looks for a D^0 candidate, then given this candidate one looks for a matching π^+ to form a D^{*+} candidate and makes a tight cut on that mass. In some cases this cut can dramatically reduce the background under the D^0 invariant mass spectrum.[3]

Our findings are not highly encouraging. Briefly, we found that the small mass difference is still large enough that for a thermal D^{*+} meson the laboratory D^0 - π^+ opening angle spans a large range. We can make some kinematic cuts to accept less than one π^+ per D^0 candidate in an average central Au-Au event. This increases the signal-to-background ratio, but the net loss of signal decreases its overall statistical significance. It is possible that selecting the high energy tail of the D distribution will make possible both the secondary vertex selection and the use of special D^{*+} decay kinematics, but this method is sensitive to details of the transverse momentum distribution of the D mesons.

---

[1] STAR Note 127.
[2] STAR Note 160.
[3] D. Cinabro *et al.*, CLEO Collaboration, Phys. Rev. Lett. **72**, 1410 (1994).

7.10 Scale-distorted Gaussians and HBT "Wiggles"

J.G. Cramer

The Hanbury-Brown-Twiss interferometry technique is widely used in ultra-relativistic heavy ion measurements with pions and other Bose-Einstein particles to extract information on source geometry and duration. The technique is primarily sensitive to the 2nd moment, i.e., width, of the source distribution. However, deviations from a Gaussian source shape will produce "wiggles", i.e., oscillations of a few percent around a value 1, in the momentum space correlation at large relative momentum. These, in principle, can be used to gain more source-shape information.

We have demonstrated this phenomenon in Monte Carlo simulations using non-Gaussian source distributions and find that the wiggle amplitudes are stronger for the correlation of 3 or more particles than for the more standard 2-particle correlations. This work was described in an Annual Report contribution last year.[1] Unfortunately, the HBT analyses of experimental data that have been performed up to now are based on at most a few thousand events, so the statistics are not sufficient to support investigation of this phenomenon. However, HBT analysis of CERN data with 10^4 to 10^6 high-multiplicity events should soon provide the needed statistics.

Our Monte Carlo simulations up to now have used simple but unphysical shapes, e.g., sharp-edge spheres and hemispheres. The next step in this investigation is to devise more physically reasonable non-Gaussian source shapes having significant 3rd moments (skewness) and 4th moments (kurtosis). One suggested technique for achieving this[2] is to add higher Gaussian derivatives as Laguerre polynomials in an Edgeworth expansion. This technique offers the advantages that distributions have analytic integrals and that distribution moments are coefficients of the expansion. Unfortunately, the resulting distributions are not positive-definite and are therefore unphysical.

We have devised an alternative prescription for producing a physically reasonable non-Gaussian source shape, *the scale-distorted Gaussian*. The procedure is to replace the Gaussian function *G(x)* with *G(f(x))*, where *f(x)* is a scale distortion function. To produce an unsymmetric distribution function which has a significant 3rd moment and skewness, we have used an arc-tangent scale-distortion function $\mathrm{afn}(x,a_3) = 2\arctan(x/a_3)/\pi$ and $f_3(x,d_3,a_3) = x[1-d_3\mathrm{afn}(x,a_3)]$. The Type-3 scale-distorted Gaussian function is therefore $G_3(x,\sigma) = Exp[-(f_3(x,d_3,a_3))^2/(2\sigma)]/\sqrt{2\pi}$. Typically, a_3 is set to 0.1 and d_3 is varied between 0.0 (a standard Gaussian) and 1.0 (a limiting case in which the right side of the distribution is constant out to infinity).

To produce a Gaussian-like function that has a significant 4th moment and kurtosis, i.e., is either more flat-topped or sharper that a normal Gaussian, we have used a modified Gaussian scale-distortion function $\mathrm{gfn}(x,a_4) = 2Exp[-x^2/(2a_4]-1$ and $f_4(x,d_4a_4) = x[1-d_4\mathrm{gfn}(x,a_4)]$. The Type-4 scale-distorted Gaussian function is therefore $G_4(x,\sigma) = Exp[-f_4(x,d_4,a_4))^2/(2\sigma)]/\sqrt{2\pi}$. Typically, a_4 is set to 2.5 and d_4 is varied from -0.5 (a "sharp" Gaussian) to 1.0 (a "flat-top" Gaussian).

The disadvantage of using functions like these is that their integrals cannot be calculated analytically, and thus distribution moments must be calculated numerically. On the other hand, the strong advantages are (1) the functions produced are guaranteed to be positive-definite, (2) they are fairly simple to calculate, and (3) they are fairly simple to incorporate in Monte Carlo calculations. We are now modifying our HBT Monte Carlo program to include these new distribution shapes, which will permit investigation of this phenomenon with more realistic source distributions.

---

[1] Nuclear Physics Laboratory Annual Report, University of Washington (1994) p. 48.
[2] T. Csörgö, private communication, (1993).

7.11 "No-Background" maximum likelihood HBT analysis

J.C. Cramer

The probability density function for the "signal" in HBT interferometry i.e., the probability density of finding a correlated particle pair with relative momentum $\underline{Q}$ from a source of geometry $\underline{R}$, is $S(\underline{Q},\underline{R}) = [1+C(\underline{Q},\underline{R}))]G(\underline{Q},\underline{R}))B(\underline{Q})/N(\underline{R})$, where $C(\underline{Q},\underline{R})$ is the reduced correlation function, $G(Q)$ is the Coulomb correction, and $B(Q)$ is the uncorrelated background distribution. The background distribution $B(\underline{Q})$ in the standard approach to HBT analysis is constructed by correlating the momenta of particles from separate and therefore uncorrelated collisions.

The probability normalization factor is $N(\underline{R}) = N_0 + N_1(\underline{R})$, where $N_0 = \int_\Omega G(\underline{Q})B(\underline{Q})d\underline{Q}$, a constant independent of $\underline{R}$, and $N_1(\underline{R}) = \int_\Omega C(\underline{Q},\underline{R})G(\underline{Q})B(\underline{Q})d\underline{Q}$, a function of $\underline{R}$. Here Ω is the complete space of all allowed $\underline{Q}$ values. We define the normalization correction factor $M(\underline{R}) = N_1(\underline{R})/N_0$, so that $N(\underline{R}) = N_0(1+M(\underline{R}))$ and note that for expected R-values $M(R) \ll 1$.

A Maximum Likelihood fit to data using this function can be performed by minimizing the function $L(\underline{R}) = -\sum_{i=1}^{K} \ln S(\underline{Q}_i,\underline{R})$, where i is the index specifying all measured particle pairs and K is the total number of pairs. This function can be rewritten as:

$$L(\underline{R}) = -\sum_{i=1}^{K} \ln\,[1+C(\underline{Q}_i\underline{R},)]G(\underline{Q}_i)B(\underline{Q}_i)/N_0[1+M(\underline{R})]$$

$$= -\sum_{i=1}^{K} \ln[1+C(\underline{Q}_i,\underline{R})] - \sum_{i=1}^{K} \ln G(\underline{Q}_i) - \sum_{i=1}^{K} \ln\, B(\underline{Q}_i)$$

$$+ \sum_{i=1}^{K} \ln N_0 + \sum_{i=1}^{K} \ln[1+M(\underline{R})]. \qquad (1)$$

Of the terms in Equation (1), only first and last depend on $\underline{R}$. Thus, minimizing $L(\underline{R})$ by varying $\underline{R}$ is equivalent to minimizing $L_1(\underline{R})$, as defined by:

$$L_1(\underline{R}) = K \ln[1+M(\underline{R})] - \sum_{i=1}^{K} \ln[1+C(\underline{Q}_i,\underline{R})]$$

$$\cong K\,M(\underline{R}) \_ \sum_{i=1}^{K} \ln[1+C(\underline{Q}_i,\underline{R})] \qquad (2)$$

where the last line is uses the approximation $\ln[1+M(\underline{R})] \cong M(\underline{R})$.

If we use the approximation $M(\underline{R}) \rightarrow 0$ to eliminate the implicit background dependence of the first $M(\underline{R})$-dependent term in Equation (2), it will have two consequences. First, the probability density function for the signal $S(\underline{Q})$ will no longer be a true probability. This has no effect on the fit. Second, the $S(\underline{Q})$ function will tend to be slightly larger for large R-values than for small R-values. Therefore, approximating $M(\underline{R}) \approx 0$ will cause the maximum likelihood fit to be slightly biased toward smaller values of R. For the case of single-event HBT analysis, where the fit to data is only used as a guide for selecting an ensemble of events that are characterized by unusually large radii, a small monotonic bias toward smaller radii should be quite acceptable. Thus, Equation (2) with $M(\underline{R}) = 0$ can be used without calculating a background to perform HBT analysis on single high-multiplicity events in ultra-relativistic heavy ion collisions.

7.12 Scaled topological measures

J.G. Reid and T.A. Trainor

For this project we use the scaling behavior of topological properties of point sets to infer the nature of the parent or generating process. To carry out such an analysis on a data set it must first be binned over a range of scale. To do this we simply take the embedding space of the data set and divide it into (rectangular) bins of characteristic size e. We then increase the size of the bins, and repeat the process until we have analyzed the entire scale range of interest. However, the analysis is not quite so simple due to aliasing that results from the density variations between the binnings. Our solution to this is to 'dither' (phase shift) the binnings of the space at each scale value and form an ensemble average of the relevant quantities over the dithered binnings to reduce the aliasing effects.

With the binning problem under control we examined the scale behavior of the entropy, information and dimension of various point sets. There is a continuum of defined entropies (each with its own information and dimension), of which the standard thermodynamic (Gibbs) entropy is one, and we must in general consider this continuum as a function of scale. To keep things as simple as possible we usually consider only the 0th (Kolmogorov) and 1st (Gibbs) order entropies, but it is important to note that this analysis can be extended to include whatever entropy measures are of interest. By examining a Poisson-filled embedding space we find that the analysis behaves just as we expect for the Kolmogorov quantities; however we are still investigating details of the Gibbs quantities.

Since the main purpose of this analysis is to identify density variations in scale which would be missed by classical point set correlation analysis we have also investigated the analysis of simple hierarchical point distributions. These are point sets whose only significant features are scaled density variations. We have been very pleased with these results. For these simple hierarchies the scaled dimension behaves exactly as we expect: the dimension reaches peaks at each scale level of the hierarchy and falls off in between. The scaled dimension is very nearly the simple sum of the dimension fields of each hierarchy level.

Another important characteristic of the data that can be determined by this analysis is the scaled set volume. We have only recently begun this part of our analysis, but it is already very promising. At large scale the analysis sees the perimeter of the data set, since at this level the analysis can only see prominent features. As the scale decreases and approaches the point at which classical volume determinations are made the calculated volume approaches the classical value. Finally, our analysis continues beyond this point into the small-scale region. The 'volume' eventually corresponds to the length of a space-filling curve through the data. Below this scale level the volume approaches asymptotically the total number of points in the set.

We are pleased with the progress of this scaled topological analysis, and we expect to concentrate on applications in the near future, particularly for STAR triggering.

7.13 Entropy analysis of STAR EM calorimeter energy distributions

J.G. Reid and T.A. Trainor

The STAR electromagnetic calorimeter can provide important information regarding both the early stages of a high-energy nucleus-nucleus collision and the subsequent evolution through hadronization. Because of its fast response to energy deposition the EM calorimeter may be an especially valuable part of the STAR trigger system. We have developed an algorithmic approach to triggering based on information entropy analysis which may quickly be able to determine the degree of correlation in a particular event energy distribution, and therefore serve as a model-independent trigger criterion.

Information entropy analysis is sensitive both to isolated features and to slower variations in density. To test the analysis we obtained twenty simulated proton-proton events produced by the standard event generator HIJING and used a simpler event simulator to generate data for A-A events.

For the Kolmogorov (capacity) entropy, as the scale of the binning system approaches the base width of an isolated jet this entropy is reduced with respect to that of a uniform (Poisson-distributed) energy distribution. Once the scale is comparable to the jet size there will be no further such reduction because there are no more empty bins to reject. Thus by identifying the minimum with scale of the corresponding capacity dimension-change (Δd_0) we can determine the size and spacing of the prominent jets for p-p collisions. One such event analysis is shown in the top panels of Fig. 7.13-1. By examining ensembles of such p-p jet events we can formulate trigger conditions based on information-related quantities such as dimension which will permit fast selection of special event classes. The bottom panels of Fig. 7.13-1 show an ensemble of p-p events which exhibit the degree of variation of the dimension-change distribution for a given event generator.

The Gibbs (information) entropy may seem redundant for analyzing the prominent jets of a p-p system, but it is essential in analyzing heavier A-A collision systems. With any A-A event there will be few or no void areas in the data because we expect to see a background of so-called minijets. This background makes the Kolmogorov entropy much less useful since it depends on identifying rejected bins to 'find' distribution features. The Gibbs entropy on the other hand depends only on density variations. Thus, the minimum in the Gibbs dimension-change (Δd_1) will be an indicator of the point in scale at which all of the significant density features have been identified. This tells us at which scale our smallest features occur for A-A events. The minijet background problem is especially serious for standard jet-finding algorithms, and is an important motivation for this new approach.

Since there is a continuum of entropies which correspond to information contained in higher-order correlations we can extend our analysis to include any of these which may be found useful. At present we have concentrated our efforts on developing the analysis system itself with jet distributions and triggering in mind. In future work we hope to understand in more detail the relationship of the jet-minijet distribution to changes in the scaled dimension for both the Gibbs and Kolmogorov entropies.

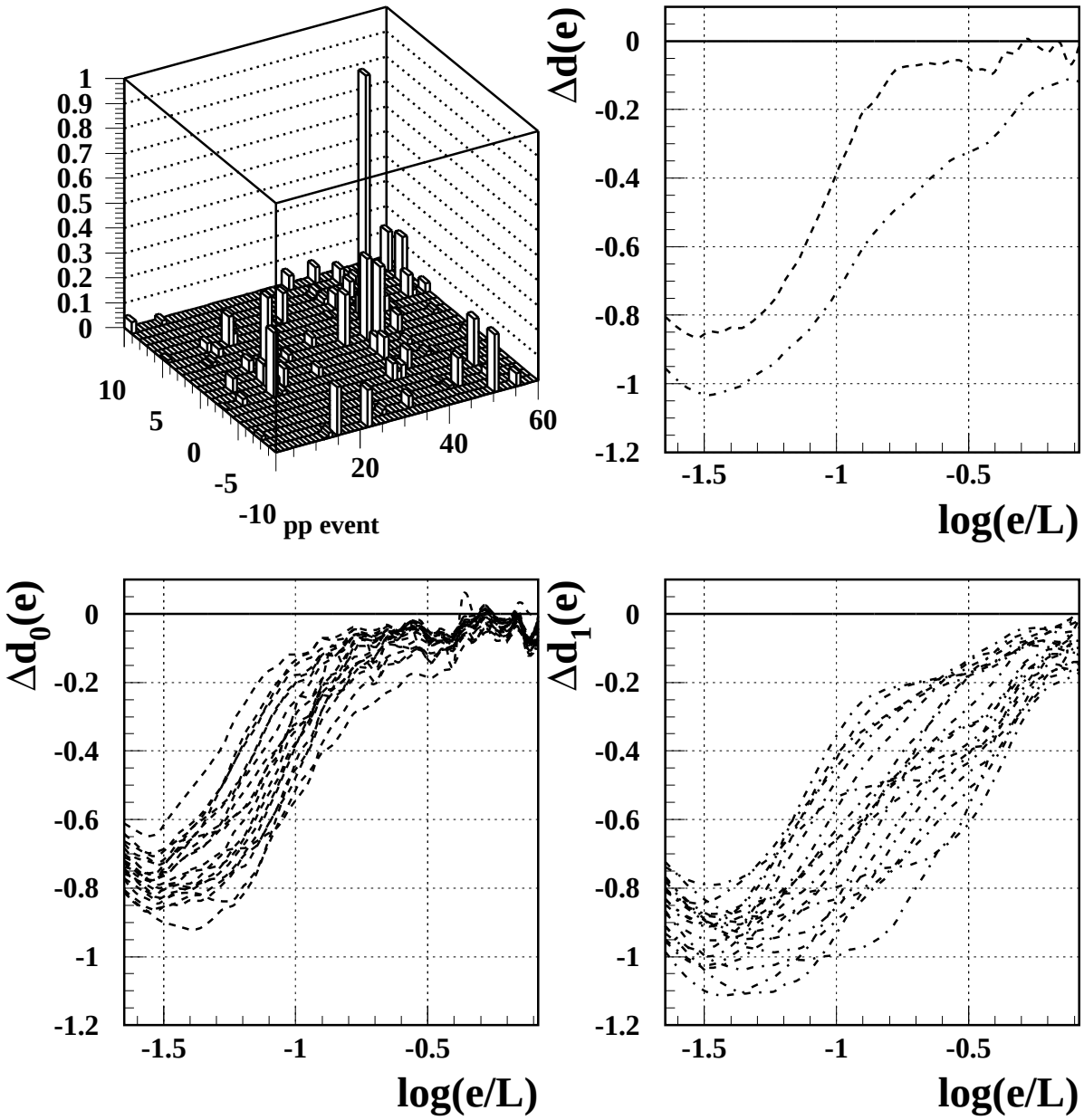

Fig. 7.13-1. Dimensions lowering analysis of single event calorimeter jet distribution (top) and similar analysis of an ensemble of events (bottom).

EXTERNAL USERS

8.1 Ball Aerospace

E.W. Smith* and G.A Geissinger*

This was the fourth in a series of experiments performed on a variety of opto-electronic circuit elements using the University of Washington Van de Graaff accelerator. This experimental program is intended to permit simulations of the performance of different optical circuit designs in radiation environments such as those encountered in spacecraft applications and in nuclear reactors. The irradiated components can be assembled in our lab at Ball Aerospace to simulate a variety of different circuit designs and the effect of different dose levels on the individual components can be analyzed.

*Ball Aerospace Systems, Group, Electro-Optics and Cryogenics Division, Boulder, CO 80306.

9.0 ELECTRONICS, COMPUTING AND DETECTOR INFRASTRUCTURE

9.1. Electronic equipment

G.C. Harper, A.W. Myers and T.D Van Wechel

Projects undertaken by the electronics shop this year included the following:

a. Vertical and horizontal steering power supplies, with a -600 volts to +600 volts range, were designed and constructed for the terminal ion source (see Section 10.3).

b. A circuit was designed and constructed for the cluster experiment to drive the voltage on the inflector plates with a calibrated ramp voltage generated by the multi-channel analyzer.

c. A voltage to frequency converter circuit was constructed for the cluster experiment to provide an output frequency proportional to the current measured by a Keithley picoammeter.

d. A portable data acquisition rack, including three NIM bins and a CAMAC crate, was assembled for weak interaction studies.

e. Preliminary design of the clock generator circuit for the 13/12 high energy buncher (see Section 10.7) and design of modifications to be made to the low energy buncher controller for phase locking to the 13/12 high energy buncher were started.

f. The current preamp for the SNO neutral current detector (see Section 2.3) has been proto-typed and tested. Ten preamps assembled from discrete components are presently being constructed and will be sent to Los Alamos. The major part of the circuitry of the 112 preamps for the neutral current detector will be fabricated on hybrid circuits.

g. A prototype 30 nsec delay line for the SNO neutral current detector has been constructed. Some development work is still required as there are some wave form aberrations on the present prototype.

h. An Analog Devices AD606 log amp evaluation board has been tested for use with the SNO neutral current detector. Originally, the rise time of the log amp was approximately 400 nsec which is unsatisfactory for this application. We were able to modify the circuit to improve the rise time to approximately 25 nsec.

i. Two Ortec 113 preamps were modified. Ten 270 nSec delay cables and several signal and power cables were constructed for the new electron detector for the "Mass-8" experiment.

j. A Sun microcomputer workstation and CADENCE electronic design system software were acquired to facilitate board layout and circuit analysis for the SNO and EMIT projects.

9.2 VAX-based acquisition systems

M.A. Howe, R.J. Seymour and D.W. Storm

Our three data acquisition systems consist of Digital Qbus-based VAXStation 3200s running VMS v4.7a. We use VWS/UIS as the "windowing" software. Each VAXstation supports a BiRa MBD-11 controlled CAMAC crate. Our principal VAXStation BA-23's cabinet is cabled into a BA-23 CC expansion cabinet. It has an MDB-11 DWQ11 Qbus to Unibus converter driving our old PDP 11/60's Unibus expansion bay. That system's peripherals include a CMD CQD-220/TM SCSI adapter, a Seagate ST41650 1.38 gigabyte disk, a TTI CTS-8210 8mm tape, a DEC IEQ11 IEEE-488 bus controller, and a DEC DRV11-J. The Unibus bay contains a DR11-C, our Printronix lineprinter controller and a Unibus cable to the MBD-11.

Our main CAMAC system contains interface modules for our dozen Tracor Northern TN-1213 ADCs. Those ADCs and other CAMAC modules are gated by an in-house built synchronization interface, which includes routing-Or capabilities, and 32 10-digit 75 MHz scalers.

Additional CAMAC space is available for our LeCroy 2249s, 2228s and 2551s. We have two FERA 4300B ADCs, and two Phillips 7186 TDCs.

The other two acquisition systems consist solely of the VAXstation's BA-23 using an Able Qniverter to cable directly to a stand-alone MBD-11. Unlike the "principal" system, these do not control non-CAMAC-based equipment.

All three systems run acquisition software based upon TUNL's XSYS, with major modifications to their DISPLAY program.

TUNL's XSYS software includes an EVAL language compiler which generates VAX-native code. Our "version" of that compiler is limited to 1024 longwords of VAX sorting code per MBD channel. One Mass-8 experiment required far more space, so we completely replaced the EVL-generated code section by a pre-compiled Fortran subroutine set. Interface subroutines were created to provide easier access to the raw incoming event buffers. We still require an EVL routine to be used, but only for histogram storage coordination.

9.3 Data analysis and support system developments

J.G. Cramer, M.A. Howe, R.J. Seymour, D.W. Storm and T.A. Trainor

All of our offline analysis VAXes are running VMS v5.5-2. We have acquired several additional VAXstation 3200s which have been surplussed from the Physics Department. These are becoming deskside systems, Qbus board-testing systems and an additional data acquisition system. Our cluster now consists of five VAXstation 3100s, two VAXstation 3200s, a VAXstation 2000 and an AXP 3000/400. Three more 3200s are about to be added to the cluster itself.

The AXP 3000/400 (Alpha) has 96 megabytes of memory, 1- and 4-gigabyte disks, a CDrom, a 19 inch color display, and occasional 8mm Exabyte tape drives attached to its external SCSI port. It is currently running OpenVMS v1.5. As members of the Digital's Campus Software License Grant program, we have implemented Digital's Fortran, C and C++ as its principal languages.

We use TGV's Multinet to provide our cluster with TCP/IP access to the Internet. Our primary Internet address is npl.washington.edu (128.95.100.10). The UW Campus dropped all BitNet support last summer, so our only access to BitNet systems is via off-campus gateways.

Our 8 megabyte VAX 11/780 finally died last March. It has been replaced by one of the VAXstation 3200s, with DHv11s now driving our connections to twenty-odd local rs232 terminals. Since the 11/780's boot disk was already on a Qbus extension to its Unibus, migration of the disk drives was trivial. The only major peripheral which did not make the transition to the Qbus was our 9-track tape drive, but it can be driven by a controller attached to another of our 3200s. There has been little demand for its services since the advent of 8mm systems.

Another VAXstation 3200 serves as the Linac's control and display system.

Our NA35, NA49 and STAR work depends upon our two HP 9000/710s, which have been updated to HP-UX v9.03 and v9.05. One (Mist) has been moved to Germany during John Cramer's sabbatical. The splitting of the two cross-referencing systems was accomplished primarily by adding disks to the to-be remote system, and putting Mist's disks on the remaining system. This allowed links and pointers to gradually be migrated to better locations while still maintaining the desired level of service to each. Cramer's system then moved to CERN for the NA49 run in November, then back to Munich in December. Our remaining 9000/710 (Sand) is providing world-visible World Wide Web (WWW) service of programs and data related to those projects, as well as a growing library of other NPL documents, including our annual reports (try http://sand.npl.washington.edu/home.html). We have added two HP 712/60 workstations, also running HP-UX v9.05.

The November NA49 run at CERN also marshaled all of our Tektronix xp338 X-terminals. They were preconfigured here to ease their arrival in Geneva. At CERN they were hosted by "Mist", which we had configured remotely.

The SNO group's arrival added a fleet of networked Macintoshes to this otherwise all-VMS (with a few PCs) laboratory. Their impact on the cluster has been little more than traffic on the common ethernet and usage of the Alpha. As a part of the SNO group support, we have installed a Sun SparcStation 20, running SunOS v4.1.4, to provide CADENCE circuit layout facilities to our electronics shop. We are still early on the learning curve in providing seamless support to that system.

Our in-house PCs now include a Pentium P90 system for general lab AutoCAD duties. We are gradually providing TCP/IP software to the PCs.

We still provide some system management services for the Institute for Nuclear Theory and the Physics Nuclear Theory group. Their three remote-site DECstation 5000/200s have been replaced with four AXP 3000/600s, two running OSF/1, and two running OpenVMS. Principal system support for those machines is now handled by Physics, with our site providing fall-back assistance and additional expertise. The two groups are still using three VAXstation 3200s which are located in our building.

9.4 SControl, an object oriented program for the control of large physics experiments

J.G. Cramer, P.B. Cramer* and M.A. Howe

SControl is an object-oriented control system construction set written to develop the slow control main console for CERN experiment NA49. It was written in C++ over a period of seven months and contains more than 250 classes. Developed on an HP 9000 series 700 system, SControl has an X11 based user interface that is graphic, mouse-driven, and "friendly". Although developed for a particular experiment, SControl is a run-time configured program that could find general use.

SControl uses a book metaphor to present parameter data on an hierarchy of display pages, with each page showing the system or sub-system that is to be controlled or monitored. Connections are made between the pages with hyper-links so the page hierarchy can be structured in as much detail as required. Each page can represent the overall system, a sub-system, a sub-sub-system, or can be a composite of information drawn from a number of systems. The hyper-links can be made to conform to any irregular shape and can be attached to custom bit-mapped images, buttons, or text.

Each page consists of a device layer and a logic layer. The device layer contains objects which convey information to the operator. A large number of devices are available and include digital and analog meters, switches, sliders, charts, and graphs. The underlying logic layer consists of objects which are used for data processing and include a wide selection for receiving, processing, altering, transmitting, and archiving slow control parameter data. Data display or processing objects are selected from pull down menus, placed on the screen, and connected into the desired configuration using the mouse. Custom built X11 bit map images can be added to the system by placing the image file into a file folder. Images can be used as backgrounds on either the device layer or the logic layer.

Parameter data comes from network connected satellite processors via TCP/IP and is placed in a shared memory data base in the SControl host computer. SControl extracts parameter data from the data base as objects which are then processed by passing through the connected logic layer objects. A data flow model is used by the processing objects. Each object processes its data only if valid data is present on all of its inputs. Because the data resides in shared memory, more than one SControl program can be running at any given time.

SControl provides an integrated alarm system page which displays up to five levels of alarms from **NOTICE** to **EMERGENCY**. Alarms are triggered as needed by connections made in the data processing networks on the logic layers. All alarms display the parameter name, value, and time triggered. Alarms can be acknowledged. A log is kept of alarm acknowledgment activity. Clearing a serious alarm requires that the operator's name be entered into the log also. Alarms can display additional help information that comes from a custom file that operators can edit.

During the November 1994 NA49 test run SControl received data from IBM PC and Macintosh computers running LabView and custom software. The program successfully prepared data-bank structures of slow control parameter information for the data acquisition system, and maintained a separate time-structured archive of operational system data parameters (see Section 7.4).

*Max -Planck-Institut für Physik, Föhringer Ring 6, D-80805 München, Germany.

10. VAN DE GRAAFF, SUPERCONDUCTING BOOSTER AND ION SOURCES

10.1 Van de Graaff accelerator operations and development

D.T. Corcoran, G.C. Harper, M.A. Howe, C.E. Linder, A.M. Myers, T.D. Van Wechel and W.G. Weitkamp

In June 1994 we finished the last steps in the major upgrade of the tandem.[1] We now have a pelletron charging system, new resistors, a terminal control computer system and spiral inclined field beam tubes in the tandem.

Delivery of our titanium spiral inclined field beam tubes[2] was originally scheduled for January 1994, but was delayed because of problems with high voltage tests of the first tube section. The tube was disassembled and micro impurities were found in the titanium electrodes. The tubes were rebuilt with new electrodes and successfully tested individually to voltages of over 5 MV. The tubes were delivered in April and the installation was complete by June. The installation was normal; the tubes fit properly.

The stability of the beam accelerated by this completed system is truly impressive. Formerly the vertical jitter of the beam leaving the tandem was ± 5 mm; now it is unobservable. Terminal voltage stability is illustrated by the fact that the corona current meter formerly fluctuated about ± 10 μA; now the fluctuation is typically $\pm$ 1 μA. Recently, a proton beam was accelerated to 0.3 MeV, with a tandem transmission of 19%. Since part of the beam energy was provided by the ion source, the tandem terminal voltage was actually only 0.07 MV. Prior to the upgrade it would have been impossible to accelerate this low an energy beam. The improved stability has also been important in tuning the beam through the booster, which has tight specifications for beam stability in position, pulse timing and energy.

The transmission of the accelerator for heavy ions has also improved. Prior to the upgrade we found that we could get at most a factor of 4 more current on the high energy cup than on the low energy cup when accelerating ^{40}Ca at a terminal voltage of 8.5 MV. (This corresponds to a transmission of 50%.) Recently we observed a factor of 7 under similar conditions (88% transmission).

The rate at which we can take the tandem to high voltage has not improved as much as we expected. For one thing, we expected the tandem to dry out more quickly after a tank opening with a pelletron than with a belt because the pellet chain should absorb less moisture; this hasn't been the case. For another thing, we find the tubes condition quite slowly. We have had episodes of x-ray production in the low energy tube. These x rays will eventually condition away. Fortunately, with sufficiently patient conditioning, the machine eventually functions adequately at high voltage. We have run the terminal voltage briefly at 9.7 MV but have not yet attempted a data run above 9 MV.

A problem with the pelletron is keeping the charging power supplies alive and the series resistors intact when the tank sparks. The wire wound resistors inside the tank provided as part of the installation proved unreliable. We presently have a string of carbon resistors in place but these are still not able to withstand repeated sparking. Adjusting the spark bars on the pelletron pulleys helped but did not cure the problem.

The new column resistors were described last year.[3] In conjunction with the test installation of the terminal ion source (see Section 10.3) we recently removed and measured 72 resistors which have been in the column for about 12 months. By using a 9 V battery and a nanoammeter and by comparing the resistors to a standard resistor, we can measure to a precision of about 0.5%. We found that the average resistance had decreased 0.5% but the rms spread in values had not changed. This rate of change is an order of magnitude smaller than that of our previous resistors.

---

[1]Nuclear Physics Laboratory Report, University of Washington (1993) p. 86 and *ibid* (1994) p. 66.
[2]Manurfactured by Dowlish Developments - High Voltage Engineering Europa.
[3]Nuclear Physics Laboratory Report, University of Washington (1994) p. 68.

During the year from March 1, 1994 to February 28, 1995 the tandem pellet chains operated 3775 hours. Additional statistics of accelerator operations are given in Table 10.1-1.

Table 10.1-1. Tandem Accelerator Operations
March 1, 1994 to February 28, 1995

	Activity	Days Scheduled	Percent
A.	Nuclear Physics Research, Ion Sources Alone	23	6
B.	Nuclear Physics Research, Tandem Alone		
	Light Ions	16	5
	Heavy Ions	3	1
	Subtotal	19	6
C.	Nuclear Physics Research, Booster and Tandem Coupled		
	Light Ions	11	3
	Heavy Ions	114	31
	Subtotal	125	34
D.	Outside Users		
	Ball Aerospace Systems Group	3	1
E.	Other Operations		
	Tandem Development	62	17
	Tandem Maintenance	85	23
	Unscheduled Time	49	13
	Subtotal	195	53
	Total	365	100

10.2 Alpha source and ion source deck improvements

D.I. Will and J.A. Wootress

A simplified vacuum system and the addition of spark surge-suppression have improved the reliability of our dual charge-exchange alpha source.[1] This source had been assembled from parts of our old Lamb-shift polarized source.[2] About ten years ago these were added to a small elevated platform[3] shared with the UNIS[4] (Universal Negative Ion Source, an old sputter source used for Accelerator Mass Spectrometry,[5] (AMS). Because of time constraints and regular use of the UNIS, the isolation of elevated parts, the suppression of spark transients, the filtering of input gas and the vacuum system were not redesigned then.

Recently, dripping condensation both from a liquid nitrogen solenoid valve for the diffusion pump baffle and from a liquid nitrogen gas purifying trap caused increasing sparking with subsequent damage to flow switches and tripping of breakers. The UNIS when used for AMS required such a liquid nitrogen cold baffle for rapid cycling of the vacuum system each time the twenty samples in the changer wheel were replaced. The cold baffle actually decreased pumping speed for noncondensable gases such as the helium used in the alpha source. Since little AMS is now performed on site at our laboratory, this baffle was removed (while retaining a -20 degrees C refrigerated baffle to impede backstreaming). The foreline was simplified with standard KF flanges (better known in the U.S. as QF or Quick Flanges) at the same time. Ultimate vacuum before these steps was 1 microTorr without liquid nitrogen and 0.2 microTorr with. Now the ultimate is 0.3 microTorr. Furthermore, the typical operating vacuum with alpha source gas load, which was 3 to 6 microTorr before removal, now is 1 to 2 microTorr confirming that pumping speed for noncondensables has been tripled.

To completely eliminate the need for liquid nitrogen, the gas purifying cold trap was replaced by a dessicant/molecular sieve trap followed by an oxygen getter trap. In addition, spark transients are now blocked by ferrite cores and shunted to ground by transorbs to protect the flow switches and sensitive circuit breakers.[6] Finally, proper high voltage shielding has been added around the doubly elevated power supplies for the duoplasmatron filament, bottle magnet, and arc. The source has recently run for one week without active tending or maintenance.

On our main ion source deck[7] all three forelines were rebuilt to allow easy attachment/detachment of a Varian Portatest 936 helium leak detector to the output of each turbomolecular pump effectively in place of the mechanical forepump. This permits detection of substantially smaller leaks than either parallel forepumping with Portatest and mechanical pump together, or direct pumping on the vacuum chamber with the Portatest.

---

[1]Nuclear Physics Laboratory Annual Report, University of Washington (1986) p. 54.
[2]Nuclear Physics Laboratory Annual Report, University of Washington (1973) p. 11; (1974) p. 13; (1975) p. 18; (1976) p. 22; (1977) p. 157.
[3]Nuclear Physics Laboratory Annual Report, University of Washington (1983) p. 72; (1984) p. 76.
[4]Nuclear Physics Laboratory Annual Report, University of Washington (1975) p. 22; (1976) p. 26; (1980) p. 167; (1986) p. 53.
[5]Nuclear Physics Laboratory Annual Report, University of Washington (1994) pp. 30-31.
[6]Nuclear Physics Laboratory Annual Report, University of Washington (1992) p. 78.
[7]Nuclear Physics Laboratory Annual Report, University of Washington (1985) p. 87; (1986) p. 71; (1987) p. 63.

10.3 Tandem terminal ion source

J.F. Amsbaugh, G.C. Harper, M.A. Howe, C.E. Linder, A.W. Myers, D.W. Storm, T.D. Van Wechel and W.G. Weitkamp

This year tests of the RF discharge source purchased from NEC were performed. The source was specified to deliver 400 μamps of $^{1}H^{+}$ and 200 μamps $^{4}He^{+}$ using a standard 2 mm diameter aluminum canal. The gas load was specified to be of the order of 1 to 2 mTorr-l/sec. The emittance of the source was specified to be about 3π *mm mrad*$\sqrt{\text{MeV}}$. We have purchased a 1 mm diameter canal in addition to the standard canal. We expected a source with a 1 mm canal to deliver about 60 μamps of $^{3}He^{+}$ with a gas load of about 0.2 mTorr-l/sec and an emittance of about 0.75π *mm mrad*$\sqrt{\text{MeV}}$.

Bench tests with a 2 mm diameter canal have shown that the source with the extractor/einzel assembly that was built in house produces a maximum of 200 μamps of unanalyzed beam using ^{1}H gas with a measured gas load of 4.7 mTorr-l/sec. An unanalyzed beam of about 110 μamps using ^{4}He as the gas has been measured. This $^{4}He^{+}$ beam had a focused FWHM of 1.5 mm and estimated emittance of 3.5π *mm mrad*$\sqrt{\text{MeV}}$. Bench tests with a 1 mm diameter canal have produced 32 μamps of unanalyzed beam using ^{4}He with a measured gas load of 2.0 mTorr-l/sec and a focused FWHM of 1.3 mm. The emittance of the $^{4}He^{+}$ beam from the 1 mm canal is estimated to be about π *mm mrad*$\sqrt{\text{MeV}}$. The bench tests were done using a variable frequency RF source and a broadband amp capable of producing 200 W of forward power. The beam intensity was found to level off at about 50 W and seemed to be independent of frequency.

The source, with the 1 mm canal, was then installed in the terminal of the Van de Graaff. The foil changer was removed from its port, which is 60° off of the beam axis, and in its place the RF discharge source and extractor/einzel assembly were installed. A double focusing dipole magnet with bending radius 14 cm and bending angle 60° was installed in the foil box. The poles of the magnet were made of 8C ferrite and permanently magnetized to 2500 Gauss. The column gradient of the high energy end was changed to accommodate the low energy (20 keV) beam. The power supplies and the gas leak valve were controlled remotely using the terminal computer. The RF oscillator used during these tests was one purchased from NEC and designed to be used with the source.

An unanalyzed beam of 22 μamps using ^{3}He gas was measured before the magnet. An analyzed beam of 3 μamps of $^{3}He^{+}$ was measured on a flap just after the magnet. Analyzed currents of order 0.1 μamps were measured for what appears to be $^{14}N^{+}$ and $^{16}O^{+}$. With the terminal at 3 MV, the current measured at the high energy cup was 2.8 μamps. The gas consumption measured was 1.3 mTorr-l/sec.

Disassembly of the source showed that the beam spot size on the flap in front of the magnet was 6 mm in diameter as predicted by the optics program that was used to model the beam transport. The magnet frame exhibited some discoloration from beam impingement and cusp shaped discoloration was also present on the post magnet flap and steering plates. The 93% transmission measured from the magnet to the high energy cup was encouraging. The reason for the poor transmission through the magnet is unknown and will be studied further outside of the Van de Graaff. There is a possibility that cylindrical electrostatic inflection plates will be tested in place of the magnet.

10.4 Terminal computer

G.C. Harper, M.A. Howe, A.W. Myers and T.D. Van Wechel

The computer which controls the terminal vertical and horizontal steerers, the stripper foil mechanism, the gas stripper canal position, and the stripper canal gas delivery system was operated approximately 3775 hours with about 3000 sparks. During the past year we upgraded our system to include an 8 channel DAC board which required us to add a second Group 3 device interface module.

This 8 channel DAC board was added to support the terminal ion source (see Section 10.3). The Gordo computer software, which is external to the tank and controls the microprocessor based controller via fiber optics, had to be upgraded to support the Terminal Ion Source. A software module was written for the DAC channels and minor modifications were made to the communication modules so that the DAC objects in Gordo could receive commands from the linac control system (CSX). A corresponding extension was made to CSX to hold the DAC values in its data base and display those values on the touch screens in the control room.

In the annual report last year, we reported as a problem an occasional unrequested foil increment during the power up or power down sequence of the terminal computer. We determined that this was being caused by 28 VDC being available at the foil changer mechanism when the computer digital outputs came up in a default high state which allowed the foil changer to increment one foil. This was also found to be the case upon power down, the computer would go to default high and 28 VDC would be present allowing the foil changer to increment. To solve this problem we did two things. First we changed the default settings of all of the digital channels to a low state. Second, we added a 5 second time delay card between 28 VDC and the 28 VDC input on the digital interface feed-through board on the inside of the inside enclosure.

Prior to tank close out, we always conduct tank close-out checks. During one of these checks, after we had been conducting signal checks and voltage tests on our computer, we found that we did not have motor outputs on two channels. We determined that during our testing we must have grounded these two outputs. This caused the motor driver I.C.'s to fail. We replaced these I.C.'s and the computer tested satisfactorily. To help keep this problem from happening again, we redesigned the motor output interface board which is the inside interface board for the outside enclosure. On this redesigned interface board we added fuses to all eight motor lines (4 motor forward and 4 motor reverse lines).

10.5 Booster operations

J. F. Amsbaugh, D. T. Corcoran, G. C. Harper, M. A. Howe, D. W. Storm, D. I. Will and
J. A. Wootress

During the period March 1, 1994 to Feb. 28, 1995 , the booster was operated for 124 days, as compared to 81 days in the same period a year earlier and to 48 days in the same period two years earlier. This increase is in spite of the shutdown of the tandem for installation of the new beam tubes.

Beams ranged in mass from ^{4}He to ^{60}Ni, and included ^{12}C, $^{16,18}O$, and ^{40}Ca. This year there were more runs and more days with ^{40}Ca than any other beam, as was the case last year.

In May we opened cryostats #2 and #5 to replace a total of three couplers. During the latter part of the year we have been unable to operate three resonators, due either to a stuck coupler, a coupler or rf power cable which is intermittently open circuit, and what appears to be a bad rf monitor cable (inside the cryostat). These will be repaired when there is an opportunity to do so.

We continue to operate the low beta resonators at an average field of 3.0 MV/m and the high beta ones at average of 2.4 MV/m. Most of these resonators were plated when the linac was being assembled over eight years ago. Approximately four of them were replaced with replated ones three or four years ago.

All the Leybold-Hereaus turbomolecular pumps with greased steel bearings have been replaced with units with greased ceramic bearings. These continue to give good service, in general. One pump failed at 14k hours, which is disappointing, but several others have much longer running times.

We had no compressor failures this year. Our oldest compressor now has run for 71k hours, and the other two have run for 41k hours in one case and 12k hours in the other case.

10.6 Cryogenic operations

M.A. Howe, D.I. Will and J.A. Wootress

The booster linac is cooled by liquid helium which is thermally shielded by liquid nitrogen. The liquid nitrogen is delivered in lots of ~6000 gallons by semitrailer tanker. In 1994 liquid nitrogen consumption of 198,900 gallons was 12% less than that in previous years since a precool heat-exchanger leak now prohibits the use of the liquid nitrogen assist in our Koch Process Systems 2830 Helium Refrigerator.[1] The helium is purchased as high purity bulk gas and liquified by our helium refrigerator. Usage of 170,800 SCF in 1994 was down 23% from that in 1993. Indeed, usage for April through December 1994 (after the leaky heat-exchanger was isolated) projects to an annual rate of 109,300 SCF, down 51% from that in 1993 and slightly less than typical for years before 1992.

The following table summarizes our maintenance for 1994 January 1 to 1994 December 31:

Item	In Use	Major Services	Times Performed
Refrigerator			
Cold Box	99%	warm/pump/purge	1
Main Dewar	100%	warm/pump/purge	0
Top Expander	~4451 Hrs	warm/pump/purge	21
	~100 RPM	main, valve rod and valve seals	1
		wristpin, crank, and cam follower brngs	1
		flywheel bearings and belts	1
Middle Expander	~8084 Hrs	warm/pump/purge	17
	~120 RPM	main, valve rod and valve seals	1
		wristpin, crank, and cam follower brngs	1
		flywheel bearings and belts	1
		replaced alternator	1
Wet Expander	~4631 Hrs	warm/pump/purge	6
	~40 RPM	main, valve rod and valve seals	1
		wristpin, crank, and cam follower brngs	1
		flywheel bearings and belt	1
		trimmed both piston lengths	1
		replaced DC drive motor/generator	1
Distribution System	99%	warm, pump, purge lines	8

This final table shows screw compressor history here as of 1995 March 13:

Item	Total	1994	Status	Maintenance
RS-1	71,424 hours	8359 hours	running	none
RS-2	55,958 hours	0 hours	phases shorted	core removed 1993
RS-2a	12,191 hours	8030 hours	running since 1993	none
RS-3	22,752 hours	0 hours	shorted to ground	core removed 1990
RS-3a	40,549 hours	8562 hours	running since 1990	none

[1]Nuclear Physics Laboratory Annual Report, University of Washington (1994) p. 75.

10.7 Development of a high energy buncher operating at 13/12 the linac frequency

D. Corcoran, D.W. Storm and K. Swartz

The linac operates at a frequency of 148.8 MHz, but the low energy buncher is operated at 1/12 this frequency in order to provide useful time separation between bunches. It is able to put about 70% of the dc beam from the ion source into a bunch which is bunched further before the linac and then accelerated. The low energy buncher spreads the remaining 30% of the dc beam out between the bunches. The high energy buncher, which is a single super conducting resonator identical to those in the first part of the linac, also bunches part of this remaining beam on each of the 11 linac rf cycle not synchronized with the low energy buncher. This beam is accelerated and makes small but significant beam bursts in between the main bunches produced by the low energy buncher. Ideally the high energy buncher would be operated at the same frequency as the low energy one, but to make a high voltage accelerating (or bunching) device operating at such low frequency is difficult.

K. Swartz realized that if the high energy buncher were operated at a frequency chosen so that the difference between its frequency and the linac frequency was equal to the low energy buncher frequency, then the beam which was outside the main bunch would not be bunched into the accelerating phase bucket of the linac, but the low energy buncher, high energy buncher, and linac could all be phased so that the main bunch would be properly bunched again by the high energy buncher and then accelerated.

We briefly considered the possibility of lowering the frequency of one of our low beta superconducting resonators by capacitively loading the drift tube. This would require, however, a rather large capacitance with a corresponding very small gap. Shortening the quarter wave resonator, on the other hand, is a straightforward way to raise the frequency. Using the same model calculation that we used to design the high beta resonators, we determined that shortening the resonator by 1.77 inches, in the region where the inner conductor has its minimum radius, would increase the frequency by a factor of 13/12. The shortening was accomplished by parting the outer conductor and inner conductor, removing a total of 1.77 inches, and vacuum brazing the parts back together. This process was done in stages, first testing the calculation using a defective resonator body, and then removing slightly less than the full length from the final resonator in order to verify the frequency. The calculation gave the right space within 0.01 inch, and the frequency error after the final machining was well within the 10 kHz tolerance for final tuning.

The resonator has been brazed and the braze joint ground back to produce a smooth groove without any gap. We expect to plate and test the resonator in late March and early April. Since the resonator is shorter than the present high energy buncher resonator, it will fit in the same cryostat with simply an extension tube connecting the liquid helium tank.

10.8 Design of support structure for three large NaI counters

D. W. Storm

We presently have a single large shielded sodium iodide detector which is used in Cave II. It is placed on a platform which is only big enough for this single counter to be operated on one side of the beam.

We have arranged to borrow two equally large sodium iodide detectors and plan to operate all three at once, with two on one side and the third on the other side of the beamline. Consequently we are planning to build a platform 13' by 14' and to move the scattering chamber a few feet downstream so it can be placed in the center of the rectangular platform.

The platform will be supported on the floor of the cave basement, which is a 12" thick reinforced concrete slab, lying on compacted sand. The platform will have 18 legs supporting a flat framework of steel I-beams with a maximum of 4.5' space between beams. On top of these beams we will put six slabs of reinforced concrete which will be leveled to make a flat floor. We plan to mount the detectors on air pads, and the floor must be flat enough for operation of the airpads.

As of mid March, the concrete platforms have been ordered, the steel design is complete and the steel is ordered.

11. NUCLEAR PHYSICS LABORATORY PERSONNEL

Faculty

Eric G. Adelberger, Professor
John G. Cramer, Professor
Hans Bichsel, Affiliate Professor
Ludwig de Braeckeleer, Research Assistant Professor
Peter J. Doe, Research Professor
Steve Elliott, Research Assistant Professor
George W. Farwell, Professor Emeritus
Gregg B. Franklin, Visiting Associate Professor[1]
Pieter M Grootes, Research Professor, Geological Sciences and Physics[2]
Jens H. Gundlach, Research Assistant Professor
Isaac Halpern, Professor Emeritus
Blayne R. Heckel, Professor
John Lestone, Research Assistant Professor
R.G. Hamish Robertson, Professor
Kurt A. Snover, Research Professor
Derek W. Storm, Research Professor; Director, Nuclear Physics Laboratory
Thomas A. Trainor, Research Associate Professor
Robert Vandenbosch, Professor
William G. Weitkamp, Research Professor; Technical Director, Nuclear Physics Laboratory
John Wilkerson, Professor

Research Staff

Marcus Beck, Research Associate
Joseph V. Germani, Research Associate
Jun Jien (Felix) Liang, Research Associate
Steven D. Penn, Research Associate
Thomas D. Steiger, Research Associate
Yue Su, Research Associate[3]
Josephus P. van Schagen, Research Associate
Danzhao Ye, Research Associate[4]
Zhiping Zhao, Research Associate
Xianzhou Zhu, Research Associate[5]

Predoctoral Research Associates

Qazi Rushdy Ahmad
James C. Beck
Jeffery D. Bierman
Thomas Brown[7]
Pakkin Chan
Alexander D. Cronin
Ziad Drebi[8]
Michael Harris
Wei-Dong Jiang[6]
Michael P. Kelly
Diane M. Markoff
Alan W.P. Poon
Gregory L. Smith
Alejandro Sonzogni
Kenneth Swartz
David C. Wright

---

[1]Permanent Address: Carnegie Mellon University, Pittsburgh, PA.
[2]Now at Christian Albrechts Universitaet, Kiel, Germany.
[3]Now at Room 102, Building 32, Beijing 100026, PRC.
[4]Now at University of Chicago, IL.
[5]Now at 13859 Azelea Circle, Tampa, FL.
[6]Now at OUM and Assoc., Bellevue, WA.
[7]Now at Lawrence Livermore National Laboratory, Livermore, CA.
[8]Now at Univ. of Al-Fateh, Tripoli, Libya.

Professional Staff
John F. Amsbaugh, Research Engineer
Gregory C. Harper, Research Engineer
Mark A. Howe, Research Engineer
Duncan Prindle, Research Scientist
Richard J. Seymour, Computer Systems Manager
H. Erik Swanson, Research Physicist
Timothy D. Van Wechel, Electronics Engineer
Douglas I. Will, Research Engineer

Technical Staff
Dean T. Corcoran, Engineering Technician
James Elms, Instrument Maker
Louis L. Geissel, Instrument Maker, Student Shop Leadman[9]
Carl E. Linder, Engineering Technician
Allan Myers, Electronics Technician
Hendrik Simons, Instrument Maker, Shop Supervisor
John A. Wootress, Accelerator Technician
Steve Zsitvay, Instrument Maker

Administrative Staff
Barbara J. Fulton, Administrative Assistant
Karin M. Hendrickson, Office Assistant

Part Time Staff
Michael Adams[10]
Ryan Allen
Stephen Bailey
Chris Bond[10]
Sara Chanthaseny
Ralph Chestine
Dawneen Davis[10]
Adam Di Vergilio
Eric Dorman
Joseph Dossum[10]
James Evan III[10]
Arin Goldberg[10]
Karsten Isaacson
Tim Kalka
Jason Knox[10]
John McGrath
Adam Miller[10]
Jeffrey Reid
Michael Strombach
Peter Venable[10]
Eleanor Warfield[10]
David Weston[10]

[9]Retired.
[10]No longer associated with NPL.

12. DEGREES GRANTED, ACADEMIC YEAR, 1994-1995:

"Radiocarbon dating of pollen by accelerator mass spectrometry," Thomas Alexander Brown, Ph.D. Thesis, (Geophysics) University of Washington (1994).

"Spin-induced shape changes in light-medium mass compound nuclei," Ziad M. Drebi, Ph.D. Thesis, University of Washington (1994).

13. LIST OF PUBLICATIONS FROM 1994-95

Published papers:

"Potentials that permit a uniqueness theorem," D.F. Bartlett and Y. Su, Amer. J. Phys **62**, 683 (1994).

"Qualité du rayonnemént en radiobiologie: application phénomenologique de la microdosimetrie," P. Pihet, H. Bichsel and H.G. Menzel, J. Chimie Physique et de Physico-Chimie Biol. **91**, 1261 (1994).

"Energy deposition by relativistic heavy ions in thin argon absorbers," M. Pfützner, H. Geissel, G. Münzenberg, F. Nickel, Ch. Scheidenberger, K.-H. Schmidt, K. Sümmerau, T. Brohm, B. Voss and H. Bichsel, Nucl. Instrum. Methods B **86**, 213 (1994).

"Cluster impact fusion and cluster size distributions," R. Vandenbosch, J. Neubauer, D.I. Will, T.A. Trainor and D. Ye, Nucl. Instrum. Methods B, **88**, 116 (1994).

"Current status of the ^{14}C AMS program at the University of Washington," T.A. Brown, G.W. Farwell and P.M. Grootes, Proceedings of the 6th International Conference on Accelerator Mass Spectrometry (1993), Nucl. Instrum. Methods B **92**, 16 (1994).

"Using maximum likelihood analysis in HBT interferometry: bin-free treatment of correlated errors," J.G. Cramer, D. Ferenc and J. Gazdzicki, Nucl. Instrum. Methods A **351**, 489 (1994).

"Shape changes and isospin purity in highly excited light-mass nuclei," M. Kicinska-Habior, K.A. Snover, J.A. Behr, C.A. Gossett, J.H. Gundlach, Z.M. Drebi, M.S. Kaplan and D.P. Wells, Nucl. Phys. A **569**, 17C (1994).

"Results from SAGE (The Russian-American Gallium Solar Neutrino Experiment)," J.N. Abdurashitov *et al.*, Phys. Lett. B **328**, 234 (1994).

"Gamow-Teller strength in the β-decay of ^{36}Ca," W. Trinder, E.G. Adelberger, B.A. Brown, Z. Janas, H. Keller, K. Krumbholz, V. Kunze, P. Magnus, F. Meissner, A. Piechaczek, M. Pfützner, E. Roeckl, K. Rykaczewski, W.-D. Schmidt-Ott and M. Weber, Phys. Lett. B. **348**, 331 (1995).

"Origin of empirical threshold for dissipative fission," R. Vandenbosch, Phys. Rev. C **50**, 2618 (1994).

"Measurements of the electric and magnetic form factors of the proton from $Q^2 = 1.75$ to 8.83 $(Gev/c)^2$," L. Andivahis *et al.*, Phys. Rev. D **50**, 5491 (1994).

"Fusion-fission cross sections for ^{32}S + ^{138}Ba and ^{48}Ti + ^{122}Sn at near-barrier energies," A. Charlop, J. Bierman, Z. Drebi, S. Gil, A. Sonzogni, R. Vandenbosch, and D. Ye, Phys. Rev. C **51**, 623 (1995).

"D-D fusion induced by oxygen clusters impacting deuterated ice targets," J.F. Liang, R. Vandenbosch, D.I. Will, Phys. Rev. A **51**, 1691 (1995).

"Absence of anomalous entrance channel effects in sub-barrier heavy ion fusion," A. Charlop, J. Bierman, A. Garcia, D. Prindle, A.A. Sonzogni, R. Vandenbosch, D. Ye, S. Gil, F. Hasenbalg, J.E. Testoni, D. Abriola, M. di Tada, A. Etchegoyen, M.C. Berisso, J.O. Fernandez-Niello and A.J. Pacheco, Phys. Rev. C **49**, R1235 (1994).

"Electric form factor of the neutron from the $^2\mathrm{H}(\vec{e},e',\vec{n})^2\mathrm{H}$ reaction at $Q^2 = 0.255$ (GeV/c)^2," T. Eden *et al.*, Phys. Rev. C **50**, 1749 (1994).

"Energy of the 'hot CNO cycle' $^{13}\mathrm{N}(p,\gamma)$ resonance and the ^{18}Ne mass," P.V. Magnus, E.G. Adelberger and A. García, Phys. Rev. C **49**, R1755 (1994).

"The Coulomb dissociation of ^{8}B and the $^7\mathrm{Be}(p,\gamma)^8\mathrm{B}$ reaction at low energies," T. Motobayashi, N. Iwasa, Y. Ando, M. Kurokawa, H. Murakami, J. Ruan (Gen), S. Shimaura, S. Shirato, N. Inabe, M. Ishihara, T. Kubo, Y. Watanabe, M. Gai, R.H. France III, K.I. Hahn, Z. Zhao, T. Nakamura, T. Teranishi, Y. Futami, K. Furataka and Th. Delbar, Phys. Rev. Lett. **73**, 2680 (1994).

"Modern tests of the universality of free fall," E.G. Adelberger, Journal of Classical and Quantum Gravity **11**, A9 (1994).

"Energy loss of 70 MeV protons in tissue substitute materials," T. Hiraoka, K. Kawashima, K. Hoshina and H. Bichsel, Phys. Med. Biol. **39**, 983 (1994).

"New tests of the universality of free fall," Y. Su, B.R. Heckel, E.G. Adelberger, J.H. Gundlach, M. Harris, G.L. Smith and H.E. Swanson, Phys. Rev. D **50**, 3614 (1994).

"Natural wormholes as gravitational lenses," J.G. Cramer, R.W. Forward, M.S. Morris, M. Visser, G. Benford and G.A. Landis, Phys. Rev. D **51**, 3117 (1995).

"Constraints on coupling constants through charged σ photoproduction," T. Mart, C. Bennhold and C.E. Hyde-Wright, Phys. Rev. D **51**, R1074 (1995).

"Quantum mechanics and Bell's inequalities," R.T. Jones and E.G. Adelberger, Phys. Rev. Lett. **72**, 2675 (1994).

"β-decay of ^{37}Ca," W. Trinder, E.G. Adelberger, Z. Janas, H. Keller, K. Krumbholz, V. Kunze, P. Magnus, F. Meissner, A. Piechaczek, M. Pfützner, E. Roeckl, K. Rykaczewski, W.-D Schmidt-Ott and M. Weber, Phys. Lett. B, **349**, 267 (1995).

"Beta-delayed γ-ray emission in ^{37}Ca decay," A. Garcia, E.G. Adelberger, P.V. Magnus, H.E. Swanson, D.P. Wells, F.E. Wietfeldt. O. Tengblad and the ISOLDE collaboration, Phys. Rev. C **51**, R439 (1995).

"Search for entrance-channel effects in sub-barrier fusion reactions," A. Charlop, J. Bierman, Z. Drebi, A. Garcia, S. Gil, D. Prindle, A. Sonzogni, R. Vandenbosch and D. Ye, Phys. Rev. C **51**, 628 (1995).

"Fusion cross sections in systems leading to ^{170}Hf at near-barrier energies," S. Gil, F. Hasenbalg, J.E. Testoni, D. Abriola, M.C. Berisso, M. di Tada, A. Etchegoyen, J.O. Fernandez Niello, A.J. Pacheco, A. Charlop, A.A. Sonzogni and R. Vandenbosch, Phys. Rev. C **51**, 1336 (1995).

"Parity mixing of the 0^+ -0^- I=1 doublet in ^{14}N," V.J. Zeps, E.G. Adelberger, A. Garcia, C.A. Gossett, H.E. Swanson, W. Haeberli, P.A. Quinn and J. Sromicki, Phys. Rev. C **51**, 1494 (1995).

"Radiative decays of the 16.6 and 16.9 MeV states in ^{8}Be and tests of CVC in the A=8 multiplet," L. De Braeckeleer, E.G. Adelberger, J.H. Gundlach, M. Kaplan, D. Markoff, A.M. Nathan, W. Schief, K.A. Snover, K.B. Swartz and D. Wright, in press, Phys. Rev. C **51**, 2778 (1995)..

"Gamma decays of proton unbound levels in ^{37}K," P.V Magnus, E.G. Adelberger and N. Cabot, Phys. Rev. C, **51**, 2806 (1995).

"Strange particle production in nuclear collisions at 200 GeV per nucleon," T. Alber *et al*. (the NA35 Collaboration), Z. Phys. C **64**, 195 (1994).

"Modern tests of the universality of free fall," E.G. Adelberger, in *Experimental Gravitation*, ed. by M. Karim and A. Qadir, Inst. of Physics Publishing, Bristol and Philadephia, p. A9 (1994).

Papers submitted or to be published:

"Ultradipole radiation from low-energy heavy-ion reactions," M.Kicinska-Habior, K.A. Snover, A. Maj, Z. Drebi, D. Ye and M. Kelly, Proceedings of the XXIX Zakopane School of Physics (Zakopane, Poland, 1994) Acta Phys. Pol. B, in press.

"Bragg curves for different shape ionization chambers," H. Bichsel, submitted to Med. Phys.

"Progress and prospects in neutrino astrophysics," J.N. Bahcall, K. Lande, R.E. Lanou, J. Learned, R.G.H. Robertson and L. Wolfenstein, Nature, in press.

"Measurement of the polarization of a pulsed electron beam with a Möller polarimeter in the coincidence mode," K.B. Beard *et al*., Nucl. Instrum. Methods, to be published.

"Transverse momentum dependence of Bose-Einstein correlations in 200A GeV/c S + A collisions," D.T. Alber *et al*. (the NA35 collaboration), Phys. Rev. Lett., to be published.

"^{36}Ca decay and the Isobaric Multiplet Mass Equation," A. Garcia, E.G. Adelberger, P.V. Magnus, H.E. Swanson, F.E. Wietfeldt, O. Tengblad and the ISOLDE Collaboration, submitted to Phys. Rev. C.

"Temperature dependence of the level-density parameter," J.P. Lestone, submitted to Phys. Rev. C.

"Analysis of α-particle multiplicities in ^{19}F + ^{181}Ta reactions leading to evaporation residues," J.P. Lestone, submitted to Phys. Rev. C.

"Spin-induced shape changes in light-medium mass compound nuclei," Z.M. Drebi, K.A. Snover, A.W. Charlop, M.S. Kaplan, D.P. Wells and D. Ye, submitted to Phys. Rev. C.

"Inclusive positive pion photoproduction," K.G. Fissum, H.S. Caplan, K.G.R. Doss, E.L. Hallin, D.M. Skopik, J.M. Vogt, M. Frodyma, D.P. Rosenzweig, D.W. Storm, G.V. O'Rielly and K.R. Garrow, submitted to Phys. Rev. C.

"Two-pion Bose-Einstein correlations in nuclear collisions at 200 GeV/nucleon," D. Ferenc *et. al*. (the NA35 Collaboration), Z. Phys., to be published.

"Neutrino," J.F. Wilkerson, McGraw-Hill Encyclopedia of Science and Technology, Eighth Edition, to be published.

Abstracts and other conference presentations by NPL personnel:

"Fusion cross sections and linear momentum transfer for ^{14}N and ^{16}O-induced reactions," A.A. Sonzogni, A. Elmaanni, C. Hyde-Wright, W. Jiang, D. Prindle, R. Vandenbosch, J. Dinius, G. Cron, D. Bowman, C.K. Gelbke, W. Hsi, W.G. Lynch, C. Montoya, G. Peaslee, C. Schwarz, M.B. Tsang, C. Williams, R. DeSouza, D. Fox and T. Moore, abstract presented at Gordon Conference, June, 1994.

"SControl, an object-oriented program for the slow control of large physics experiments," M.A. Howe, J.G. Cramer and P.B. Cramer, published in proceedings of AIHEN95 (Artificial Intelligence for High Energy area Nuclear Physics), Pisa, Italy, April 1995.

"Natural wormholes as gravitational lenses," J.G. Cramer, M. Visser, M.S. Morris, R.W. Forward, G. Benford and G.A. Landis, contributed to the 17th "Texas" Symposium on Relativistic Astrophysics, Munich, Germany, Dec. 12, 1994, to be printed in Conference Proceedings.

"Operating experience with the upgraded UW Tandem," W.G. Weitkamp, D.T. Corcoran, G.C. Harper, M.A. Howe, C.E. Linder, A.W. Myers and T.D. Van Wechel, Symposium of North Eastern Accelerator Personnel, Western Michigan University, 1994.

"A terminal ion source for the UW tandem," G.C. Harper, Symposium of North Eastern Accelerator Personnel, Western Michigan University, 1994.

"A terminal computer for the UW tandem," G.C. Harper, Symposium of North Eastern Accelerator Personnel, Western Michigan University, 1994.

"Neutrino astrophysics: a research briefing," J.N. Bahcall, K. Lande, R.E. Lanou, J. Learned, R.G.H. Robertson and L. Wolfenstein, Report to National Academy of Sciences/National Research Council.

"Direct neutrino mass determinations," R.G.H. Robertson, Invited Summary Paper, Snowmass Workshop on Neutrino Astrophysics and Cosmology, June 30, 1994.

"Neutrino physics summary," R.G.H. Robertson, Invited Report to APS DPF Long-Term Planning Committee, Albuquerque, NM, Aug 7, 1994.

"The solar neutrino problem: is the sun going out, or is no "nu's' good news?" R.G.H. Robertson, Public Lecture, APS DNP Meeting, Williamsburg, VA, Oct. 27, 1994.

"Neutrino physics for the masses," R.G.H. Robertson, Invited Paper, Symposium in Honor of G.T. Garvey, Los Alamos, Jan. 19, 1995.

"Impact parameter dependence of pre-equilibrium particle emission in intermediate energy heavy ion reactions," R. Vandenbosch, Invited Talk, ACS National Meeting, Anaheim, CA, April 1995.

"Light-charged particles emitted from the decay of the ^{156}Er compound nucleus," J.F. Liang, J.D. Bierman, P. Chan, M.P. Kelly, A.A. Sonzogni and R. Vandenbosch, Bull. Am. Phys. Soc. **40**, 978 (1995).

"Fusion barrier distributions extracted from cross-section measurements on the systms ^{40}Ca + ^{192}Os, ^{194}Pt," J.D. Bierman, P. Chan, M.P. Kelly, J.F. Liang, A.A. Sonzogni and R. Vandenbosch, Bull. Am. Phys. Soc. **40**, 978 (1995).

"Search for fundamentally new interactions with ranges >1 cm," J.H. Gundlach, Seventh Marcel Grossman Meeting on General Relativity, Stanford, CA, July 23-31, 1994.

"The extraction and AMS radiocarbon dating of pollen from sediment samples from an Alaskan lake," T.A. Brown, G.W. Farwell and P.M. Grootes, presented at the Second Annual PALE Research Meeting, Feb. 4-6, 1995, University of Washington, Pack Forest, Eatonvile, Washington; published internally by PALE for NSF.

"The extraction and AMS radiocarbon dating of pollen from lake sediment and peat samples," T.A. Brown, G.W. Farwell and P.M. Grootes, abstract submitted to INQUA95, Aug. 3-10, 1995, Berlin, Germany.

"Tests of the weak equivalence principle in the Earth's field," Y. Su, E.G. Adelberger, B.R. Heckel, M.G. Harris and G.L. Smith, Proceedings of the William Fairbanks Conference, Hong Kong, 1994.

"Development of a $^{3}H(p,\gamma)^{4}He$ 20 MeV calibration souce for energy calibration at the Sudbury Neutrino Observatory," A.W.P. Poon, presented at the Bakan School of Particles and Cosmology, Baksan, Russia, April 19, 1995, to be printed in the Proceedings.

"Results for SAGE II," S. Elliott and SAGE Collaboration, Annual Fall Meeting of the Division of Nuclear Physics, Williamsburg, VA, Oct. 29, 1994, contributed talk.

Conference presentations by collaborators of NPL personnel:

"Recent results from NA35," M. Gazdzicki for the NA35 Collaboration presented at Quark Matter '95, Monterey, CA, Jan. 9, 1995, to be printed in the Conference Proceedings.

"Two-pion interferometry in central sulfur-nucleus collisions at 200 GeV per nucleon," T. Alber for the NA35 Collaboration presented at Quark Matter '95, Monterey, CA, Jan. 9, 1995, to be printed in the Conference Proceedings.

"Antibaryon production in S-nucleus collisions at 200 GeV per nucleon," J.Günther for the NA35 Collaboration presented at Quark Matter '95, Monterey, CA, Jan. 9, 1995, to be printed in the Conference Proceedings.

"Transverse energy distributions and nuclear stopping in Pb + Pb at 160 GeV per nucleon," S. Margetis for the NA35 Collaboration presented at Quark Matter '95, Monterey, CA, Jan. 9, 1995, to be printed in the Conference Proceedings.

"Strange particle and anti-proton production in S + nucleus collisions at 200 GeV per nucleon," S. Margetis for the NA35 Collaboration, present at the 8th Meeting of the Division of Particles and Fields of the APS, Albuquerque, NM, Aug. 2, 1994, to be printed in the Proceedings.

"Stopping and two pion Bose-Einstein correlation results from CERN experiment NA35," J.T. Mitchell for the NA35 Collaboration, presented at the 8th Meeting of the Division of Particles and Fields of the APS, Albuquerque, NM, Aug. 2, 1994, to be printed in the Proceedings.

"Transverse momentum dependence of Bose-Einstein correlations in 200A GeV/c S + A collisions," R.J. Morse for the NA35 Collaboration, presented at the 5th Conference on the Intersections of Particle and Nuclear Physics, St. Petersburg, FL May 31, 1994, to be printed in the Proceedings.

"Hadron production in S + nucleus collisions at 200 GeV/nucleon," S. Margetis for the NA35 Collaboration, presented at the 10th Winter Workshop on Nuclear Dynamics, Snowbird, Utah, Jan. 15, 1994, to be printed in the Proceedings.

"Bose-Einstein correlations in nuclear collisions at 200 GeV/nucleon," Daniel Ferenc and the NA35 Collaboration, invited paper presented at the XXIXth Rencontres de Moriond, QCD and High Energy Hadronic Interactions, March 19, 1994, Meribel, France, to be printed in the Proceedings.

"Time projection chambers in NA35 and NA49," P. Jacobs for the NA35 and NA49 Collaborations, presented at the Winter Workshop on Nuclear Dynamics, Key West, FL, Jan. 31, published in Proceedings, Advances in Nuclear Dynamics, 217 (1994).